Contract No:

This document was prepared in conjunction with work accomplished under Contract No. DE-AC09-08SR22470 with the U.S. Department of Energy (DOE) Office of Environmental Management (EM).

Disclaimer:

Flowsheet Testing for Strip Effluent to Slurry Mix Evaporator Modifications at the Defense Waste Processing Facility

D.P. Lambert

J. R. Zamecnik

April 2015

SRNL-STI-2015-00002, Revision 0

DISCLAIMER

Printed in the United States of America

Prepared for
U.S. Department of Energy

Keywords: *Slurry, sludge, SRAT, SME, SEFT, strip effluent*

Retention: *Permanent*

Flowsheet Testing for Strip Effluent to Slurry Mix Evaporator Modifications at the Defense Waste Processing Facility

D.P. Lambert
J. R. Zamecnik

April 2015

Prepared for the U.S. Department of Energy under contract number DE-AC09-08SR22470.

Savannah River National Laboratory™
OPERATED BY SAVANNAH RIVER NUCLEAR SOLUTIONS

REVIEWS AND APPROVALS

AUTHORS:

D.P. Lambert, Process Technology Programs Date

J. R. Zamecnik, Process Technology Programs Date

TECHNICAL REVIEW:

C.J. Martino, Process Technology Programs Date

M.S. Williams, Process Technology Programs Date

APPROVAL:

D.H. McGuire, Manager Date
Process Technology Programs

S.L. Marra, Manager Date
Environmental & Chemical Process Technology Research Programs

E.J. Freed, Manager Date
DWPF/Saltstone Facility Engineering

ACKNOWLEDGEMENTS

The authors wish to acknowledge the assistance of M. E. Stone, D. G. Sumpter, M. F. Williams, H. K. Hall, J.W. Duvall, V. J. Williams, R. J. Workman, W. B. Matthews, and D. A. Foreman for performing the necessary lab-scale process simulations to complete this task.

The authors also wish to thank W. T. Riley, T. L. White, D. R. Best, K. L. Wyszynski, and B. G. Wall for their efforts and dedication in analyzing the majority of the process samples in the face of very tight deadlines. Sample analysis assistance was also provided by SRNL Analytical Development personnel including T. L. White, A. A. Ekechukwu.

The authors wish to thank M. F. Williams, M. S. Williams, and J. M. Pareizs in preparing the offgas instruments for these runs and for data analysis at the completion of these runs.

The authors wish to acknowledge DOE's Office of Environmental Management for financial support and the Defense Waste Processing Facility/Saltstone Facility Engineering organization for their program sponsorship of this research.

EXECUTIVE SUMMARY

Savannah River Remediation plans to add strip effluent to the Sludge Receipt and Adjustment Tank (SRAT) and/or the Slurry Mix Evaporator (SME) during processing in the Defense Waste Processing Facility (DWPF). At the present time, strip effluent is added only to the SRAT, but this flowsheet change is planned to allow more flexibility in processing the large volume of strip effluent produced by the Modular Caustic-side Solvent Extractant Unit (MCU) or the Salt Waste Processing Facility (SWPF).

Four process demonstrations of the coupled flowsheet for SRAT and SME cycles were performed using SB8-Tank 40 simulant. These runs were patterned after run SB8-D5 (a previous coupled experiment completed in developing the SB8 flowsheet and utilizing the same sludge simulant, addition of Actinide Removal Product (ARP), and acid addition). Differences from run SB8-D5 included much higher noble metal concentrations and very long strip effluent addition times (equivalent to 38,000 gallons of Strip Effluent, including 30,000 gallons of Strip Effluent added to the SME), which combined to make this a very challenging set of runs.

The main difference between the runs was that three strip effluent combinations (original solvent based on BobCalix/nitric acid, new solvent based on MaxCalix/boric acid, and a blend of the two) were used. A fourth run was performed without solvent and using water as the strip effluent solution to see whether the solvent or strip effluent acid had any impact on processing, particularly hydrogen generation.

Although allowing a large addition of strip effluent to either the SRAT or SME offers obvious operational advantages, it also requires a longer time at temperature than typical DWPF batches, which may lead to higher hydrogen generation, higher ammonia production, higher formate destruction, lower Reduction/Oxidation (REDOX) Ratio, higher potential for foaming and coil fouling, and higher yield stress and consistency. Although these impacts could be carefully controlled, consistent processing (same sludge, ARP, strip effluent, and decon water volume for each SRAT and SME batch), should lead to consistent product chemistry. Processing at the maximum volumes of strip effluent, whether in the SRAT, SME or both increases the likelihood of the process problems listed above and may require remediation of the SME product with nitric or formic acid to achieve the desired glass REDOX. Due to the high pH of the SME product leading to higher yield stress and consistency, the melter feed pump may have more difficulty feeding to the melter without dilution.

Some of the highlights of the testing are summarized below:

- The destruction of formate was very high in all runs, but especially high in the two runs with the highest hydrogen generation. The SME formate destruction varied from 29.3 to 70.7% for the four runs, much higher than the 2% measured in a similar run during SB8 blend qualification. This led to a high generation of CO_2, which could increase the potential for foamovers.
- Due to the high anion destruction rates, and the fact that formate and nitrate destruction happens at different rates, the resulting SME product REDOX was much more oxidizing than targeted. In all four tests, the SME product would have required remediation with added formic acid to meet the REDOX target. If a SME product in DWPF was remediated, it would require a remediation plan to be drafted to add formic acid, resampling and reanalysis of the SME to demonstrate that the REDOX target was met before transferring the SME product to the MFT. After remediation of the SME product in DWPF, the next SME batch might be even higher in hydrogen generation due to the addition of fresh formic acid for remediation.
- The pH of the SRAT and SME products (9-10 for SRAT products, 10 for SME products) were very high compared to typical simulant testing. The high pH SME products typically are significantly thicker rheologically. The long processing times and high noble metal concentrations were responsible for the high anion destruction and high product pH. Note that

although the equivalent of 30,000 gallons of strip effluent was added during SME processing, the pH of the SME product was almost the same for the three runs with acid in the strip effluent and the run with no added acid.

- It should be noted that in two of the runs, one of the two heating rods used was likely responsible for the high hydrogen generation and rod fouling. Heating rod T8 was very hot relative to the Heating rod T4, which would lead to increased fouling and hydrogen generation. Heating rod T8 averaged more than 11˚C hotter than heating rod T4 during run SB8-D6 and 12˚C hotter during run SB8-D8. Material fouling the heating rods requires an increase in power to the heating rod to maintain the boilup rate, which in turn causes higher local temperature at the point of fouling. With hydrogen generation having a strong relationship to temperature, fouling can cause a significant increase in hydrogen generation.
- Fouling of the heating rods in the SME cycles was noted in the two experiments with the highest hydrogen generation rates. This led to longer processing times for both of these experiments as the targeted boilup rate could not be maintained.
- Very high hydrogen generation was experienced in two of the four runs (SB8-D6 and SB8-D8). The hydrogen generation was so high in run SB8-D6 that the SRAT purge was used for most of the SME cycle to keep from exceeding the 1 volume % hydrogen limit. The peak SME hydrogen generation was 0.568 and 0.229 lb/hr DWPF Scale respectively in runs SB8-D6 and SB8-D8. Both runs had a peak hydrogen generation rate higher than the 0.223 lb/hr DWPF SME limit.
- One of the objectives of the testing was to determine the impact of the three combinations of strip acid and solvent on processing, especially hydrogen generation. Because of the wide variability between the two rigs, no conclusion on this impact can be drawn based on this study.
- There was significant ammonia generation in these runs.
- The calculated pH of the SMECT condensates was 1.3-1.7, suggesting that no nitric acid addition is necessary to control the SMECT pH from 1 to 3. Eliminating the nitric addition to the SMECT may minimize mercury dissolution.

The testing performed was very aggressive, with high noble metals concentrations and very large strip effluent additions, which led to long processing times and high anion destruction. The objective was that this testing could demonstrate that this flowsheet change could be processed for any future sludge batch, even with very high SWPF strip effluent volumes. Based on the testing completed, an endorsement of the flowsheet change for adding strip effluent to the SME is not currently warranted.

Although the planned testing did not provide a strategy for processing strip effluent in the SME, there are likely some sludge batches (with lower noble metal activity than that tested) where processing strip effluent in the SME would be feasible. In addition, smaller additions of strip effluent in the SME are also more feasible than the 15-30,000 gallons tested.

This testing is a reminder that the chemistry throughout DWPF SRAT and SME processing is complicated and can lead to variable results depending on the temperature of the heating surface, the time for processing, the boilup rate, acid addition rate, etc. It also demonstrates the need for completing nearly identical processing with each SRAT and SME batch to produce melter feed that is at the expected REDOX target. Longer processing at temperature is expected to lead to more oxidizing melter feed and will likely require remediation of the SME product with formic acid. The time it takes to develop a remediation plan, add formic acid and resample/reanalyze the SME product may negate any time savings expected from using idle SME time to process strip effluent.

This flowsheet change to add strip effluent in the SRAT or SME would be much easier to implement with the nitric-glycolic flowsheet than the nitric-formic flowsheet. The lack of hydrogen generation and lower reaction rates for destruction of glycolate and nitrate make producing melter feed without remediation

more likely. The higher processing volumes expected after startup of SWPF will make processing in the SRAT and SME much longer and will likely be easier to process using the nitric-glycolic flowsheet. Future testing to implement the Strip Effluent to SME flowsheet should be performed using the nitric-glycolic flowsheet.

Additional testing should be completed prior to implementing the flowsheet change in DWPF:

1. Repeat the experiments for each sludge batch with sludge batch levels of noble metals and mercury added to the best sludge simulant for that sludge batch.
2. Complete experiments using planned sludge batch maximum amounts for sludge, ARP, strip effluent, and acid stoichiometry. If SWPF is not operational, do not use SWPF volumes of ARP and strip effluent for testing.
3. Test adding strip effluent to the SME using the nitric-glycolic flowsheet.
4. The testing should be completed using any lessons learned from this testing (see below).

The following improvements to SRNL testing methodology is recommended and will be implemented in future experiments with high strip effluent volumes in the SRAT or SME:

1. Repeat experiments using new, temperature-matched heating rods to minimize testing differences from probe to probe. Perform a water run before testing to demonstrate a low measured differential temperature between rods.
2. Complete scoping experiments before beginning the experimental set to determine the anion destruction in order to be able to accurately predict the REDOX in subsequent experiments. This would require the anion destruction during segments of the cycles such as strip effluent addition in SRAT or SME; decon water evaporation in SME, and process frit slurry evaporation to more accurately predict the final melter feed composition.
3. Complete analysis and review data for the SME product and resulting glass REDOX before performing the next experiment in the series.

TABLE OF CONTENTS

LIST OF TABLES

LIST OF FIGURES

LIST OF ABBREVIATIONS

ACTL	Aiken County Technology Laboratory
AD	Analytical Development
ARP	Actinide Removal Process
CPC	Chemical Process Cell
CQ	Caustic quench
DWPF	Defense Waste Processing Facility
FAVC	Formic Acid Vent Condenser
FTIR	Fourier Transform Infrared (Spectrometry)
GC	Gas Chromatograph
HMDSO	Hexamethyldisiloxane
IC	Ion Chromatograph
ICP-AES	Inductively Coupled Plasma-Atomic Emission Spectroscopy
KMA	Koopman Minimum Acid Equation
SE	Modular Caustic-side solvent extraction Unit
MS	Mass Spectrometer
MWWT	Mercury Water Wash Tank
m/z	MS mass-to-charge ratio
NOx	$NO + NO_2$
NyOx	$NO + NO_2 + N_2O$
PEG	Poly(ethylene)glycol
PSAL	Process Science Analytical Laboratory
PSED	Polymeric siloxane ethoxylated derivative
R&D	Research and Development
REDOX	Reduction-Oxidation potential
SE	Strip Effluent
SEFT	Strip Effluent Feed Tank
SME	Slurry Mix Evaporator
SMECT	Slurry Mix Evaporator Condensate Tank SRAT
SRAT	Sludge Receipt and Adjustment Tank
SRNL	Savannah River National Laboratory
SWPF	Salt Waste Processing Facility

TIC	Total Inorganic Carbon
TMS	Trimethylsilanol
TOC	Total Organic Carbon
TTR	Task Technical Request
TSR	Technical Safety Requirement
TTQAP	Task Technical & Quality Assurance Plan

1.0 Introduction

Savannah River Remediation (SRR) plans to add strip effluent to either the Sludge Receipt and Adjustment Tank (SRAT) or Slurry Mix Evaporator (SME) during processing in the Defense Waste Processing Facility (DWPF). At the present time, strip effluent is added only to the SRAT, but this flowsheet change is planned to allow more flexibility in processing the large volume of strip effluent (SE) produced by the Modular Caustic-side Solvent Extractant Unit (MCU) or Salt Waste Processing Facility (SWPF).

SRNL was requested by a DWPF Task Technical Request (TTR) to perform simulant studies to support a flowsheet change to add strip effluent to either the SRAT or SME.[1] This task was technical baseline research and development, but the requirements of DOE/RW-0333P were not applicable. SRNL developed a task technical and quality assurance plan (TTQAP) for the proposed scope of work.[2] E7 procedures relevant to this task are outlined in the quality assurance (QA) matrix of the approved TTQAP. Details of simulant preparation were recorded in controlled laboratory notebook SRNL-NB-2012-00108. Details of the process simulations were recorded in electronic laboratory notebook O7787-00055-16. These notebooks contain sufficient data to reproduce the simulant preparation and simulant testing as well as containing processing data recorded manually every twenty minutes during DWPF process simulations.

Details of simulation liquid and slurry sample analyses (final results only presented in this report) were recorded in controlled laboratory notebooks held by either the Process Science Analytical Laboratory (PSAL) or SRNL Analytical Development (AD). Special data not recorded by the above methods, such as rheological flow curves, are included in the main body or the appendix (rheology) of this report. Software used in performing the DWPF simulations conforms to the requirements of E7, 5.0, Software Engineering and Control. Additional details related to QA and the implementing procedures within SRNL can be found in the QA matrix pages at the end of the TTQAP[2].

Four process demonstrations of the coupled flowsheet for SRAT and SME cycles were performed for the sludge-only flowsheet using SB8-Tank 40 simulant. These runs were patterned after run SB8-D5 (same sludge simulant, same addition of Actinide Removal Product or ARP, same acid addition). The results of the above four SRAT/SME tests are documented in the body of this report below (Section 3.2).

2.0 Experimental Procedure

Four lab-scale SRAT/SME runs were performed with Tank 40 simulants. Testing was completed at the Aiken County Technology Laboratory (ACTL). The four SB8 SRAT/SME runs occurred in pairs (the first pair was completed the week of November 11, 2014 and the second pair was completed the week of December 1, 2014. All runs were performed using round-the-clock operations.

The SRAT cycles were completed as coupled processing, meaning that a sludge, ARP, and strip effluent simulant were added during the SRAT cycle. The scaled equivalent of 6,000 gallons of SB8-D sludge, 1,050 gallons of ARP, and 8,000 of gallons strip effluent were added during SRAT processing. The only change from run to run was the strip effluent acid and the added solvent.

The SME cycles were completed with both added process frit and strip effluent. No previous testing has included strip effluent in the SME cycle. The strip effluent added in two separate steps to simulate the scaled addition of 30,000 gallons of strip effluent. 15,000 gallons of strip effluent was added to the SRAT product at the beginning of the SME cycle, followed by the addition of process frit and the concentration of the SME product. Samples were pulled at this point (SME #1 samples). 15,000 additional gallons of

strip effluent was added to the SME#1 product to complete the SME cycle. Samples were pulled at this point (SME #2 samples).

2.1 Sample Analytical Methods

The automated data acquisition system developed for the 4-L lab-scale SRAT/SME was used to collect electronic data on a computer. Collected data included SRAT slurry temperature, bath temperatures for the cooling water to the SRAT condenser and Formic Acid Vent Condenser (FAVC), slurry pH, SRAT mixer speed and torque, air and helium purge flows (helium is used as an internal standard and is set to 0.5% of the nominal SRAT air purge flow), temperatures in the SRAT condenser, FAVC, and ammonia scrubber, the individual temperatures of the two heating rods, the total rod current draw, and the total rod power consumption (to permit calculation of time-dependent heat transfer coefficients between the rods and slurry).

For slurry samples, anions were determined by ion chromatography (IC) using the new caustic quench method developed by Tom White[3]. Approximately 10 mL of sample is pulled in a 15 mL sample bottle and weighed. Two mL of 50 wt% sodium hydroxide are added to the sample bottle and reweighed. A 100-fold weighted dilution of the caustic quenched sample with water is followed by filtration to remove the remaining insoluble solids. IC results were obtained on the SRAT and SME products. For condensate and supernate samples, anions were diluted with water prior to analysis. SRAT and SME product slurry samples were submitted to PSAL for mercury analysis by ICP-AES. Simulants, SRAT products, and SME products were analyzed by PSAL for slurry and supernate density using the Anton-Parr DMA-4500 density instrument.

Four SRAT and eight SME product samples were submitted to AD for total inorganic carbon (TIC) and total organic carbon (TOC) analysis (12 total samples). Samples from the ammonia scrubber reservoir vessel and SRAT and SME products were analyzed by AD using cation chromatography for the ammonium ion.

As a part of the testing, samples of the SRAT and SME dewater condensate were analyzed for the standard suite of elements by ICP-ES, including silicon. Antifoam molecules terminate in end groups composed of multi-methyl siloxanes, so silicon is a potential marker for volatilized or steam stripped antifoam lost from the SRAT slurry. The test cannot discriminate between silicon derived from antifoam and silicon from the SiO_2 in the slurry, but it can bound potential antifoam losses to the condensate related to Si.

2.2 Chemical Process Cell

The 4-L lab-scale SRAT equipment was used for these tests. A photo of a typical 4-L rig is shown in Figure 1. The SRAT vessel was insulated when at processing temperatures. The trimmed SRAT receipt volume was about 3.0 L.

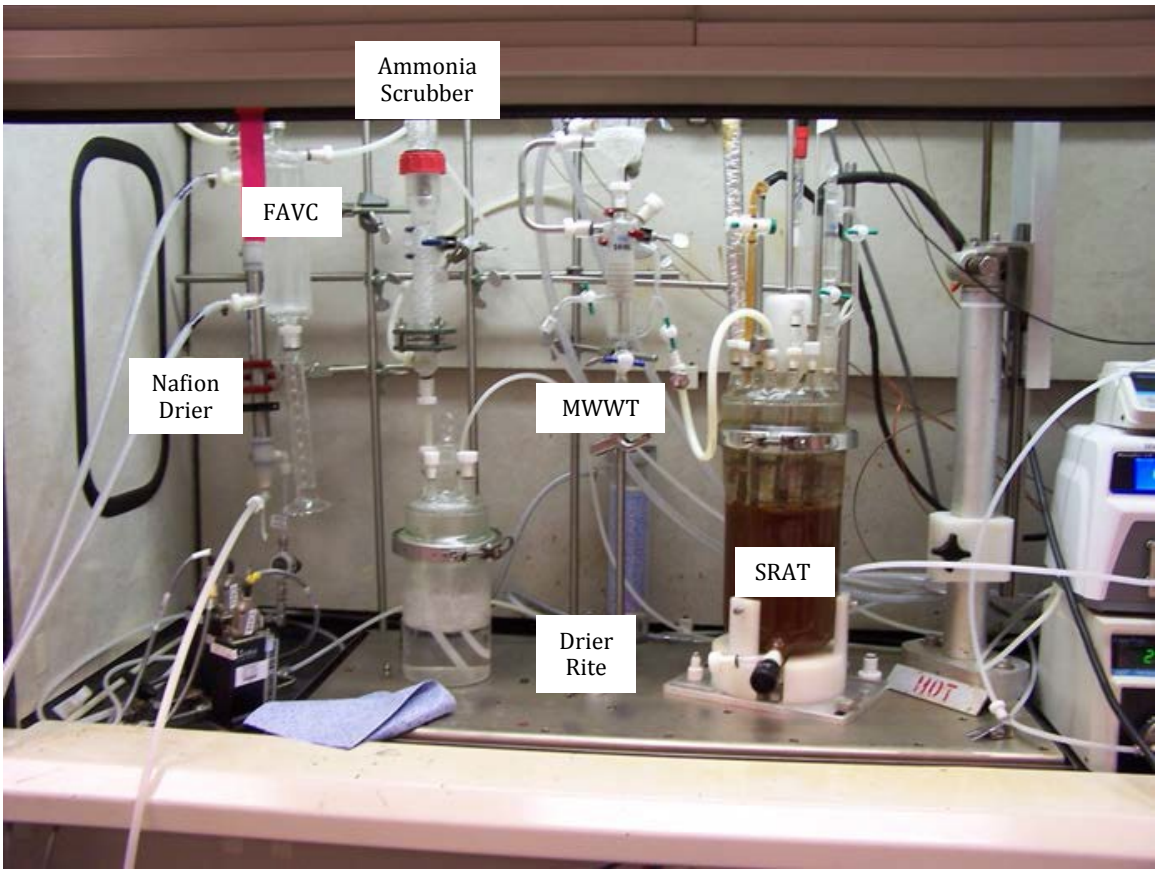

Figure 2-1. Lab-scale SRAT Apparatus

The modified lab-scale SRAT rig design was used (off-center agitation, heating rods). More details about the new design are in the CPC equipment set-up reference[5]. The air purges to the rig equipment were treated by the FTIR air purifier to remove almost all moisture and CO_2.

The reservoir below the ammonia scrubber was charged with a solution of 749 g of de-ionized water and 1 mL of 50 wt.% nitric acid. Condensates from the SRAT and SME were not drained into this reservoir. The dilute acid reservoir solution was recirculated by a MasterFlex driven Micropump gear pump at about 300 mL per minute to a spray nozzle at the top of the scrubber packing section. The main purpose of the lab-scale ammonia scrubber is to collect ammonia vapor in the SRAT/SME condenser off-gas for quantification of ammonia generation, whereas the main purpose of the DWPF SRAT and SME ammonia scrubbers is to prevent build-up of ammonium nitrate crystals in the off-gas system.

Initial simulant acid calculations were based on the Koopman minimum acid (KMA) requirement equation (all terms have units of moles/L slurry).

$$\frac{moles\ acid}{L\ slurry} = base\ equivalents + Hg + soluble\ TIC + nitrite + 1.5 \times (Ca + Mg + Mn)$$

A stoichiometric factor of 120% was used in all tests and included Actinide Removal Process (ARP) slurry and dilute acid from the SE added in both the SRAT and SME. A parallel acid calculation was also performed using the current DWPF algorithm (Hsu equation) for comparison[7]:

$$\frac{moles\ acid}{L\ slurry} = [base\ equivalents\ + 2 \times total\ TIC + 0.75 \times nitrite + 1.2 \times Mn + Hg]/L$$

The results of the acid calculations for the trimmed simulants are summarized in Table 2-1. The table also includes the actual acid additions made based on 120% of the Koopman minimum acid equation and the equivalent DWPF stoichiometric factors (percent) to go from the DWPF acid equation (Hsu equation) values to the actual acid additions.

Table 2-1. Stoichiometric Acid Calculation Results, mol acid/L trimmed slurry

Slurry	Hsu Eqn. moles/L	Hsu Eqn. DWPF	Koopman Min. moles/L	KMA Factor
SB8-D	1.80	125%	1.88	120%

The calculated stoichiometry by both the Hsu and KMA equations were based on the sum of the sludge simulant acid demand plus the ARP simulant acid demand.

Total acid demand was partitioned between formic and nitric acids using the current reduction – oxidation (REDOX) equation.[4] The REDOX target was set to 0.20 $Fe^{2+}/\sum Fe$ for SB8-D6 and SB8-D7 and 0.10 for SB8-D8 and SB8-D9. Assumptions of 28.4% formate loss and of 8.0% nitrite-to-nitrate conversions were also made to allow the REDOX prediction to be performed. Oxalate was assumed to be 10% destroyed. The collective anion change assumptions were based on the earlier SB8-D5 testing[3].

Scaled design basis DWPF SRAT/SME processing conditions were generally used. The SRAT and SME cycles, however, did not have a heel from a prior batch. R&D directions were prepared for each run and used to supplement the standard SRNL procedure for non-radioactive CPC simulations.[5]

SRAT Cycle

- Sludge, mercuric oxide, and noble metal trim chemicals were added to the vessel.
- The SRAT air purge scaled was to 230 scfm in DWPF.
- A 100 ppm antifoam addition was made prior to boiling.
- The SRAT was brought to boiling, ARP added, and the SRAT was dewatered.
- A SRAT receipt sample was pulled.
- The SRAT was cooled to 93 ºC.
- A 200 ppm antifoam addition was made and nitric acid was added at 93 °C at 2 gpm scaled.
- A 100 ppm antifoam addition was made and formic acid was added at 93 °C at 2 gpm scaled.
- A 500 ppm antifoam addition was made prior to going to boiling following acid addition.
- Boiling assumed a condensate production rate of 5,000 lb/hr at DWPF scale.
- SRAT dewatering took about 3-4 hours to produce a 27 wt. % total solids slurry.
- SE addition followed dewatering. SE addition/dewatering replaced the majority of the reflux time in the coupled flowsheet test.

SME Cycle

- The SME air purge was scaled to 74 scfm in DWPF.
- A 100 ppm antifoam addition was made at the start of the SME cycle.
- Canister decontamination water additions and dewaterings were not simulated.

- 15,000 gallons of SE at DWPF scale was added at the beginning of the SME cycle. This is almost 24 hours of SE addition and dewatering.
- Two frit 418-water-formic acid additions were made targeting 36% waste loading.
- The SME was dewatered following each frit slurry addition.
- The final SME solids target was 45 wt.%. Samples were pulled (SME#1).
- 15,000 gallons of SE at DWPF scale was added at the end of the SME cycle. This is an additional 24 additional hours of SE addition and dewatering (SME#2).
- The final cycle was considered complete and samples were pulled.

SRAT and SME product slurries were sampled once the vessel contents had cooled to 90° C while still mixing.

Additional SRAT and SME product samples were taken from each run after the product had cooled further for compositional and solids analyses as well as for rheological characterization of each slurry. The MWWT and FAVC were drained and the condensates weighed after both the SRAT and SME cycles. Elemental mercury was separated from the aqueous phase in the post-SRAT MWWT sample when possible, and the mass of the mercury-rich material determined.

Gas chromatograph off-gas data were scaled to DWPF flow rates. The calculation methodology has been previously documented.[6] An internal standard flow is established with helium. Other gas flow rates are determined relative to helium by taking the ratio of the two gas volume percentages times the helium standard flow. These results are normally scaled by the ratio of 6,000 gallons of fresh sludge divided by the volume of fresh sludge in the simulant SRAT charge. In the SB8 flowsheet simulations, the scaling was performed assuming the volume following pre-concentration was equivalent to 6,000 gallons at DWPF scale. Identical logic was used to convert MS off-gas data to DWPF-scale flow rates.

Noble metals were trimmed at 125% of the HM values while mercury was trimmed at 1% total solids basis. The ARP slurry was assumed to have no noble metals and mercury based on sample results that show negligible entrained sludge solids content in the slurry (slurry is essentially MST and salt solution). The targets are summarized in Table 2-2. The potential for hydrogen generation was impacted due to the high noble metal concentration and long processing times.

Table 2-2. Mercury and Noble Metal Targets

Hg	Rh	Ru	Ag	Pd
0.9840	0.0445	0.2542	0.0164	0.0925

Values given in Table 2-2 are based on the combined total solids (sludge solids plus ARP solids). All four of the runs started from the same untrimmed simulant and had identical insoluble species.

Table 2-3. Targeted Mass of Sludge, ARP and SE Added to Each Test

Component	ACTL, ml	ACTL, g	DWPF, gal
Sludge pre-concentration	3,233	3,750	6,820
Sludge post-concentration	2,845	3,300	6,000
ARP	529	557	1,050
SRAT SE	3,793	3,797	8,000
SME#1 SE	7,112	7,119	15,000
SME#2 SE	7,112	7,119	15,000
Total SE	18,017	18,035	38,000

2.3 Offgas Sampling Equipment

Raw chromatographic data were acquired by gas chromatograph (GC) on samples of the FAVC exit off-gas stream using a separate computer interfaced to the data acquisition computer. The chilled off-gas leaving the FAVC was passed through a Nafion dryer in counter-current flow with a dried air stream to reduce the moisture content at the GC inlet. The dried, chilled off-gas stream was sampled by GC from the beginning of heat-up to temperature to start the SRAT cycle through most of the cool down following the SME cycle. Sampling frequency was approximately one chromatogram every four minutes.

Each experiment had a dedicated Agilent (or Inficon) 3000A dual column micro GC. Column-A can collect data related to He, H_2, O_2, N_2, NO, and CO, while column-B can collect data related to CO_2, N_2O, and water. The GCs were calibrated with a standard calibration gas containing 0.510 vol% He, 1.000 vol% H_2, 20.10 vol% O_2, 50.77 vol% N_2, 25.1 vol% CO_2 and 2.52 vol% N_2O. The calibration was verified prior to starting the SRAT cycle and after completing the SME cycle. Room air was used to give a two point calibration for N_2. The GC's were baked out before and between runs. During analysis of the GC data, the N_2 and O_2 concentrations were corrected with a linear correction so that the concentrations of N_2 and O_2 matched air at the beginning and end of the runs.

GC data were supplemented by parallel Extrel Core mass spectrometer (MS) readings on FAVC exit off-gas samples. Samples originated from the same part of the off-gas system as the GC samples. Samples were drawn from the off-gas lines with diaphragm pumps. The single MS can alternately monitor off-gas compositions from both hoods using its automated sampling system that switches between the samples from the two hoods. There is some drift in the MS measurement of H_2, so a linear interpolation correction versus time may be applied to the data using the pre- and post-run calibration check data.

The MS obtains data by molecular weight of ionized fragments of the original molecules. The data can be reconstructed to give quantitative concentrations for H_2, He, N_2, O_2, NO, NO_2, CO_2, and Ar. The MS signal intensities at several masses are also measured, as shown in Table 2-4. These intensity measurements accurately follow the concentrations of the species shown, but the values recorded are not the actual concentrations. The actual concentrations would be these intensity values times an unknown calibration factor.

The compounds analyzed are specified by the MS run method and are calibrated using set of six different calibration gases. GC or FTIR N2O data is used to correct for N_2O interference on the MS measured values of NO, CO_2, and N_2. The MS takes a reading every 9-10 seconds, so the time resolution of events is much sharper than that provided by the GC. The MS measures one sample for about 106-107 sec (12 readings), then there is a 29 sec delay as the sample is switched to the other sample, then that sample is analyzed for 106-107 sec; this process repeats indefinitely.

Table 2-4. Mass Spectrometer Organic Masses Measured

Mass	Indicative of:
57	Isopar™ L
58	Isopar™ L
59	Isopar™ L
73	HMDSO from Antifoam
75	TMS from Antifoam
131	HMDSO from Antifoam
147	HMDSO from Antifoam
148	HMDSO from Antifoam

The MS obtains data on one hood for about 2.2 minutes, then switches to the other hood for the same time, then switches back, and so on, so there are about 20 MS data sets per GC chromatogram on both hoods. Roughly 14,000 composition measurements were obtained during the tests.

GC and MS data were further supplemented by a MKS Fourier Transform Infrared (FTIR) spectrometer for two of the runs (SB8-D6 and SB8-D8). The FTIR is connected to the two SRAT/SME off-gas systems like the MS, but it is manually valved into one or the other for the duration of the run. Therefore, only two sets of FTIR data were obtained from the four tests. The FTIR can quantitatively measure CO_2, NO, NO_2, N_2O, H_2O, NH_3, and hexamethyldisiloxane (HMDSO) concentrations. Water and ammonia are not actually measured because these are removed by the ammonia scrubber and the Nafion dryer. The FTIR also qualitatively measured the concentration of Isopar™ L. The FTIR was also set to measure dodecane, which has a spectrum similar to Isopar™ L, so qualitative and relative measurements could be made. The FTIR obtained data roughly every 15 seconds.

After the runs were complete, an extensive data review was completed of all the offgas data from the GCs, MS and FTIR. The most reliable data for each offgas component was used but data from all three offgas analyzers were included in the analysis. Since the three analyzers sampled at different frequencies, the data were interpolated to allow a comparison of all data on the same time scale. Conversion of all data to the same time scale also allowed the cumulative amount of each gas to be calculated versus time when combined with interpolated process air and helium purge rates. The helium purge rates were adjusted slightly so that the calculated concentration of He at the beginning and end of the runs matched the concentrations measured by the GC.

2.4 Quality Assurance

Requirements for performing reviews of technical reports and the extent of review are established in manual E7 2.60. SRNL documents the extent and type of review using the SRNL Technical Report Design Checklist contained in WSRC-IM-2002-00011, Rev. 2.

3.0 Results and Discussion

3.1 Simulant Preparation and Characterization

The sludge simulant, ARP simulant and Strip Effluent Simulant are discussed in this section.

3.1.1 Sludge Simulant Sample Results

The SB8 simulant used in this testing was also used in the SB8-Tank 40 experiments. The preparation and analysis of the SB8-D simulant is discussed in section 3.1 of the SB8 Flowsheet Report[5]. The simulant composition is summarized in Table 3-1.

Table 3-1. SB8-D Sludge Simulant Composition

Element	Result	Units	Analyte	Results	Units
Al	8.1	wt% calcined solids basis	sodium	1.27	Supernate M
Ca	1.33	wt% calcined solids basis	nitrite	0.34	Supernate M
Ce	0.28	wt% calcined solids basis	nitrate	0.16	Supernate M
Cr	0.12	wt% calcined solids basis	chloride	<0.003	Supernate M
Cu	0.17	wt% calcined solids basis	sulfate	0.019	Supernate M
Fe	22.4	wt% calcined solids basis	fluoride	<0.03	Supernate M
K	0.14	wt% calcined solids basis	carbonate	0.14	Supernate M
La	0.073	wt% calcined solids basis	aluminate	0.12	Supernate M
Mg	0.29	wt% calcined solids basis	oxalate	0.035	Supernate M
Mn	7.2	wt% calcined solids basis	phosphate	<0.006	Supernate M
Na	20	wt% calcined solids basis	potassium	0.007	Supernate M
Ni	2.31	wt% calcined solids basis	total solids	18.72	wt% slurry basis
P	0.091	wt% calcined solids basis	insoluble solids	10.19	wt% slurry basis
Pb	0.013	wt% calcined solids basis	soluble solids	8.53	wt% slurry basis
S	0.36	wt% calcined solids basis	calcined solids	14.36	wt% slurry basis
Si	1.46	wt% calcined solids basis	slurry density	1.160	g/mL
Ti	0.021	wt% calcined solids basis	supernate density	1.076	g/mL
Zn	0.053	wt% calcined solids basis	base equivalents	0.856	mol/L slurry
Zr	0.13	wt% calcined solids basis	TIC	2,152	mg C/kg slurry
Hg	0.984*	Wt% total solids basis	*Calculated, not measured		

3.1.2 ARP Simulant Sample Results

The ARP simulant used in this testing was also used in the SB8-Tank 40 experiments. The preparation and analysis of the ARP simulant is discussed in section 3.1 of the SB8 Flowsheet Report. The simulant composition is summarized in Table 3-2.

Table 3-2. ARP Simulant Composition

Element	Result	Units	Analyte	Results	Units
Al	1.27	wt% calcined solids basis	sodium	1.27	Supernate M
Ca	0.00	wt% calcined solids basis	nitrite	0.34	Supernate M
Ce	0.00	wt% calcined solids basis	nitrate	0.16	Supernate M
Cr	0.00	wt% calcined solids basis	chloride	<0.003	Supernate M
Cu	0.00	wt% calcined solids basis	sulfate	0.019	Supernate M
Fe	0.00	wt% calcined solids basis	fluoride	<0.03	Supernate M
K	0.93	wt% calcined solids basis	carbonate	0.14	Supernate M
La	0.00	wt% calcined solids basis	aluminate	0.12	Supernate M
Mg	0.00	wt% calcined solids basis	oxalate	0.035	Supernate M
Mn	0.00	wt% calcined solids basis	phosphate	<0.006	Supernate M
Na	41	wt% calcined solids basis	potassium	0.007	Supernate M
Ni	0.00	wt% calcined solids basis	total solids	16.5	wt% slurry basis
P	0.00	wt% calcined solids basis	insoluble solids	9	wt% slurry basis
Pb	0.00	wt% calcined solids basis	soluble solids	7.5	wt% slurry basis
S	0.58	wt% calcined solids basis	calcined solids	12.6	wt% slurry basis
Si	0.03	wt% calcined solids basis	slurry density	1.138	g/mL
Ti	17.72	wt% calcined solids basis	supernate density	1.066	g/mL
Zn	0.00	wt% calcined solids basis	base equivalents	0.739	mol/L slurry
Zr	0.00	wt% calcined solids basis	TIC	700	mg C/kg slurry

3.1.3 Strip Effluent Composition

The only planned difference between these runs was the composition of strip effluent fed to each run. To simulate the entrainment of solvent in the strip effluent, 87 mg/kg of solvent was slowly metered in using a syringe pump. The stripping acid and solvent used for each run is summarized in Table 3-3.

Table 3-3. Strip Effluent and Solvent Used in Testing

Component	SB8-D6	SB8-D7	SB8-D8	SB8-D9
Strip Effluent	Nitric Acid	DI Water	Boric Acid	Boric Acid
Solvent	Isopar™ L	None	Isopar™ L	Isopar™ L
Extractant	BobCalixC6	None	MaxCalix	Blend of BobCalix/MaxCalix
Modifier	Cs-7SB	None	Cs-7SB	Cs-7SB
Suppressor	tri-n-octylamine	None	TiDG	Blend of TiDG and tri-n-octylamine

Note: TiDG is N, N', N''- tris(isotridecyl)guanidine

3.2 Results from Flowsheet Simulant Testing

Four Coupled SRAT/SME simulations with ARP addition prior to nitric acid and SE addition after SRAT cycle dewatering, at the start of the SME and at the end of the SME were performed. The unique features of the four runs were summarized in section 2.2. Results from process samples, off-gas analysis, and material balance calculations are organized into the sections below. Note that two sets of SME samples were taken. The first set (SME#1) refers to samples pulled after adding 15,000 gal SE, completing process frit addition and dewatering. The second set (SME#2) refers to samples pulled after adding 15,000 gal SE, completing process frit addition, dewatering, and adding an additional 15,000 gal SE.

3.2.1 SRAT/SME Processing Data

The four runs were complicated due to simulating the coupled processing (added ARP and SE in the SRAT) and due to the extended time for adding SE in the SME. For example, the same pump was used to add nitric acid, formic acid and SE, each with its own addition rate. In addition, solvent was added very slowly to simulate the solvent carryover in the strip effluent.

Four processing issues will be discussed in this section, namely, pH, heat transfer, foamovers, and accumulation of Isopar™ L at non boiling conditions. The four runs were designed to be very similar, with the only difference being the concentration of the very dilute acid and solvent in the strip effluent added.

3.2.1.1 SRAT/SME pH

The pH was measured throughout the SRAT and SME cycle. The amount of nitric and formic acid added to each run is summarized below. The total acid moles added to each run was the same. Each run had a different strip effluent and solvent. The pH is impacted by the moles of acid added, the amounts of condensed acids returned to the SRAT during dewater, and the amount of formic and nitric acid consumed during processing. The acid added with the strip effluent was approximately 6.5% of the total acid added in runs SB8-D7, SB8-D8 and SB8-D9. No acid was added with the strip effluent in run SB8-D7. The final pH of the SRAT and SME products is summarized in Table 3-4.

Table 3-4. pH of SRAT and SME Products

	SB8-D6	SB8-D7	SB8-D8	SB8-D9
Nitric Acid, mols	1.102	1.102	1.510	1.510
Formic Acid, mols	6.309	6.309	5.839	5.839
Strip Effluent Acid, mols	0.514	0	0.461	0.461
% Acid as strip effluent	6.5	0	5.9	5.9
SRAT Product pH	10.22	9.71	9.19	9.35
SME#1 Product pH	10.23	9.82	10.06	10.21
SME#2 Product pH	9.82	9.86	10.26	10.05

The addition of the strip effluent had little impact on SRAT and SME product pH. The run with no added acid (SB8-D7) had approximately the same pH as the other three runs.

The pH trend for the four runs is summarized in Figure 3-1. Note that all four runs have the same shape trend, going to a minimum pH at the end of acid addition (pH ~5) and the pH slowly increasing until it levels off (pH~9-10). Note also that the pH in the Table 3-4 is measured at room temperature (~20 ˚C) while the data in the graph is corrected to 25 ˚C. The SRAT and SME product pH is very high compared to typical simulant runs (~pH 7-8).

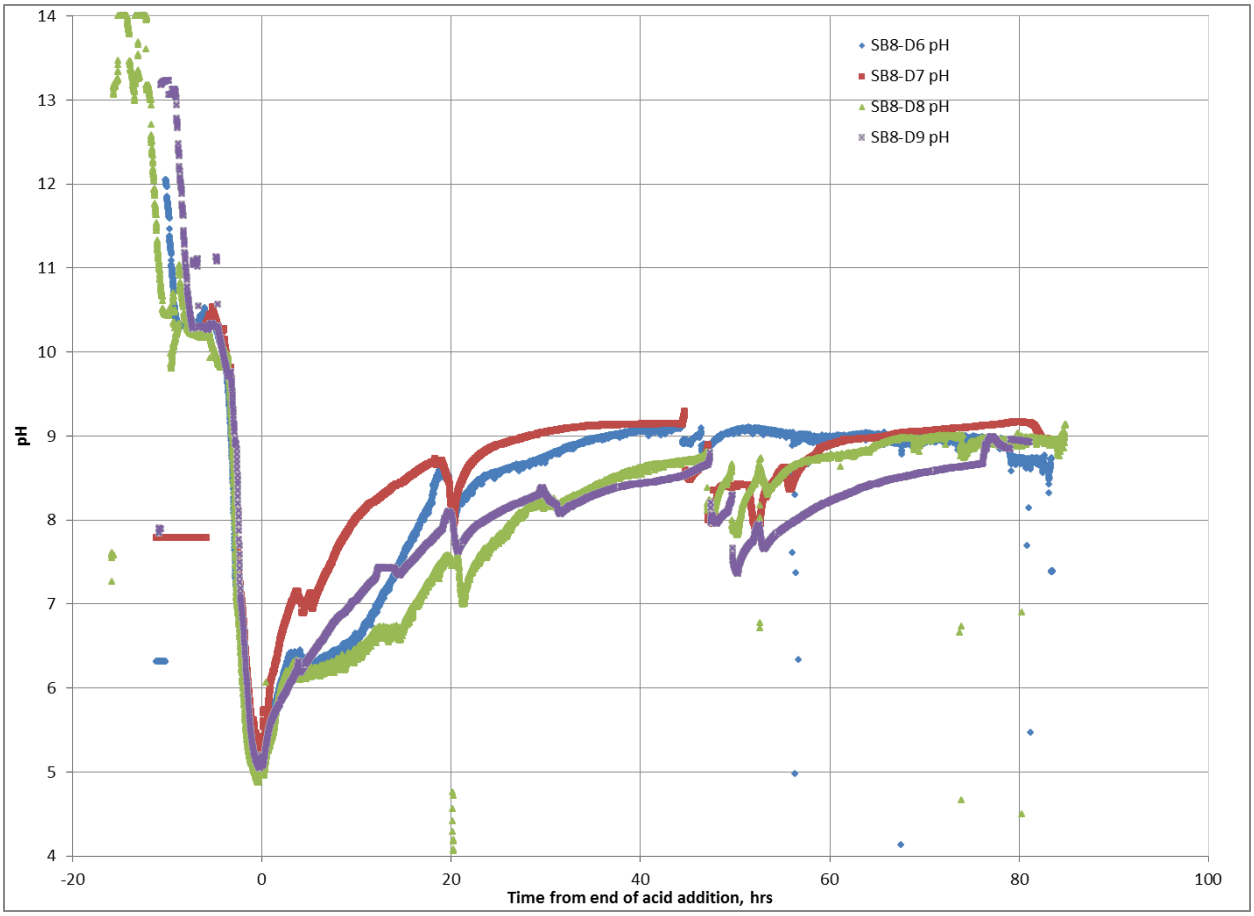

Figure 3-1. pH Trends for SRAT and SME cycles

3.2.1.2 SRAT/SME Heat Transfer

There are two rods that supply heat to the slurry (½" diameter, 4" heated length Watlow heating rods). The heat transfer coefficient is calculated from process data (heat input to rods, temperature difference between the rods and slurry, along with the calculated cross sectional area of the heated section of the rod. A two controller cascade system is used to control either the power (during boiling) or temperature (during acid addition) by supplying the wattage needed to both heating rods without allowing the temperature of the heating rods to exceed 166 ˚C, the maximum temperature of 50 psig steam in DWPF. The actual power supplied to each heating rod is not measured. The typical heat transfer coefficient during processing is 0.15-0.20 $W/cm^2 \cdot ^\circ C$ (Figure 3-2). In addition, it was expected that both heating rods would be the same temperature. In the case for the north hood (SB8-D6 and SB8-D8), the rod temperatures were not the same temperature. The heat transfer rate for each rod was calculated assuming that the power was evenly split between the two rods. The calculated difference in heat transfer coefficient between each pair of rods for each run is summarized in Figure 3-3.

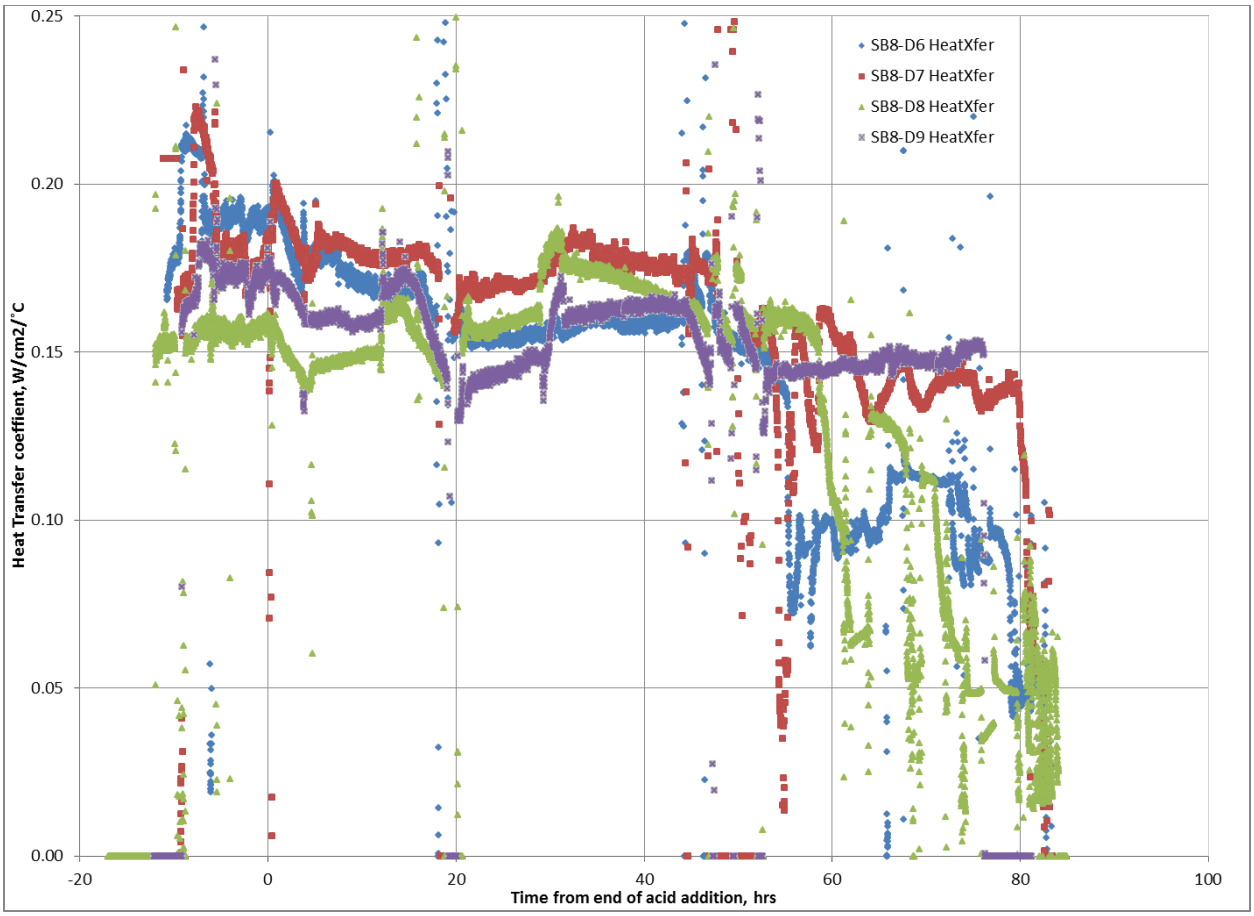

Figure 3-2. Calculated Heat Transfer Coefficient Trends for SRAT and SME Cycles

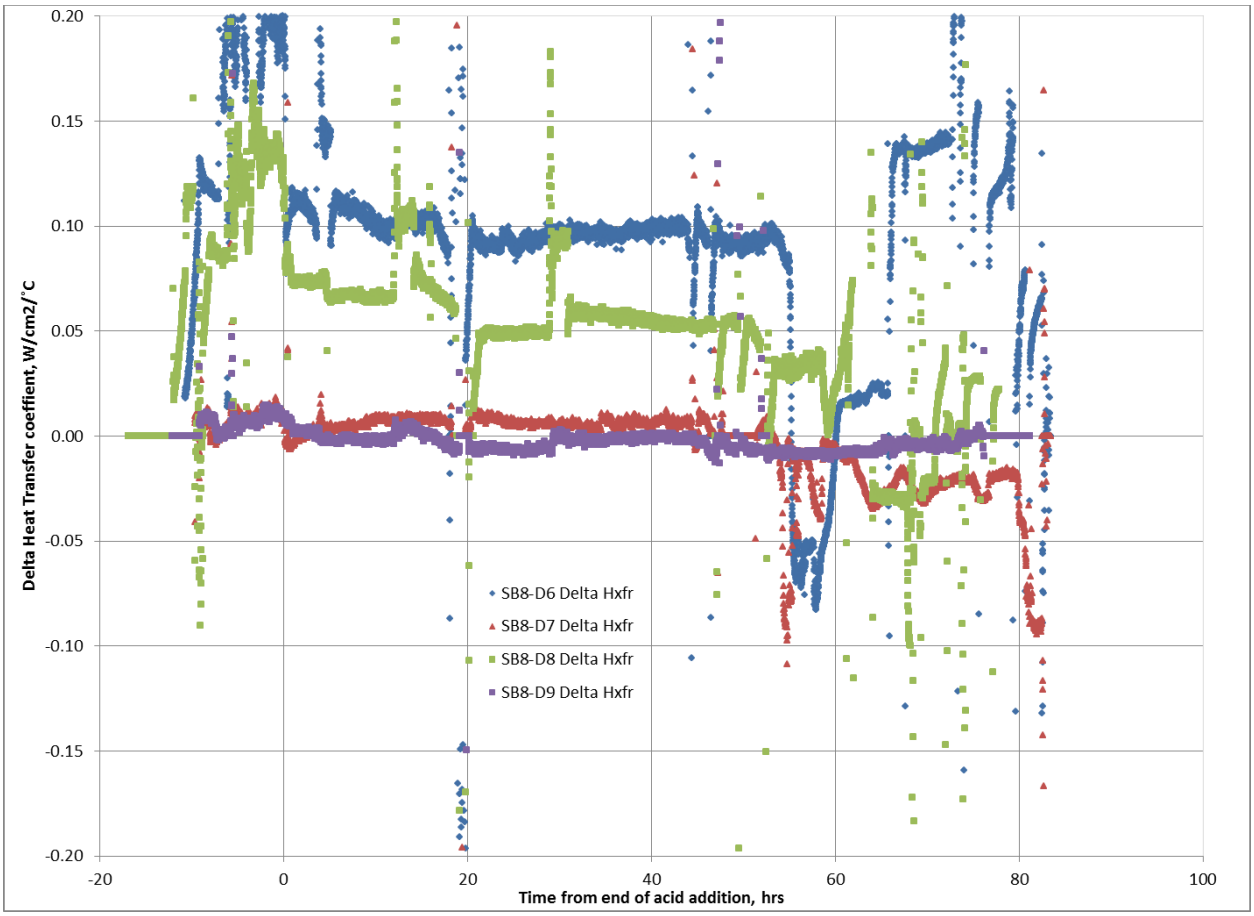

Figure 3-3. Calculated Heat Transfer Coefficient Difference for SRAT and SME cycles

In the south hood, the calculated heat transfer coefficient difference was close to zero, while in the north hood the calculated heat transfer difference was closer to 0.10 W/cm^2·˚C for SB8-D6 and 0.05 W/cm^2·˚C for SB8-D8. This difference is an indication that the hotter rod is fouling. If the fouling layer increases, the heat transfer rate decreases and the rod temperature increases until the rod temperature approaches its limit (usually set at 132 ˚C to prevent reaching the maximum steam temperature of 166 ˚C). Once this temperature limit is exceeded, the power to the rods is limited to prevent the rod temperature from exceeding the limit. As the fouling continues, the power is cut back until boiling cannot be maintained. At this point, the rod is either unplugged (so all the power is added through the other rod), which allows the agitator to scour the fouling off the rod or replaced. The jumps and drops in the heat transfer coefficient difference are indicative of unplugging and replugging one of the two rods in order to maximize the heat input. The poor heat transfer in SB8-D6 and SB8-D8 led to very low boilup rates and extended boiling time to reach the dewater targets.

The fouling not only leads to poor heat transfer, but it also leads to high hydrogen generation rate due to the very high temperatures on the skin of the heating rod. High temperatures lead to higher generation of hydrogen. The two runs with the poor heat transfer also were the two runs with significantly higher hydrogen generation (see section 3.2.2.7 for more details).

Another measure of the rod fouling is the temperature difference between the two heating rods. The data are summarized in Figure 3-4. Note that run SB8-D9 had a very small temperature difference between the

two rods, indicating little or no fouling. Run SB8-D6 had two short periods of fouling. Runs SB8-D6 and SB8-D8 had long periods of fouling throughout the SME cycle.

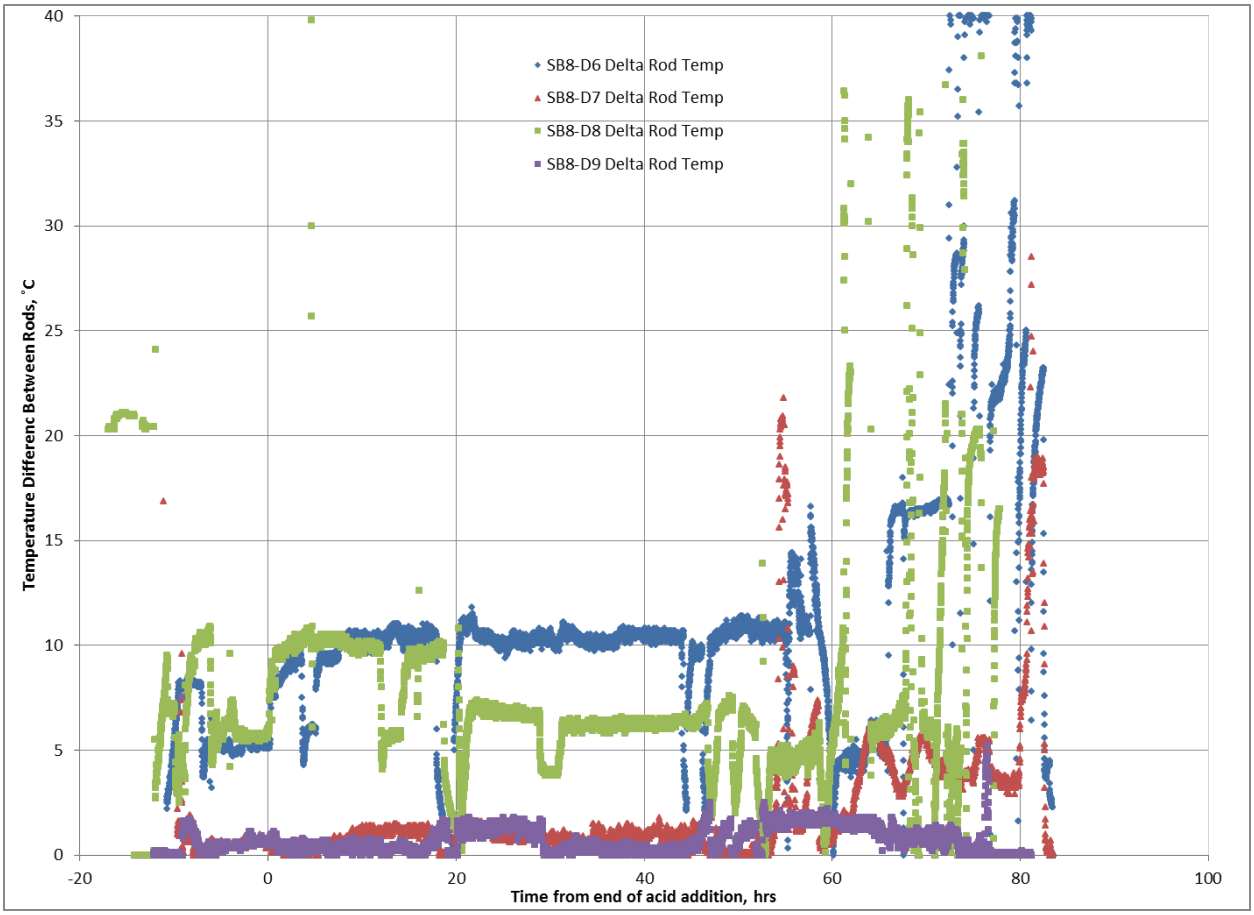

Figure 3-4. Heating Rod Temperature Difference for SRAT and SME cycles

Inspection of the heating rods after the runs demonstrated that many of the heat rods were corroded at the heat zone, likely caused by high rod temperature in air. In addition six of the twelve heating rods were identified in subsequent testing as damaged and were disposed of. Ten additional new rods were procured for future testing.

3.2.1.3 SRAT/SME Foamovers

Foamovers occurred in three of the four runs. Foaming in runs SB8-D6 and SB8-D7 led to foam in the MWWT. The foam was flushed from the SRAT condenser and MWWT by refluxing the condensate back to the SRAT. More significant foaming in run SB8-D8 led to foam filling the SRAT condenser, MWWT and ammonia scrubber. The final mass of the ammonia scrubber solution was 78 g higher in run SB8-D8 than SB8-D9 due to the foamover. The foam was drained from the MWWT and returned to the kettle then the SRAT condenser and MWWT were flushed back to the kettle by refluxing the condensate back to the SRAT. The foam in the ammonia scrubber could not be recovered as it had been diluted with 750 mL of pH 2 nitric acid solution. The foamover in run SB8-D7 was not noted by the technician. But startup of the ammonia scrubber for SB8-D9 introduced slurry into the pH 2 nitric acid solution giving it a brown color. The slurry or foam must have been leftover from run SB8-D7.

Because of the foaming in the first two runs, the R&D instructions were modified to explicitly add antifoam at various times during the testing instead of just giving the technicians instructions to add 100 ppm of antifoam each 12 hours. This was successful in preventing foam in SB8-D9 but not SB8-D8. The long processing time in the SRAT and SME, the high slurry pH, high boilup rate, and the significant offgas generation throughout the SRAT and SME cycle led to significant foam formation. More frequent antifoam additions will be needed throughout the runs to minimize the risk of foamovers in DWPF.

3.2.2 SRAT/SME Product Sample Results

Minimal sampling was completed during the run, with only samples pulled at the completion of the SRAT cycle, SME cycle #1 and SME cycle #2. The results and a discussion of these results are included in the sections below.

3.2.2.1 SRAT/SME Product Solids and Density Sample Results

There is some variability from run to run in the set of four SRAT and SME cycles that were completed. This is true especially for the SME product #2 from both run D6 and D8 where total solids was approximately 35% due to stopping the run before the final concentration was complete. Due to the rods fouling, the boilup rate was lower than planned. So the run was stopped when the planned boiling time was complete. The solids and density results for the SRAT and SME product slurries are given in Table 3-5.

To make the solids and density data easier to compare, the solids and density results were adjusted to account for the different dilutions present in the various products. The corrected solids and density results for the SRAT and SME product slurries are given in Table 3-6. Each product total solids was adjusted to give a SRAT product of 27 wt % total solids or a SME product of 45 wt % total solids. The rest of the results were adjusted to reflect the correction that dilution or concentration to reach the 27 or 45 wt% total solids. The "adjusted" results show better agreement between essentially identical runs.

Table 3-5. Solids and Density of SRAT and SME Product Samples

Sample	Total Solids wt% slurry	Insoluble Solids wt% slurry	Calcined Solids wt% slurry	Supernate Solids wt% supernate	Soluble Solids wt% slurry	Slurry Density, g/mL	Supernate Density, g/mL
D6 SRAT	26.5%	14.2%	17.5%	14.3%	12.3%	1.21	1.10
D7 SRAT	27.0%	14.1%	17.8%	15.1%	13.0%	1.20	1.10
D8 SRAT	27.0%	12.9%	18.1%	16.2%	14.1%	1.21	1.10
D9 SRAT	27.6%	12.8%	18.5%	17.0%	14.8%	1.22	1.10
D6 SME #1*	45.6%	36.3%	38.4%	14.6%	9.33%	1.39	1.11
D6 SME #2#	37.9%	29.5%	31.6%	11.9%	8.37%	1.32	1.09
D7 SME #1	52.0%	40.9%	43.9%	18.8%	11.1%	1.46	1.14
D7 SME #2	49.2%	39.7%	42.1%	15.8%	9.51%	1.43	1.11
D8 SME #1	45.0%	35.1%	37.6%	15.3%	9.91%	1.39	1.10
D8 SME #2	35.5%	27.6%	29.8%	10.8%	7.84%	1.28	1.08
D9 SME #1	46.3%	34.7%	38.4%	17.8%	11.6%	1.40	1.11
D9 SME #2	47.7%	36.5%	39.7%	17.6%	11.2%	1.42	1.12

* SME#1 refers to samples pulled after adding 15,000 gal SE, completing process frit addition and dewatering

\# SME#2 refers to samples pulled after adding 15,000 gal SE, completing process frit addition, dewatering, and adding an additional 15,000 gal SE.

Table 3-6. Corrected* Solids and Density of SRAT and SME Product Samples

Sample	Total Solids wt% slurry	Insoluble Solids wt% slurry	Calcined Solids wt% slurry	Supernate Solids wt% supernate	Soluble Solids wt% slurry	Slurry Density, g/mL	Supernate Density, g/mL
D6 SRAT Fixed	27.0%	14.5%	17.9%	14.6%	12.5%	1.22	1.10
D7 SRAT Fixed	27.0%	14.1%	17.8%	15.1%	12.9%	1.20	1.10
D8 SRAT Fixed	27.0%	12.9%	18.1%	16.2%	14.1%	1.21	1.10
D9 SRAT Fixed	27.0%	12.5%	18.1%	16.6%	14.5%	1.21	1.10
D6 SME #1 Fixed	45.0%	35.8%	37.9%	14.4%	9.2%	1.38	1.10
D6 SME #2 Fixed	45.0%	35.1%	37.5%	14.1%	9.9%	1.40	1.12
D7 SME #1 Fixed	45.0%	35.4%	38.0%	16.3%	9.6%	1.37	1.10
D7 SME #2 Fixed	45.0%	36.3%	38.5%	14.4%	8.7%	1.38	1.09
D8 SME #1 Fixed	45.0%	35.1%	37.7%	15.3%	9.9%	1.39	1.11
D8 SME #2 Fixed	45.0%	35.1%	37.8%	13.7%	9.9%	1.39	1.11
D9 SME #1 Fixed	45.0%	33.7%	37.3%	17.3%	11.3%	1.38	1.11
D9 SME #2 Fixed	45.0%	34.4%	37.4%	16.6%	10.6%	1.38	1.11

* the SRAT product results were corrected to 27 wt% total solids and the SME products were corrected to 45% total solids to remove the effect of dilution on the sample results.

3.2.2.2 SRAT/SME Product Calcined Elemental Sample Results

Calcined elemental results for the SRAT and SME product slurries from SB8-D7 through D9 are given in Table 3-7. Values are the average of two measurements from a single preparation. There is excellent agreement from run to run, as would be expected in runs where the only difference involves the composition of the SE.

Table 3-7. Calcined Elemental Results of SRAT and SME Product Samples (wt% calcined solids)

Element	D6 SRAT	D7 SRAT	D8 SRAT	D9 SRAT	D6 SME #1	D6 SME #2	D7 SME #1	D7 SME #2	D8 SME #1	D8 SME #2	D9 SME #1	D9 SME #2
SE Acid	Nitric	Water	Boric	Boric	Nitric	Nitric	Water	Water	Boric	Boric	Boric	Boric
Solvent	Bob	None	Max	Blend	Bob	Bob	None	None	Max	Max	Blend	Blend
Al	7.91	7.82	7.70	7.74	3.35	3.43	3.18	3.08	3.21	3.19	3.21	3.26
B	<0.10	<0.10	0.21	0.15	1.37	1.28	1.36	1.40	1.50	1.54	1.44	1.40
Ca	1.49	1.49	1.53	1.53	0.53	0.54	0.48	0.47	0.51	0.48	0.47	0.49
Cr	0.17	0.18	0.18	0.18	0.08	0.09	0.08	0.07	0.08	0.07	0.07	0.08
Fe	22.8	22.1	22.2	22.2	8.34	8.33	7.58	7.49	8.36	8.43	8.69	8.68
K	0.14	0.18	0.15	0.14	0.24	<0.10	0.19	0.12	<0.10	<0.10	<0.10	<0.10
Li	<0.10	<0.10	<0.10	<0.10	2.05	2.01	2.15	2.17	2.10	2.11	2.08	2.11
Mg	0.25	0.25	0.24	0.25	0.12	0.12	0.11	0.11	0.12	0.11	0.11	0.12
Mn	7.68	7.50	6.55	6.77	2.98	2.99	2.73	2.70	2.60	2.64	2.62	2.60
Na	22.8	22.3	21.0	21.9	12.3	12.5	11.9	11.6	11.5	11.8	11.6	11.8
Ni	1.56	1.59	1.70	1.75	0.66	0.69	0.61	0.59	0.62	0.61	0.61	0.63
S	0.38	0.40	0.37	0.37	0.15	0.16	0.15	0.12	0.15	0.14	0.15	0.15
Si	1.44	1.44	2.41	1.77	23.8	23.0	24.0	24.4	23.3	23.4	22.6	22.8
Ti	0.49	0.67	0.61	0.60	0.23	0.24	0.28	0.28	0.28	0.28	0.27	0.27
Zn	0.12	0.12	0.11	0.11	<0.10	<0.10	<0.10	<0.10	<0.10	<0.10	<0.10	<0.10
Zr	0.13	0.06	0.12	0.15	0.13	0.14	0.13	0.13	0.13	0.13	0.12	0.13

3.2.2.3 SRAT/SME Product Supernate Elemental Analytical Results and Calculated Percent Solubility

Data were obtained on the elements in the SRAT and SME product supernates. Many species were below detection limits or were minor species with minimal impact on processing chemistry. Other species have varying degrees of significance. Ca, Mg, and Mn are three of the more active elements chemically during the CPC, starting insoluble in the SRAT feed, typically dissolving close to 100% at some point during processing, and then partially reprecipitating by the end of the SME cycle. Table 3-8 gives a short list of SRAT product supernate results.

Table 3-8. Major SRAT Product Supernate Elements, mg/L

Element	D6 SRAT	D7 SRAT	D8 SRAT	D9 SRAT
Al	12.1	<1.00	<1.00	<1.00
Ca	9.21	5.07	39.3	13.2
K	486	604	365	388
Mg	3.66	<1.00	18.7	5.85
Mn	7.42	3.91	39.8	8.62
Na	45,700	47,700	50,400	52,700
S	849	559	594	587
Si	196	135	111	134

Selected concentrations in Table 3-8 were converted to a slurry basis and compared to the total concentration of the element to assess the partitioning of the element between soluble and insoluble species, Table 3-9.

Table 3-9. Selected SRAT Product Supernate Elements, % of total

Element	D6 SRAT	D7 SRAT	D8 SRAT	D9 SRAT
Al	0.07%	0.01%	0.01%	0.01%
Ca	0.28%	0.15%	1.13%	0.37%
Fe	0.00%	0.00%	0.00%	0.00%
K	156%	149%	108%	115%
Mg	0.66%	0.04%	3.35%	1.01%
Mn	0.04%	0.02%	0.27%	0.05%
Na	90%	94%	105%	103%
S	99%	61%	71%	68%
Si	6.07%	4.13%	2.01%	3.22%

Sodium, potassium and sulfur (sulfate) were the only highly soluble elemental species in the SRAT products. In addition, 2-6% of the Si was soluble (the silicon source was antifoam). The results are summarized in Table 3-9.

Table 3-10. Major SME Product Supernate Elements, mg/L

Element	D6 SME #1	D6 SME #2	D7 SME #1	D7 SME #2	D8 SME #1	D8 SME #2	D9 SME #1	D9 SME #2
Al	6.31	<1.00	8.67	4.16	2.52	3.84	<1.00	4.21
Ca	1.18	3.98	3.93	3.71	1.81	2.40	3.33	1.95
K	566	176	1,010	887	406	221	439	457
Mg	<1.00	<1.00	3.30	<1.00	1.27	<1.00	10.84	<1.00
Mn	<1.00	<1.00	10.11	<1.00	<1.00	<1.00	18.75	<1.00
Na	49,600	37,700	63,700	51,800	50,500	34,800	56,200	58,200
S	1,140	918	1,140	1,040	1,120	839	1,050	1,290
Si	41.4	6860	54.8	47.4	72.1	74.5	104	113

The partitioning of the elements in the supernate between phases was calculated on the basis of percent of total element mass present (as determined by the slurry elemental analysis). These percentages are given in Table 3-11.

Table 3-11. Selected SME Product Supernate Elements, % of total

Element	D6 SME #1	D7 SME #1	D8 SME #1	D9 SME #1	D6 SME #2	D7 SME #2	D8 SME #2	D9 SME #2
Al	0.01%	0.03%	0.00%	0.02%	0.03%	0.01%	0.03%	0.02%
Ca	0.06%	0.11%	0.11%	0.06%	0.03%	0.15%	0.10%	0.10%
Fe	0.00%	0.00%	0.00%	0.00%	0.00%	0.00%	0.00%	0.00%
K	63%	50%	67%	65%	36%	35%	63%	94%
Mg	0.17%	0.20%	1.48%	0.12%	0.13%	0.17%	0.36%	0.12%
Mn	0.01%	0.01%	0.11%	0.01%	0.01%	0.01%	0.04%	0.00%
Na	69%	66%	74%	71%	60%	62%	63%	58%
S	119%	137%	104%	119%	114%	118%	89%	108%
Si	0.05%	0.07%	0.07%	0.07%	0.03%	0.61%	0.03%	0.03%

Sodium, potassium and sulfur (sulfate) were the only highly soluble species in the SME products. Very little of the Si was soluble (the silicon source is frit with a small amount of antifoam).

3.2.2.4 SME Product Waste Loading Calculation Results

Waste loadings were calculated from the Li concentration in SME product and frit and from Fe concentration in SRAT product and SME product. These results are summarized in Table 3-12. The waste loading target was 36%. Results for waste loading were close to target and fairly consistent. Note that SB8-D7 did have a foamover. This is likely the reason for the lower was loading in SB8-D7.

Table 3-12. Waste Loading of SME Products

Run	Li, wt%	Fe, wt%
D6 SME #1	36.9%	36.6%
D6 SME #2	38.4%	36.5%
D7 SME #1	33.8%	34.3%
D7 SME #2	33.4%	33.9%
D8 SME #1	35.4%	37.7%
D8 SME #2	35.3%	37.8%
D9 SME #1	36.2%	39.1%
D9 SME #2	35.2%	39.1%

3.2.2.5 SRAT/SME Product Anion Sample Results

SRAT and SME product anion data are given in Table 3-13. All samples were caustic-quenched prior to analysis. The dilution of the caustic-quenched sample species by the added caustic has been removed computationally to present the results on a SRAT slurry basis prior to caustic quenching. The caustic quench preparation is very important for accurate oxalate analysis.

Table 3-13. SRAT and SME Product Anions, mg/kg slurry

Sample ID	Cl	NO_2	NO_3	C_2O_4	HCO_2	SO_4	SO_4 ICP
D6 SRAT	615	<500	25,300	6,280	53,300	1,970	2,020
D7 SRAT	720	<500	27,100	6,800	44,200	2,120	2,150
D8 SRAT	706	<500	34,900	6,500	47,900	2,120	2,000
D9 SRAT	719	<500	36,000	6,670	47,100	2,150	2,050
D6 SME #1	538	<500	19,300	5,610	28,400	1,720	1,720
D6 SME #2	<500	<500	14,100	3,430	14,400	1,390	1,510
D7 SME #1	673	<500	22,700	6,310	46,500	1,940	1,990
D7 SME #2	710	<500	18,700	5,570	35,800	1,810	1,560
D8 SME #1	571	<500	25,500	5,440	31,600	1,780	1,660
D8 SME #2	<500	<500	17,700	4,030	17,900	1,370	1,230
D9 SME #1	594	<500	28,900	5,470	37,500	1,830	1,760
D9 SME #2	621	<500	28,700	5,590	35,400	1,920	1,830

As was discussed in the solids and density section, the results were corrected to account for the different dilutions present in the various products. As a result, the rows labeled “fixed” were adjusted to give a SRAT product of 27 wt % total solids or a SME product of 45 wt % total solids. The rest of the results were adjusted to reflect the correction that dilution or concentration to reach the 27 or 45 wt% total solids. Note that there should be variability in the reactive anions (nitrite, nitrate, oxalate and formate). In addition, nitrate was added through the strip effluent in run SB8-D7. As can be seen, the concentration of chloride and sulfate were essentially constant in both the SRAT and the SME products as would be expected. SRAT and SME product anion data are given in Table 3-14.

Table 3-14. Corrected* SRAT and SME Product Anions, mg/kg slurry

Sample ID	Cl	NO_2	NO_3	C_2O_4	HCO_2	SO4	SO_4 ICP
D6 SRAT Fixed	627	<510	25,800	6,400	54,300	2,010	2,060
D7 SRAT Fixed	719	<499	27,100	6,790	44,100	2,120	2,150
D8 SRAT Fixed	706	<500	34,900	6,500	47,900	2,120	2,000
D9 SRAT Fixed	703	<489	35,200	6,500	46,000	2,100	2,000
D6 SME#1 Fixed	531	<493	19,000	5,530	28,000	1,700	1,700
D6 SME#2 Fixed	<541	<594	16,800	4,080	17,100	1,650	1,790
D7 SME#1 Fixed	582	<432	19,600	5,460	40,200	1,680	1,720
D7 SME#2 Fixed	649	<457	17,100	5,090	32,700	1,660	1,420
D8 SME#1 Fixed	571	<500	25,500	5,440	31,600	1,780	1,660
D8 SME#2 Fixed	<559	<634	22,400	5,110	22,700	1,740	1,560
D9 SME#1 Fixed	578	<486	28,100	5,320	36,500	1,780	1,710
D9 SME#2 Fixed	586	<472	27,100	5,270	33,400	1,810	1,730

* the SRAT product results were corrected to 27 wt% total solids and the SME products were corrected to 45% total solids to remove the effect of dilution on the sample results.

3.2.2.6 SRAT/SME Product Calculated Loss of Anions

The SRAT and SME product anions and a mass balance were used to calculate the loss of formate, nitrite, and nitrate. As is typical in runs with adequate added acid, the nitrite decomposition is complete. The various reactions destroying the nitrite produce NO, N_2O, NO_2, and nitrate. In a typical experiment, approximately 33% of the nitrite is converted to nitrate. If this happens there is an increase in the nitrate concentration (reported below as nitrite to nitrate conversion). In addition, the nitrate can be destroyed due to noble metal activity. In these runs, the nitrite to nitrate conversion was very low due to the complete decomposition of nitrite and the partial decomposition of nitrate. The formate and nitrate decomposition continued throughout the SME cycle also leading to large and variable nitrate and formate losses compared to typical SME cycles.

The combination of high noble metal concentration and long processing times led to high decomposition for formate and nitrate. In the SRAT cycles, a loss of about 45% of the formate is significantly higher than the 28% measured in the SB8-D5 run (lower noble metals, shorter processing time). In the SME cycle, the formate loss varied from 29 to 71%, much higher than the 2% measured in the SB8-D5 run. The SME cycle typically has low anion destruction (similar to the nitrate and formate loss in SB8-D5). However in this series of runs, the loss of formate and nitrate was both large and varied considerably from run to run. An accurate prediction of these five anion loss percentages is essential in accurately predicting REDOX. This will be discussed in more detail in 3.2.6.

Table 3-15. Changes in Major Anions

	D5	**D6**	**D7**	**D8**	**D9**
SE Acid	Boric	Nitric	Water	Boric	Boric
SRAT					
Formate Loss	28%	34.4%	45.4%	37.3%	38.3%
Nitrite Loss	100%	100%	100%	100%	100%
Nitrite-to-nitrate	8%	2.8%	10.7%	15.8%	20.5%
SME					
Formate Loss	2%	70.7%	43.7%	53.3%	29.3%
Nitrate Loss	1%	36.1%	44.9%	32.2%	19.7%

Results are susceptible to the analytical uncertainties in the IC measurements of anions in the SRAT and SME product samples as well as to uncertainty in the SRAT product mass (a key parameter in partitioning the total anion change between the SRAT and SME cycles). The SRAT product mass is calculated by several methods including a running mass balance from the beginning of the SRAT adjusted for off-gas losses, a reverse running mass balance based on the SME product mass that puts dewater masses back in and takes frit slurry addition masses out, and a calculation based on conservation of the mass of calcined oxides (adjusted for samples) from the starting sludge to the SRAT product. It is not uncommon to have a 5-10% spread in the SRAT product mass determined from the various independent calculations. The values in the table must be interpreted in the context of fairly large uncertainty bars, e.g. ±10% to the values as given (22% is probably somewhere in the 12%- 32% range).

3.2.2.7 SRAT/SME Rheology

Flow curves for the SRAT and SME products were obtained by using a Haake RS600 rheometer and the current DWPF simulant rheology protocol.[7] The up and down curves were fit to a Bingham plastic model to determine yield stress and consistency. Down flow curve data are the generally preferred choice for comparisons between systems. The data for all runs are tabulated below for the SRAT and SME Products. A rheology graph for the SRAT and both SME products is summarized Figure 3-5 and Figure 3-6. Individual rheology graphs for each run are included in Appendix B.

The calculated yield stress and consistency is summarized in Table 3-16. Design basis rheology for the SRAT and SME are shown in the table below. The SB8-D7 SME#1 product had the highest yield stress of all the runs. SB8-D6 and SB8-D8 SME#2 samples would have had an even higher yield stress if they had been concentrated to 45 wt% total solids.

In general, the yield stress and consistency increased the longer the slurry was processed (compare Figure 3-6 to Figure 3-7). The rheology concern is that this thin sludge slurry transitioned to a much thicker SME product due to the long processing time. Thick sludge slurry likely would have been too thick for processing (pumping, heat transfer, and or foaming).

Table 3-16. SRAT and SME Product Rheology Summary

Run	Insoluble Solids, wt %	Up Yield Stress, Pa	Down Yield Stress, Pa	Up Consistency, cP	Down Consistency, cP
Design Basis[8]		1.5-5		5-12	
D6 SRAT	14.2%	1.59	1.53	8.27	8.29
D7 SRAT	14.1%	7.54	3.45	11.9	16.6
D8 SRAT	12.9%	3.87	3.12	10.2	11.1
D9 SRAT	12.8%	5.56	3.99	14.4	15.3
Design basis[8]		2.5-15		10-40	
D6 SME #1	36.3%	2.76	2.92	13.1	12.5
D6 SME #2	29.5%	13.4	11.2	20.6	26.0
D7 SME #1	40.9%	8.52	15.6	33.3	27.6
D7 SME #2	39.7%	8.54	13.6	30.3	27.0
D8 SME #1	35.1%	3.32	3.77	14.6	13.6
D8 SME #2	27.6%	7.34	10.12	25.4	18.2
D9 SME #1	34.7%	4.13	5.82	21.7	17.3
D9 SME #2	36.5%	5.52	7.56	24.0	20.4

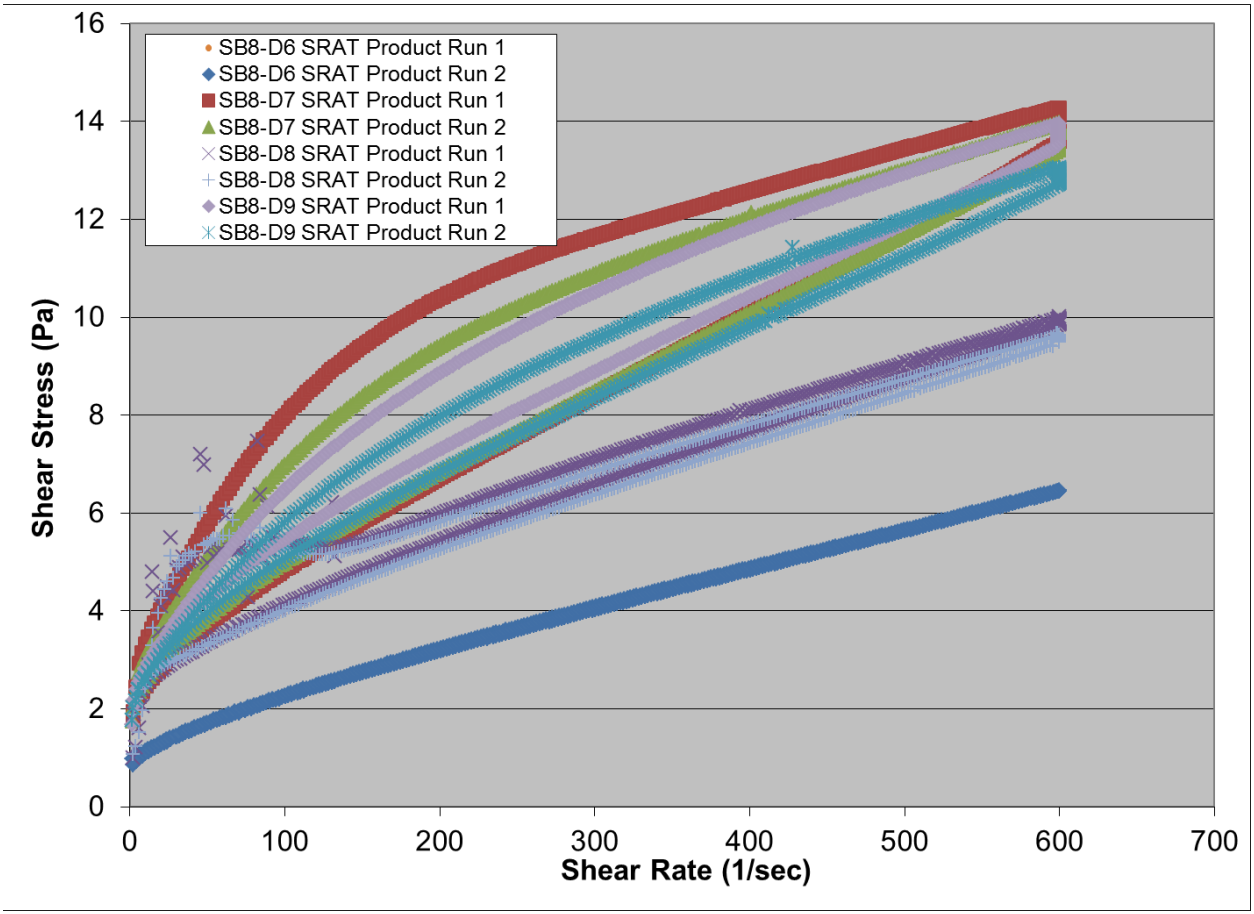

Figure 3-5. SRAT Product Rheology Curves

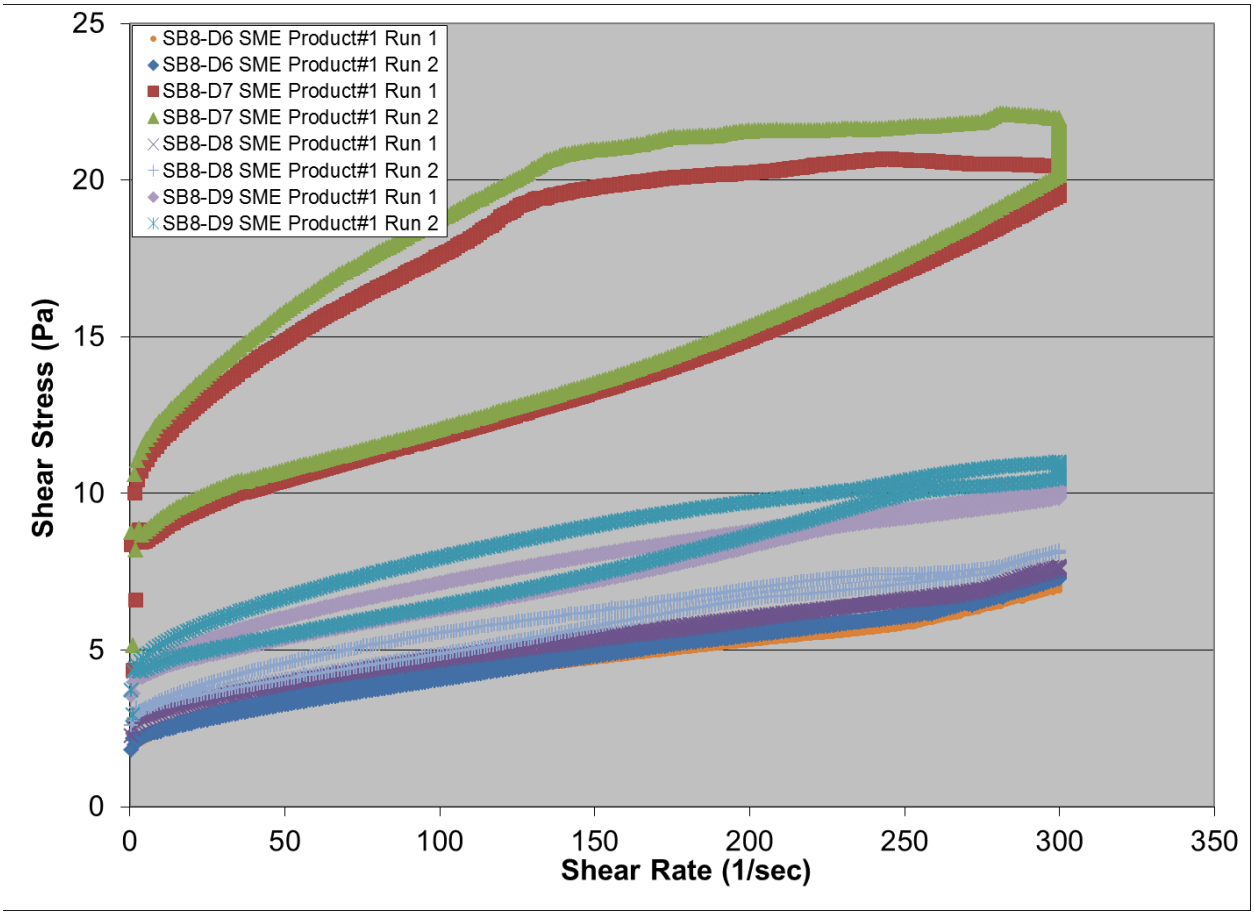

Figure 3-6. SME Product #1 Rheology Curves

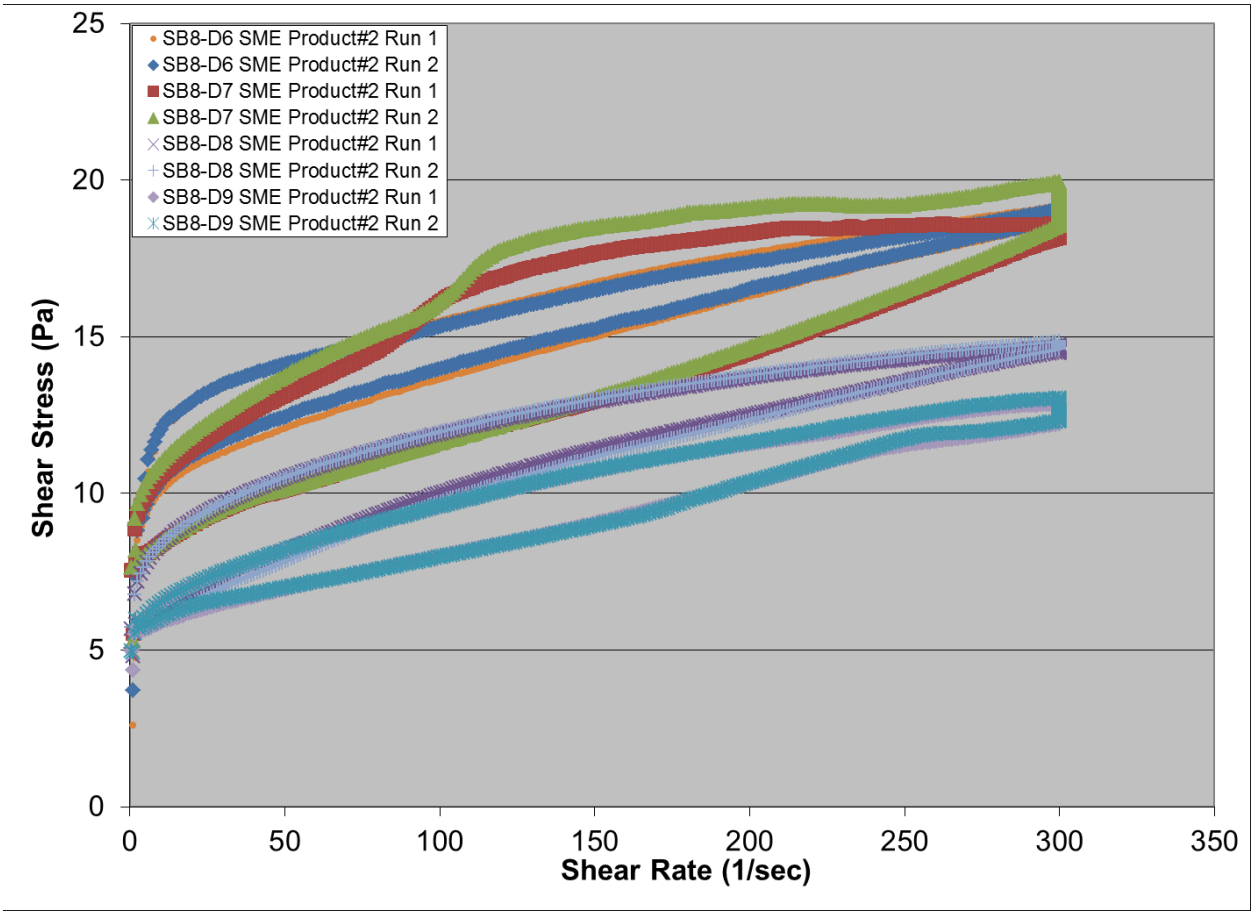

Figure 3-7. SME Product #2 Rheology Curves

3.2.3 SRAT/SME Off-gas Results

Gas samples were taken from the exit of the FAVC for analysis by gas chromatography (GC), mass spectrometry (MS), and Fourier transform infrared spectroscopy (FTIR). The results of the analysis are discussed below. Note that the offgas had to pass through the condenser, ammonia scrubber, FAVC, and Perma Pure Nafion® gas dryer prior to analysis to remove water, ammonia, solids, and nitric acid prior to analysis. The FTIR was not used in runs SB8-D7 and SB8-D9. The time delay between exiting the vessel and reaching the analyzer was estimate to be x min in the SRAT and y min in the SME.

3.2.3.1 Minor Offgas Species

Hydrogen, Isopar™ L, HMDSO, and ammonia are minor offgas species but are important as they are potentially flammable. These offgas components will be discussed below.

3.2.3.1.1 Ammonia

A small amount of ammonia was detected in the offgas by the FTIR for runs SB8-D6 and SB8-D8. (see section 3.2.4.3 for more discussion of ammonia removed by the ammonia scrubbers prior to offgas analysis). The total ammonia detected by the FTIR was 0.0378 mmol in SB8-D8 compared to 18.3 mmol from the ammonia scrubber solution meaning that >99.8% of the ammonia was removed by the ammonia scrubbers. The average ammonia concentration in SB8-D8 was 0.36 ppm_v. Ammonia was not measured

in runs SB8-D7 and SB8-D9. A graph showing the ammonia concentration throughout the runs is included as Figure 3-8.

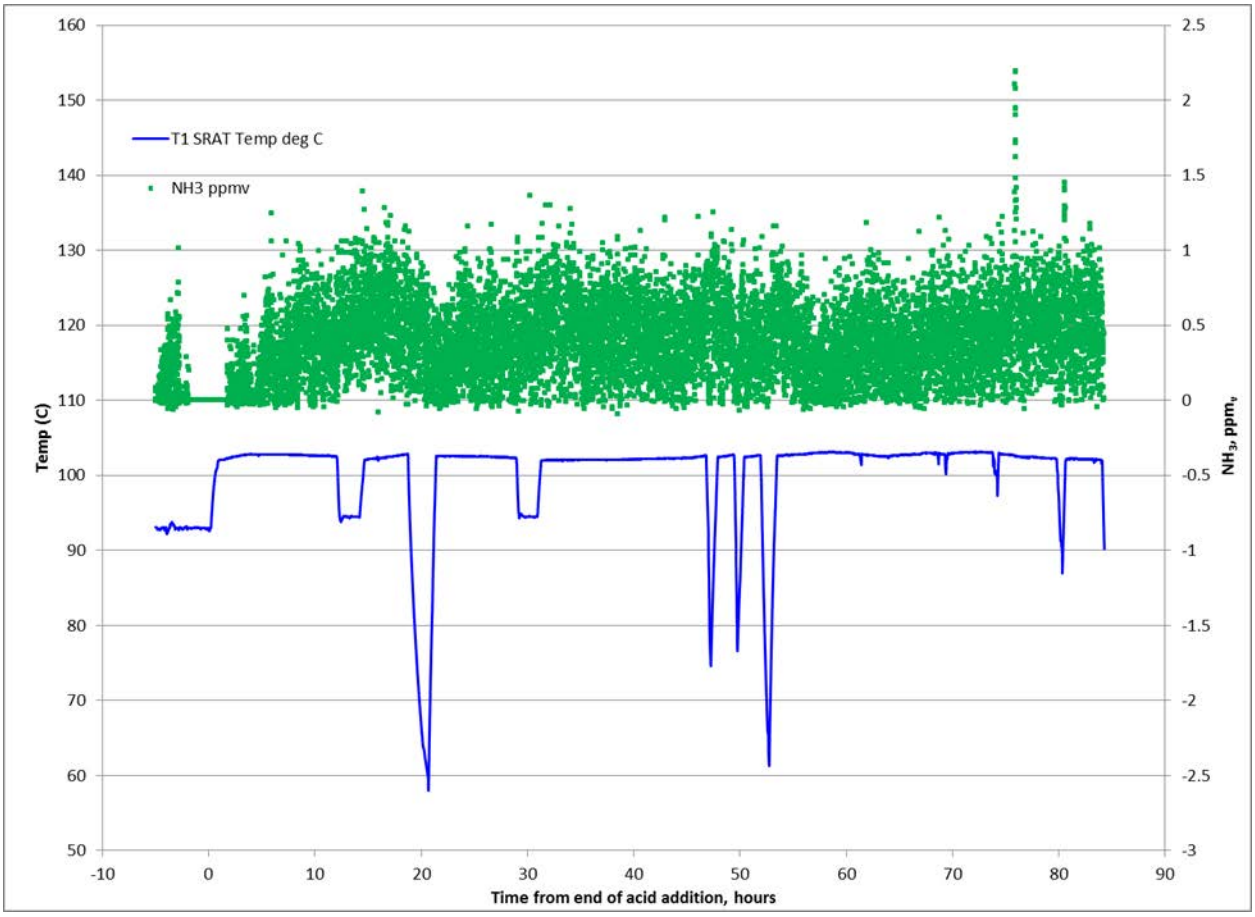

Figure 3-8. SB8-D8 Ammonia Concentration, ppm_v

3.2.3.1.2 Hydrogen

Significant hydrogen was measured in runs SB8-D6 and SB8-D8, where the DWPF SME hydrogen generation limit of 0.223 lb/hr was exceeded. It should be noted that both of these experiments were completed in the north hood with same heating rods. The north hood T8 rod was significantly hotter than the other rods due to fouling. Fouling leads to high rod temperatures and high hydrogen generation. The rod temperatures were controlled at less than 132 ˚C except during the very end of run SB8-D8 where the rod temperature exceeded 166 ˚C during the last few hours of the SME cycle in an attempt to maximize boilup in spite of significant fouling. Runs SB8-D7 and SB8-D9 had hydrogen generation rates similar to SB8-D5 and did not exceed DWPF hydrogen limits[9].

Run SB8-D6 experienced the maximum hydrogen generation rate and the maximum total hydrogen generated. The concentration of hydrogen throughout the run is summarized in Figure 3-9. Two things should be noted. First, when the heating rods were shut off, the hydrogen concentration dropped very quickly. Second, although the hydrogen peak was in the SRAT cycle, there was significant hydrogen generation in the SME cycle. In Run SB8-D6 only, the air purge was not reduced at the beginning of the SME cycle as had been planned to avoid exceeding the planned limit of 1 volume % hydrogen. Had the hydrogen limit been exceeded, the purge would have been increased anyway. The SME purge was

lowered once the hydrogen generation dropped low enough. Due to the high hydrogen generation in SB8-D6, the SRAT purge was used for most of the SME cycle. The hydrogen concentration would have been much higher had the lower SME purge been used throughout the SB8-D6 SME cycle.

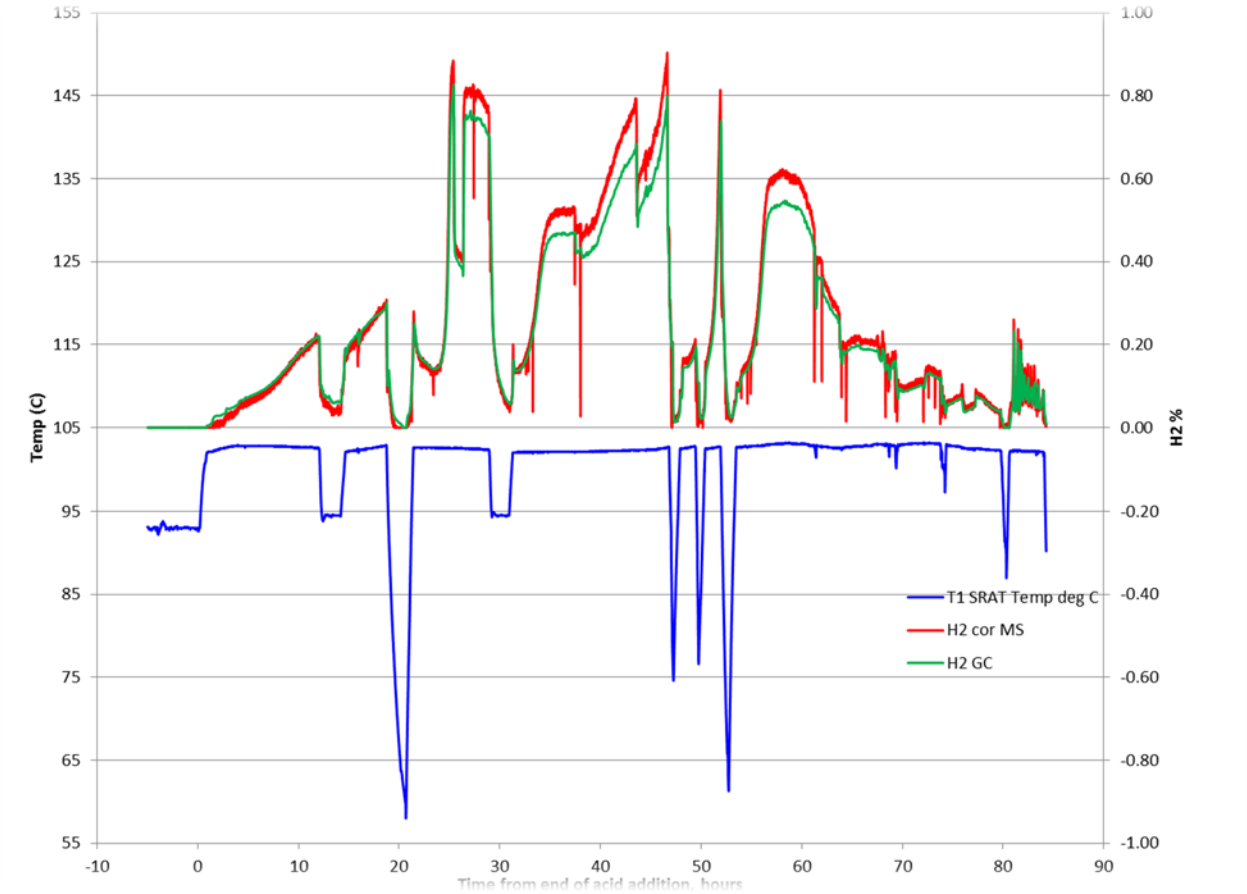

Figure 3-9. SB8-D6 Hydrogen Concentration, volume %

A graph of all of the hydrogen data is shown in Figure 3-10.The maximum H_2 concentrations and the peak hydrogen generation rates are summarized in Table 3-17.

Table 3-17. Maximum Concentrations of Hydrogen Measured by GC

Run	SRAT Maximum H_2 (volume %)	SME Maximum H_2 (volume %)	SRAT lb H_2/hr DWPF Scale	SME lb H_2/hr DWPF Scale
DWPF Limit			0.65	0.223
SB8-D5			0.085	0.070
SB8-D6	1.033	0.613	0.584	0.568
SB8-D7	0.069	0.296	0.058	0.095
SB8-D8	0.229	0.812	0.242	0.229
SB8-D9	0.083	0.109	0.069	0.030

The profile for the hydrogen generation was very different from run to run. SB8-D6 had a very large peak at 14 hours after acid addition was complete in the SRAT cycle. The hydrogen was so high at the end of the SRAT cycle that the air purge was not reduced to keep from exceeding 1 volume % hydrogen. The hydrogen was also high in run SB8-D8 but the peak was delayed until about 5 hours into the SME cycle.

There were 4 peaks in the SB8-D8 SME cycle that exceeded 0.5 volume % hydrogen. The hydrogen in runs SB8-D7 and SB8-D9 was lower but still significant. Holding all other parameters constant, an increase in formic acid concentration is expected to increase the production of hydrogen. Thus, the addition of formic acid with the frit tended to increase the hydrogen generation. Removal of formic acid to the frit as a declumping/deleaching additive would lead to less hydrogen in the SME cycle.

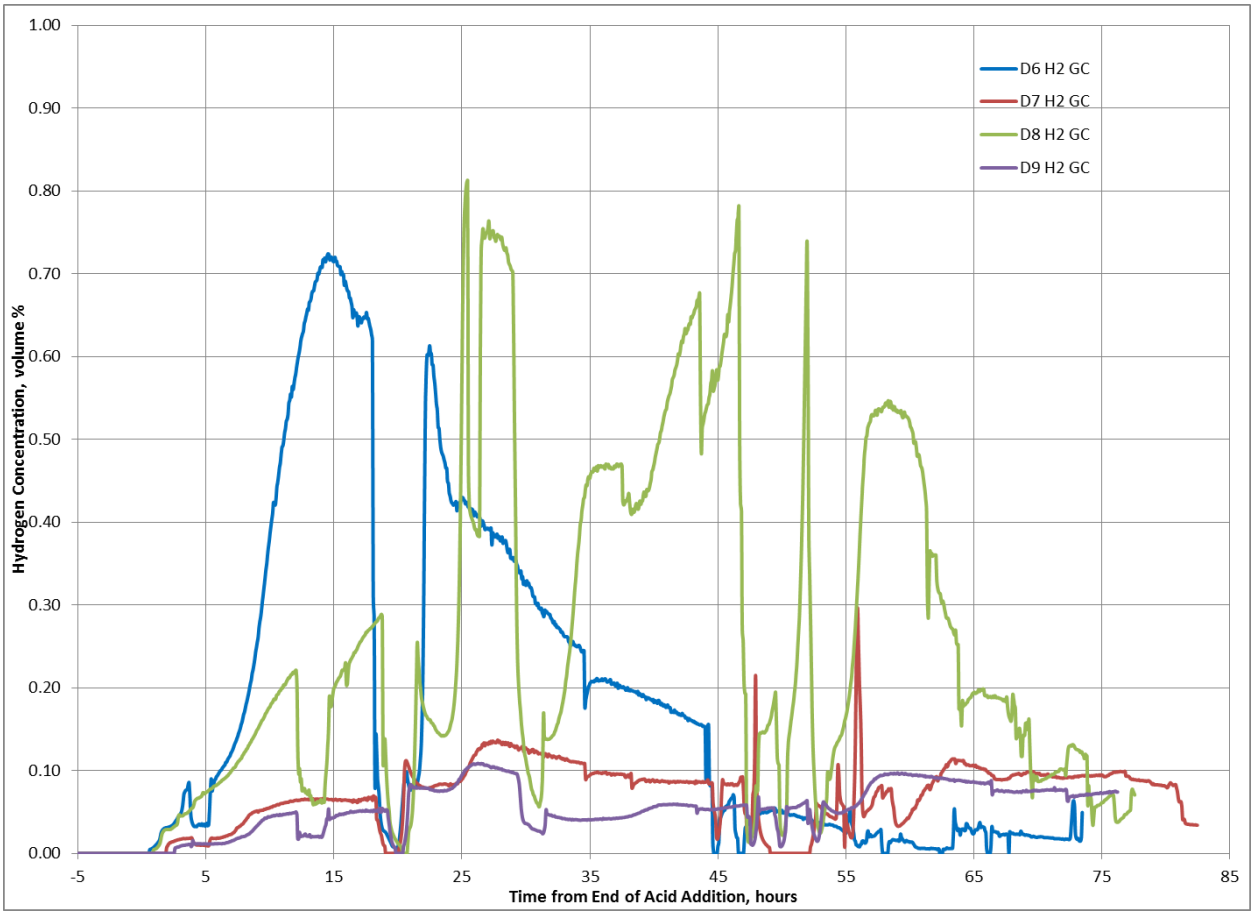

Figure 3-10. Hydrogen Concentration for all runs measured by GC, volume %

3.2.3.1.3 Solvent

Some solvent is entrained in the strip effluent. The solvent is a mixture of diluent, extractant, suppressor, and modifier. The extractant, suppressor and modifier have no significant vapor pressure and can't be detected using the offgas analyzers. The diluent is volatile and can be tracked by the FTIR and MS. The diluent is Isopar™ L. Isopar™ L is a mixture of normal alkanes, isoalkanes, and cycloalkanes. The best FTIR match for Isopar™ L is isooctane, $CH_3)_3CCH_2CH(CH_3)_2$. or dodecane, $CH_3(CH_2)_{10}CH_3$. Isopar™ L was added with the strip effluent in a separate feed using a syringe pump to simulate 87 ppm solvent (~60 ppm Isopar™ L) entrainment in the strip effluent. If the Isopar™ L flashes immediately after being fed, the expected concentration of the Isopar™ in the vapor is 74 ppm in the SRAT and 206 ppm in the SME after dilution with the air purge (ratio ~0.36). The FTIR measured dodecane concentration was ~15 ppm in the SRAT and 40 ppm in the SME (ratio ~0.38). Recall that the dodecane or isooctane is just a qualitative measure of the Isopar™ L, but the relative concentrations should be representative of the actual Isopar™ L concentrations. The higher concentration in the SME is due to the lower SME air purge.

As can be noted in Figure 3-11, the Isopar™ L concentration assuming it is dodecane, dropped from 15 to 10 ppm_v when the SRAT temperature decreased from boiling to 94.5 ˚C. It spiked from 10 to 25 ppm_v when the SRAT temperature returned to boiling, suggesting that Isopar™ L is accumulating at the lower temperature. Assuming the Isopar™ L is isooctane, the isooctane dropped from 60 to 35 ppm_v when the SRAT temperature decreased from boiling to 94.5 ˚C. It spiked from 35 to 90 ppm_v when the SRAT temperature returned to boiling. Due to the apparent accumulation of Isopar-L during the SRAT cycle, there is no justification for decreasing the minimum TSR required temperature for adding SE from boiling to 94.5 ˚C.

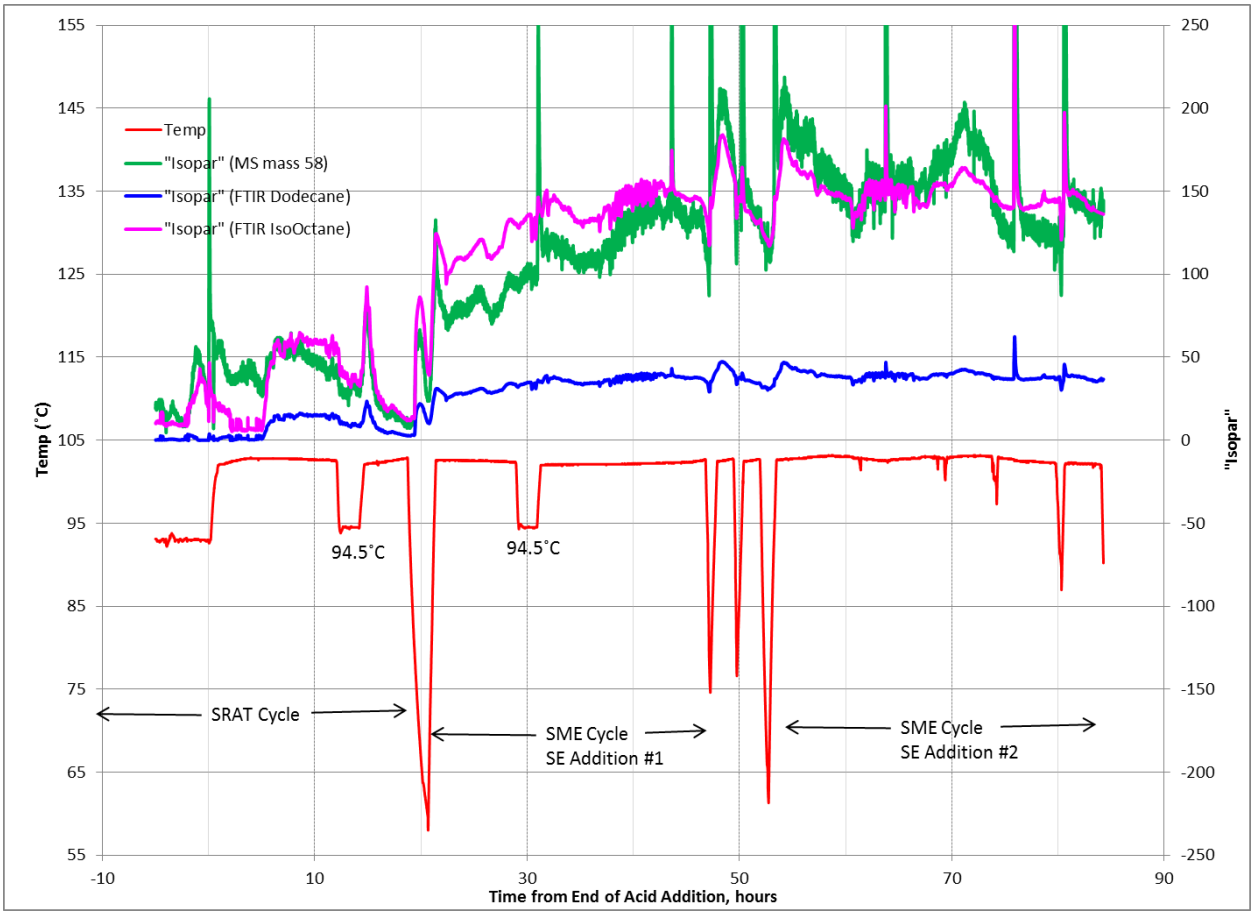

Figure 3-11. SB8-D8 "Isopar™ L" (Dodecane) Concentration, volume %

During the SRAT and SME cycles, the slurry temperature was decreased from boiling to 94.5˚C to determine whether the Isopar™ L would accumulate or whether it would evaporate and not build up. This was done for two hours during both the SRAT and SME cycles. A graph showing the Isopar™ L concentration is shown in Figure 3-12. The solvent (dodecane) did noticeably accumulate in two hours of sub-boiling testing (94.5˚C) in the SRAT.

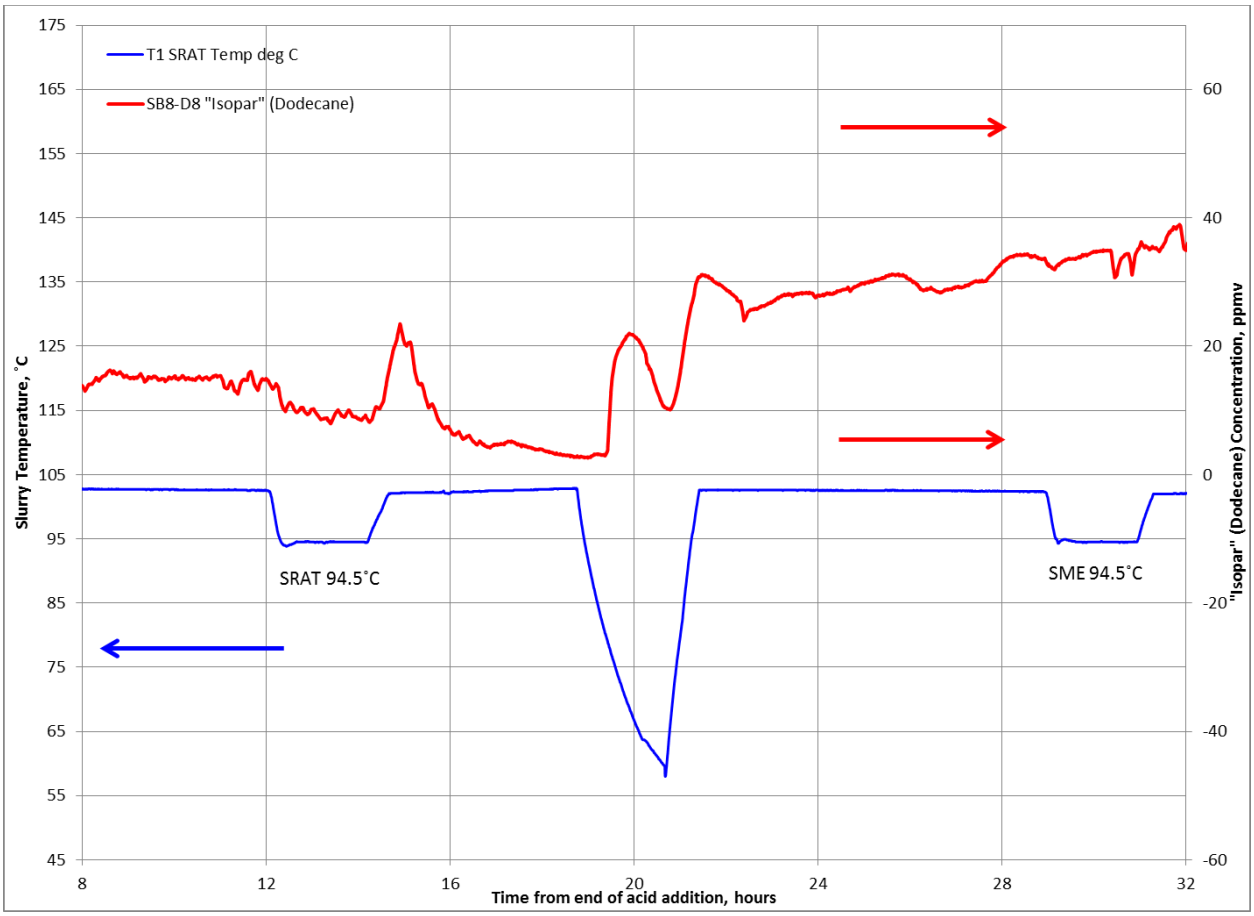

Figure 3-12. SRAT and SME Offgas Isopar Concentration

The MS signal at mass 58 tracked the FTIR “dodecane” extremely well. See graph inserted below. This relationship shows that the MS mass 58 signal is a good representation of Isopar™ L and could be used for runs without the FTIR (Figure 3-13.

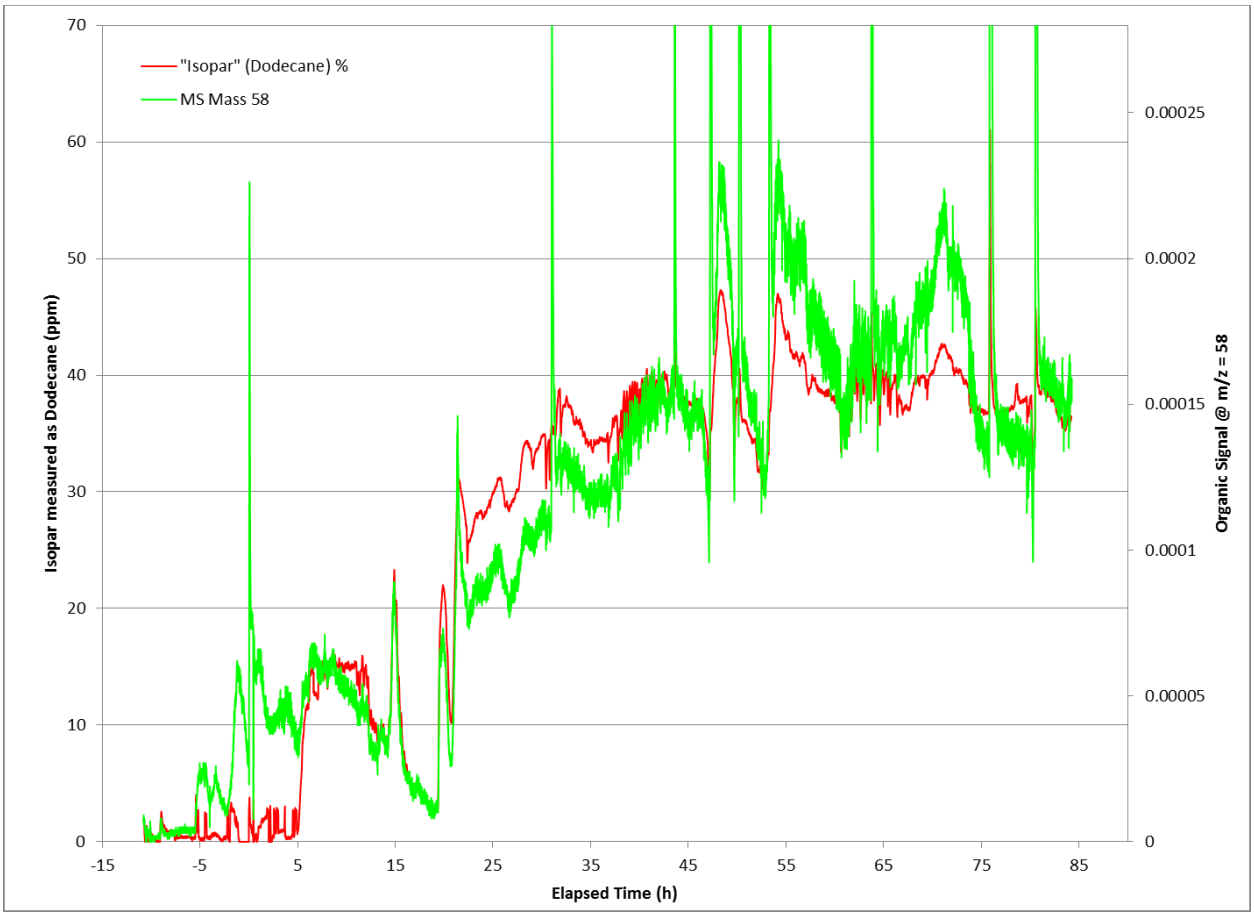

Figure 3-13. Comparison of Mass Spec Mass 58 and FTIR Dodecane as means of Tracking Isopar™ L

3.2.3.1.4 HMDSO

HMDSO is a fragment of the antifoam 747 as the molecule breaks into two pieces. HMDSO is tracked by the FTIR. Any addition of antifoam can be noted by a spike of HMDSO almost immediately after adding. Two molecules of antifoam can degrade to a one molecule of HMDSO and two molecules of polymeric ethoxylated siloxane derivatives[10]. The total moles of HMDSO (molecular weight 162.38) detected inSB8-D8 was 0.00214 moles (0.348 g). A total of 5.92 g (0.00891 moles Antifoam 747) was added in run SB8-D8. If the antifoam degraded into two pieces, this would be equivalent to 48% of the potential HMDSO. A graph of the HMDSO is included as Figure 3-14.

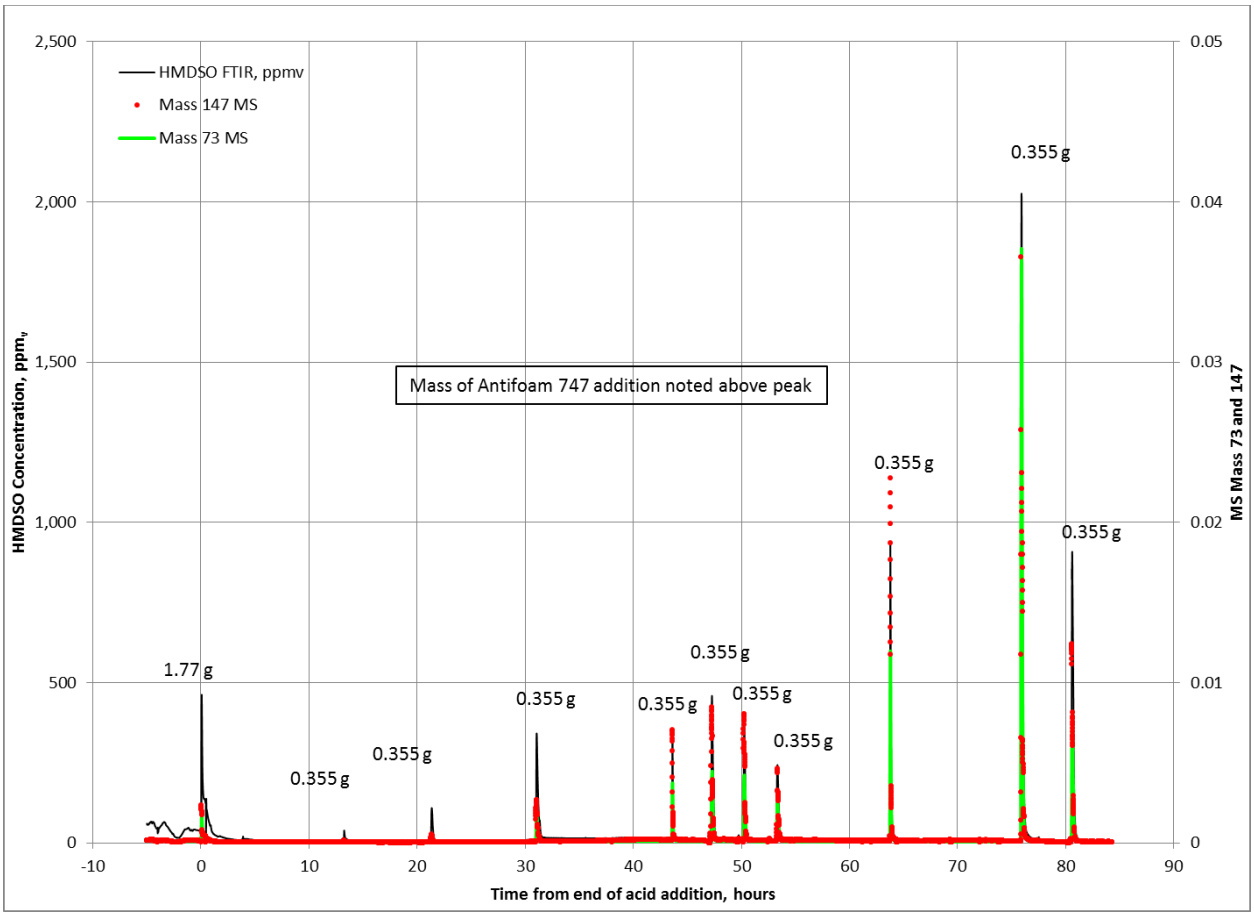

Figure 3-14. SB8-D8 HMDSO Concentration (Antifoam Additions Noted), ppm_v

3.2.3.2 Major Offgas Species

The major offgas species (CO_2, O_2, NO, NO_2, and N_2O) are shown in Figure 3-15, for the early part of the SRAT cycle. The later portion of the SRAT cycle and SME cycle for all runs are similar with declining concentrations of CO_2 and NO_x species. An Elapsed Time of zero is the end of formic acid addition.

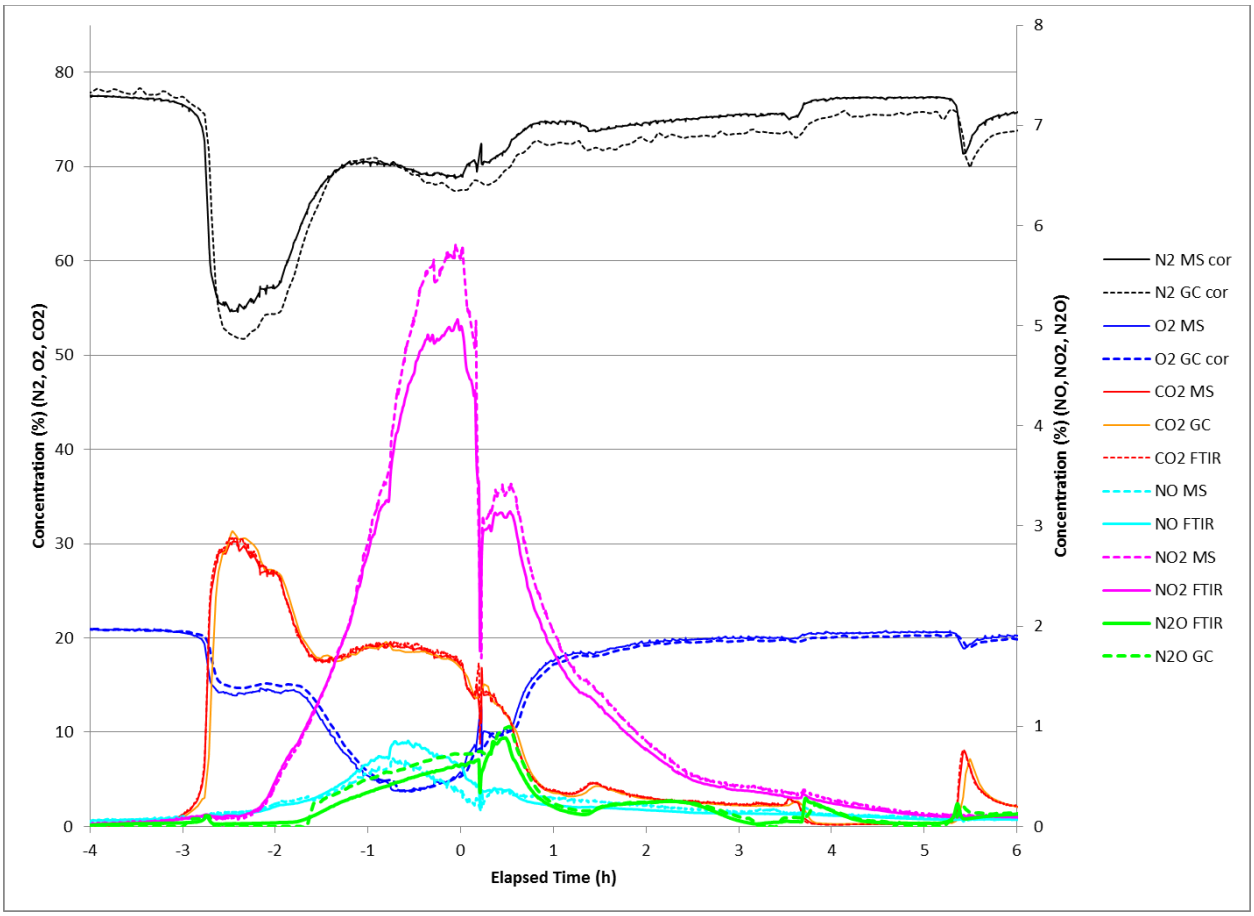

Figure 3-15. SB8-D6 Offgas Major Species Concentration (N_2, O_2, CO_2, NO, NO_2, N_2O)

There was excellent agreement between all three gas analyzers as can be seen from the graph. The other three runs had very similar concentration profiles. Note that in contrast to the glycolic acid flowsheet, there is no period where the oxygen concentration drops to zero. This is primarily due to the higher dilution purge for the nitric-formic flowsheet. More information about these gases will be provided in the nitrogen and carbon offgas sections.

3.2.3.3 Nitrogen Balance

The major nitrogen species include the nitrite and nitrate in the sludge and ARP feeds, the added nitric acid, and the degradation products of NO, N_2O, NO_2, and NH_3. In addition, NH_3 is adsorbed by the nitric acid solution that is circulated through the ammonia scrubber.

The most reactive of the nitrogen species is nitrite. In all runs, the nitrite was completely destroyed in the SRAT cycle. The destruction of nitrite produces offgas (NO, N_2O, and NO_2), nitrate in the condensate and increased nitrate in the SRAT. Once nitrite is decompose to the same eventual nitrogen containing products.

The nitrogen in the feed is summarized in Table 3-18. The nitrogen in the SRAT product and other products is summarized in Table 3-19.

Table 3-18. Nitrogen in Feed to SRAT, mol

FEED:	SB8-D6	SB8-D7	SB8-D8	SB8-D9
Strip Acid	Nitric	Water	Boric	Boric
Sludge total N in nitrite	1.16	1.16	1.16	1.16
Sludge Total N in nitrate	0.54	0.54	0.54	0.54
ARP total N in nitrite	0.04	0.04	0.04	0.04
ARP total N in nitrate	0.12	0.12	0.12	0.12
Total N in HNO3	0.51	0.51	0.97	0.97
Total N in Feed	2.36	2.36	2.82	2.82
Corrected N for Samples	**2.29**	**2.29**	**2.74**	**2.82***

* No sample mass was recorded for preARP sample, so this mass is slightly high

Table 3-19. Nitrogen in SRAT Product, mol

SRAT CYCLE PRODUCTS:	SB8-D6	SB8-D7	SB8-D8	SB8-D9
sludge product nitrate	1.42	1.53	1.94	2.01
NO_x measured (NO + NO_2 + 2*N_2O)	0.54	0.57	0.56	0.55
Scrubber nitrate	0.32	0.14	0.31	0.28
Dewater nitrate	0.30	0.44	0.04	0.50
MWWT nitrate	0.00	0.00	0.00	0.00
Total condensate nitrate	0.61	0.58	0.35	0.78
Total N in NH3, mol	0.065	0.002	0.0183	0.002
total nitrite to offgas, mol	1.22	1.15	0.93	1.34
TOTAL N IN PRODUCTS	2.64	2.69	2.87	3.34
N Delta	-0.36	-0.39	-0.13	-0.52

Table 3-20. Nitrite Decomposition Path

Nitrite Decomposition	SB8-D6	SB8-D7	SB8-D8	SB8-D9
% of nitrite to offgas	45.7%	48.0%	47.3%	46.0%
% nitrite to condensate	51.5%	48.4%	29.2%	65.7%
% nitrite to SRAT nitrate	2.9%	3.5%	23.5%	-11.7%
Acid Calc % nitrite to SRAT nitrate	2.8%	10.7%	15.8%	20.5%

3.2.3.4 Nitrogen Offgas

The predominant nitrogen species measured by the offgas instruments is nitrogen in the air purge. However, nitrogen is inert and does not participate in the reactions. As a result, the other nitrogen offgas species will be discussed. The predominant reactive nitrogen offgas species is NO_2. NO comprised approximately 10-20% of the nitrogen moles, N_2O comprised 20-40% and NO_2 comprised 50-60%. Data for all runs is summarized in Table 3-21.

Table 3-21. Nitrogen Species Production Measured by Offgas Analyzers

Generated Nitrogen Offgas Species	SB8-D6	SB8-D7	SB8-D8	SB8-D9
MS or FTIR NO	12.0%	8.0%	10.8%	21.8%
MS or FTIR NO_2	54.4%	51.1%	50.0%	58.1%
GC N_2O	33.5%	40.9%	39.2%	20.1%

No NH_3 was detected by the FTIR or MS, although a significant quantity of NH_3 was removed by the ammonia scrubber as discussed in section 3.2.3.1. NO, N_2O and NO_2 are all produced through reactions destroying nitrite. The early nitrogen profiles from run SB8-D6 is summarized in Figure 3-16.

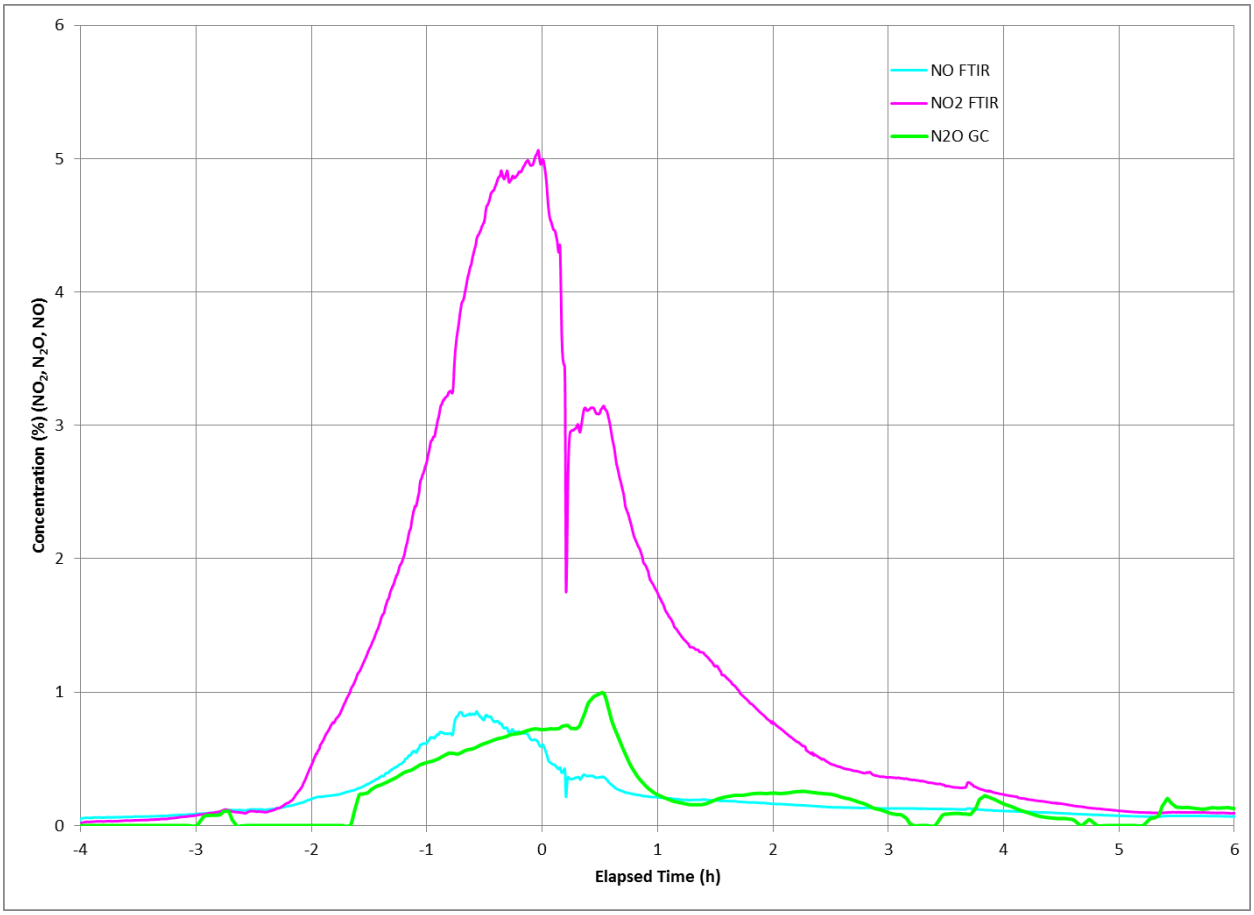

Figure 3-16. Early SRAT Cycle NO, N_2O and NO_2 Concentration for SB8-D6, Volume %

The NO, N_2O and NO_2 generation throughout the rest of the SRAT and SME cycle was very low. The addition of formic acid with the process frit and antifoam in the SME cycle led to higher (but small) NO and N_2O peaks as boiling was approached.

Figure 3-17 is a graph of the NO, N_2O and NO_2 concentration for the end of the SRAT cycle and throughout the SME cycle for run SB8-D6.

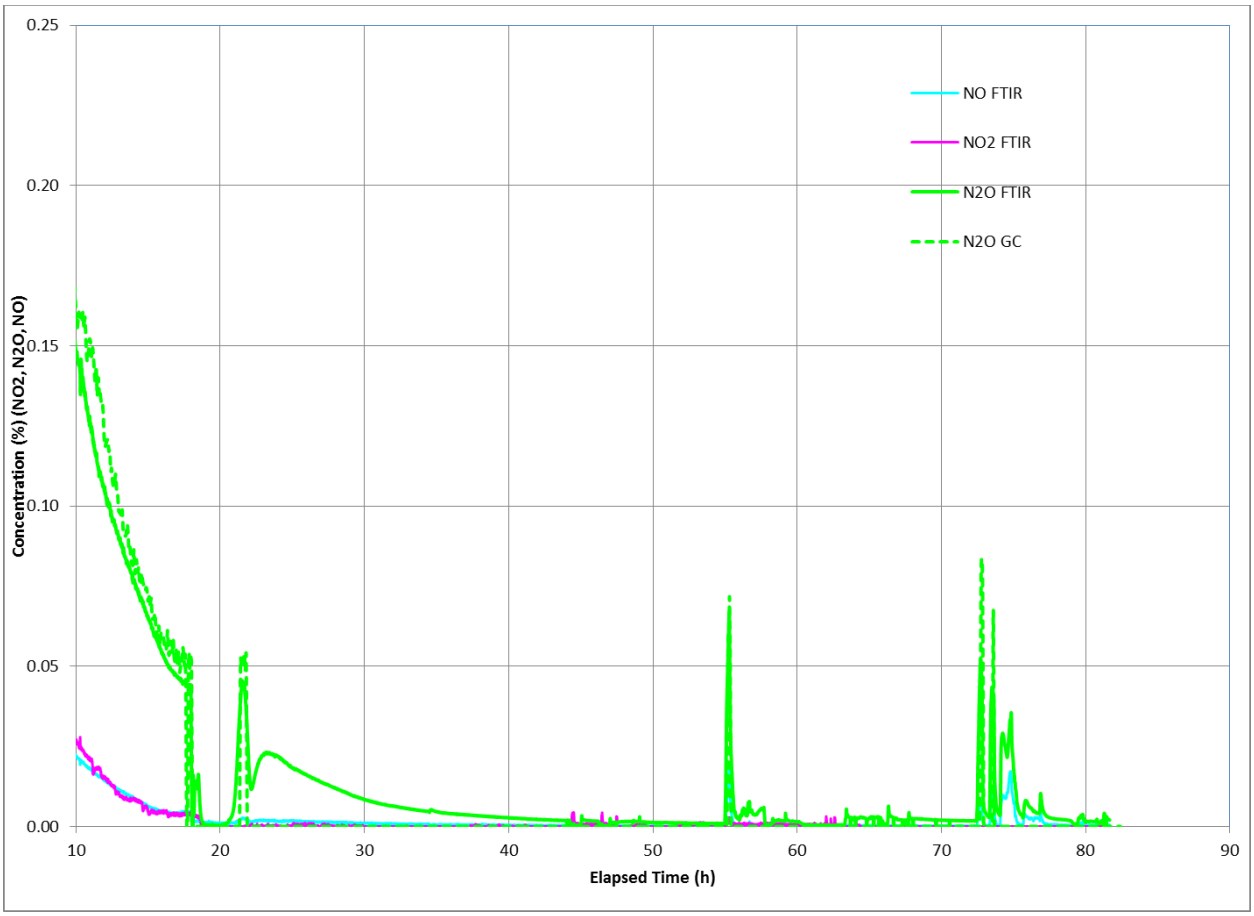

Figure 3-17. Late SRAT and SME Cycle NO, N_2O and NO_2 Concentrations for all runs, Volume %

A graph showing the NO, NO_2, and N_2O concentration for all runs are shown in Figure 3-18, Figure 3-19, and Figure 3-20. Note that the profiles for all runs for these gases are very similar. SB8-D6 and SB8-D8 had bigger NO peaks than SB8-D7 and SB8-D9. The peak in total NO_x emission for all runs occurred near the end or after the formic acid addition.

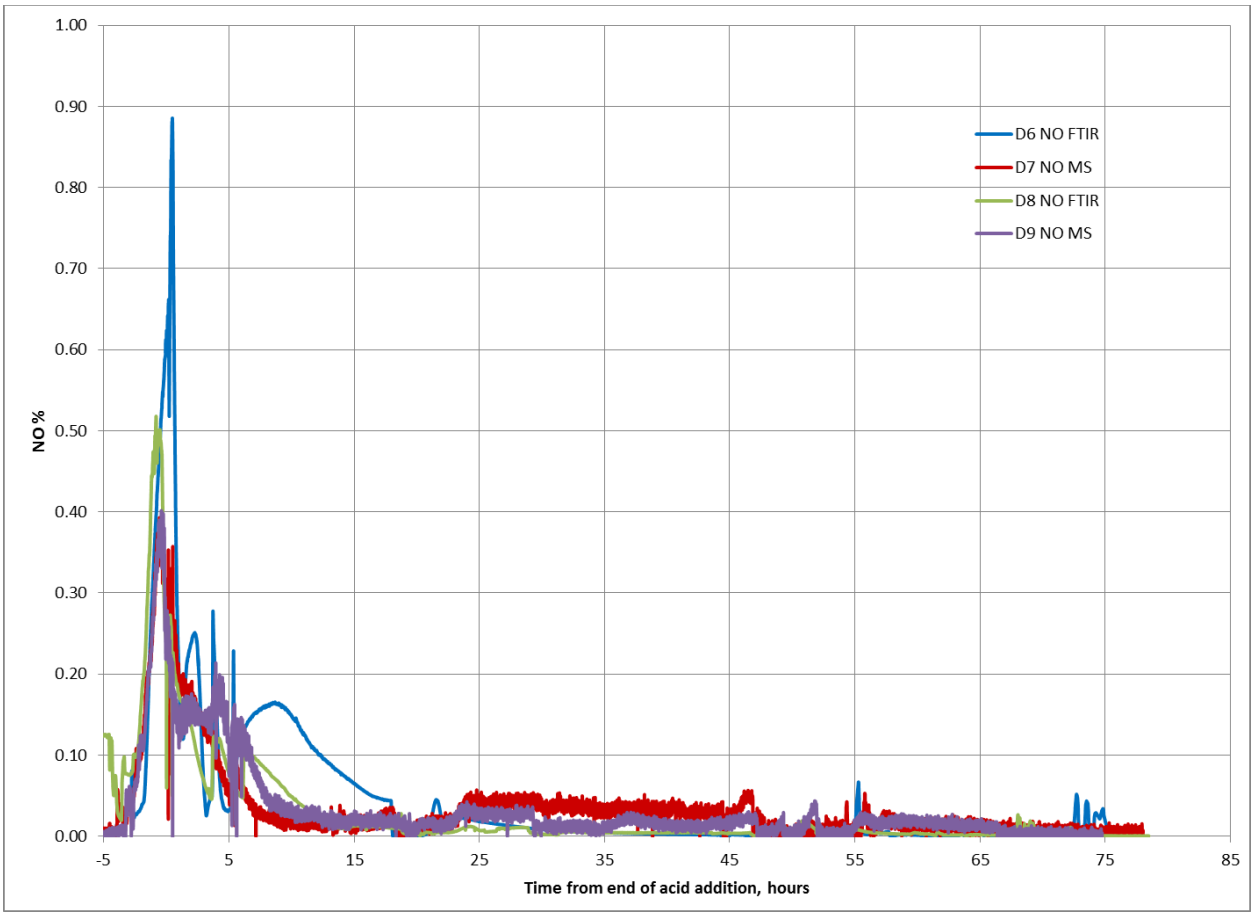

Figure 3-18. SRAT and SME Cycle NO Concentrations for all runs, Volume %

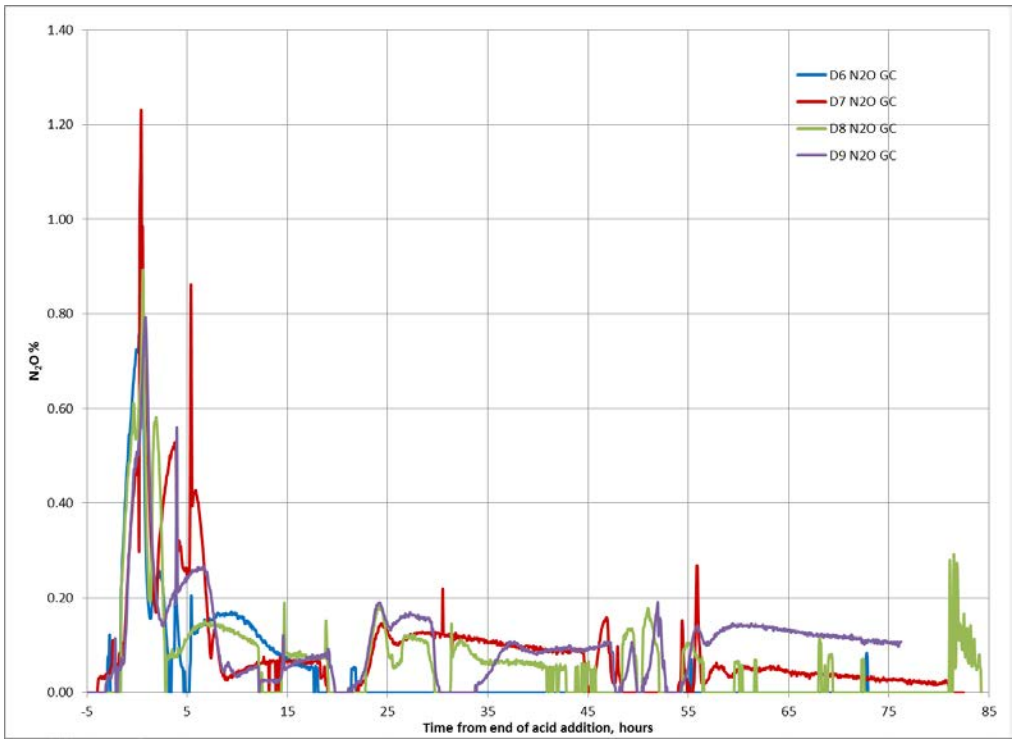

Figure 3-19 SRAT and SME Cycle N_2O Concentrations for all runs, Volume %

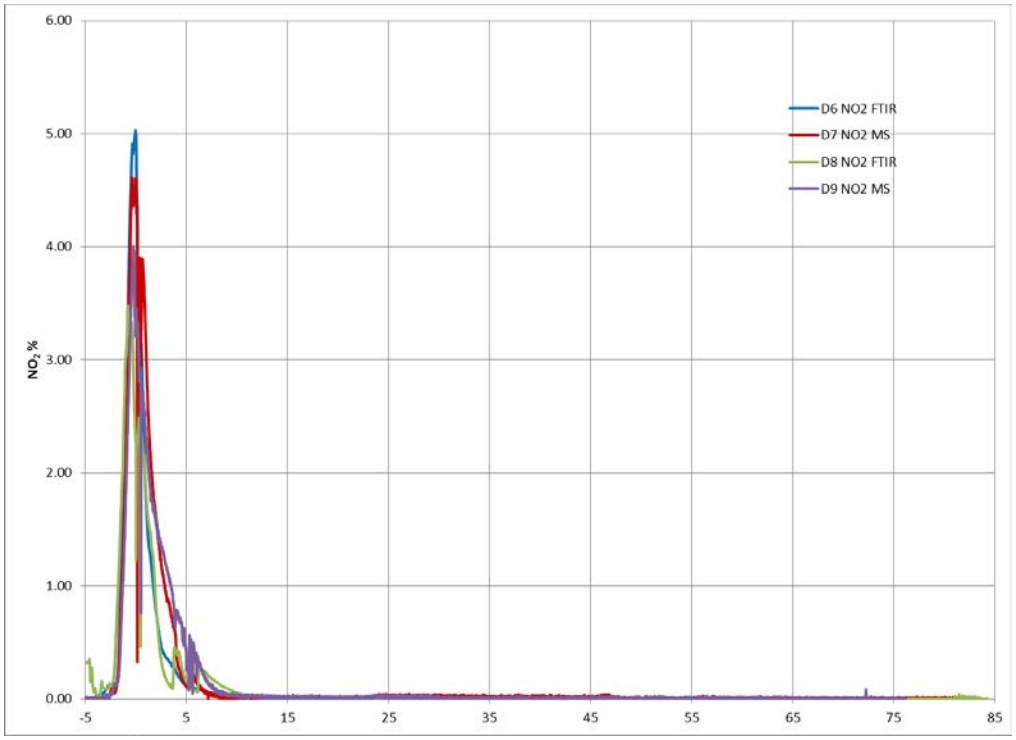

Figure 3-20. SRAT and SME Cycle NO_2 Concentrations for all runs, Volume %

3.2.3.5 SRAT/SME Carbon Results

Total carbon, total inorganic carbon (TIC), and total organic carbon (TOC) were measured by SRNL/AD in the SRAT and SME samples. TIC is essentially a measure of the carbonate in the sample and TOC is a measure of organic species, primarily formate and oxalate. In addition, the TOC can be calculated from the oxalate and formate concentration. The results are summarized in Table 3-22. The TOC results agree well with the calculated TOC results.

Table 3-22. SRAT/SME Organic Carbon Results, mg/kg slurry

TOC Reanalysis	**SB8-D6**	**SB8-D7**	**SB8-D8**	**SB8-D9**
SRAT Product	15,200	15,800	15,300	14,500
SME Product #1	9,480	13,900	11,300	12,200
SME Product #2	5,950	11,100	6,050	11,300
Calculated TOC	**SB8-D6**	**SB8-D7**	**SB8-D8**	**SB8-D9**
SRAT Product	16,300	14,200	14,900	14,800
SME Product #1	9,700	14,900	10,500	12,100
SME Product #2	5,000	11,600	6,200	11,600

Although the carbon dioxide peak is during acid addition, significant carbon dioxide continues to be produced throughout the SRAT and SME cycle. This is due to the catalytic decomposition of formate to hydrogen and CO_2. The data in Table 3-23 summarizes the total inorganic carbon analyses from SRNL/AD.

Table 3-23. SRAT/SME Inorganic Carbon Results, mg/kg slurry

Reanalysis	**SB8-D6**	**SB8-D7**	**SB8-D8**	**SB8-D9**
SRAT Product	3,500	2,490	2,420	2,080
SME Product #1	7,000	4,130	4,000	2,260
SME Product #2	4,930	5,010	4,790	3,370

Note that if formate is decomposing to hydrogen and carbon dioxide, there should be one mole of hydrogen per mole of carbon dioxide. As has been seen in other nitric-formic flowsheet runs, the carbon dioxide generation is much higher than the hydrogen generation. The data is summarized in Figure 3-21.

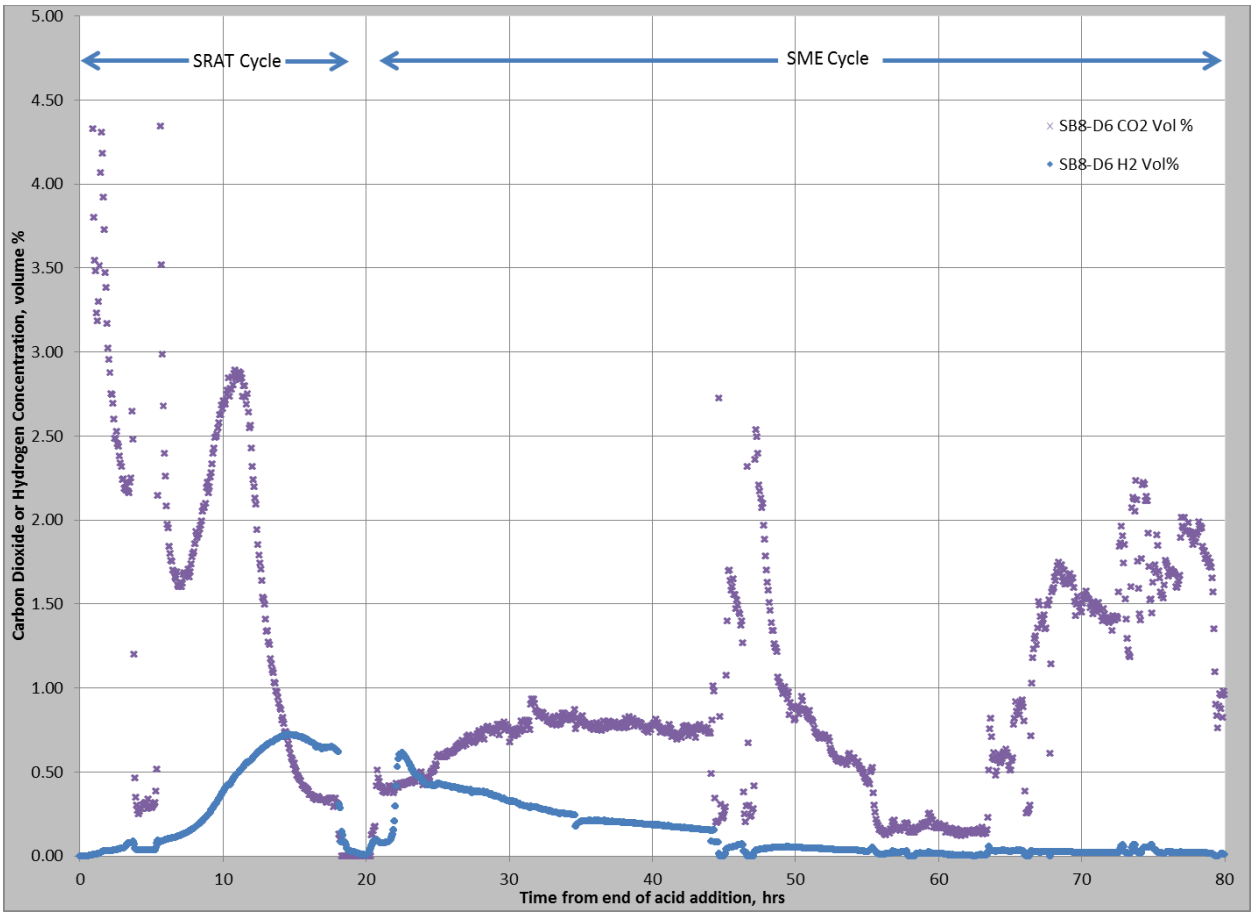

Figure 3-21. SB8-D6 GC Hydrogen and Carbon Dioxide Generation, Volume %

3.2.3.6 Carbon Balance

The major carbon species include the carbonate and oxalate in the sludge and ARP feeds, the added formic acid and antifoam, and the degradation products CO, CO_2, HMDSO (from antifoam degradation) and degraded antifoam. In addition, CO_2 is adsorbed from offgas when the slurries in the SRAT and SME cycles are caustic, so considerable carbonate can be produced during processing.

The carbon in the feed is summarized in Table 3-24. The carbon in the SRAT product is summarized in Table 3-25. The carbon measured by the offgas analyzers is summarized in Table 3-26.

Table 3-24. Carbon in Feed to SRAT, mol C

FEED:	SB8-D6	SB8-D7	SB8-D8	SB8-D9
Sludge CO_3^{--} as C	0.531	0.531	0.531	0.531
ARP NCO_3^{--} as C	0.022	0.022	0.022	0.022
Sludge oxalate as C	0.412	0.412	0.412	0.412
ARP oxalate as C	0.077	0.077	0.077	0.077
Formic added as C	6.309	6.300	5.837	5.840
Total C in Feed	7.352	7.342	6.879	6.883
Post Sample Corrected C	7.120	7.134	6.682	6.883

Table 3-25. Carbon in SRAT Product, mol C

SRAT Product:	SB8-D6	SB8-D7	SB8-D8	SB8-D9
SRAT Product Formate as C	4.121	3.446	3.670	3.614
SRAT Product Oxalate as C	0.248	0.271	0.255	0.262
SRAT Product Carbonate as C	1.014	0.728	0.695	0.598
Total C in SRAT Product	3.490	2.116	2.855	2.234
Lost Carbon	8.873	6.561	7.475	6.708

Table 3-26. Carbon in Offgas

SRAT Product:	SB8-D6	SB8-D7	SB8-D8	SB8-D9
GC CO2, mol	3.489	2.116	2.855	2.234
FTIR CO, mmol	0.000405	Not measured	0.000213	Not measured
FTIR HMDSO, mmol	0.001550	Not measured	0.002214	Not measured

3.2.3.7 Carbon Offgas

The predominant carbon offgas species is CO_2. CO comprised approximately 0.01% of the combined CO and CO_2. The initial CO_2 peak is produced from the decomposition of carbonate. The reductions of mercury, MnO2, and the reduction reaction of nitrite comprise the second peak (nitrite is mostly destroyed by the disproportionation of HNO_2 formed from the acidification of the nitrite. The remainder is destroyed by reduction by formic acid.). The CO2 then slowly decreases at the end of acid addition and the early boiling segment of the SRAT cycle. The early carbon dioxide profile is summarized in Figure 3-22.

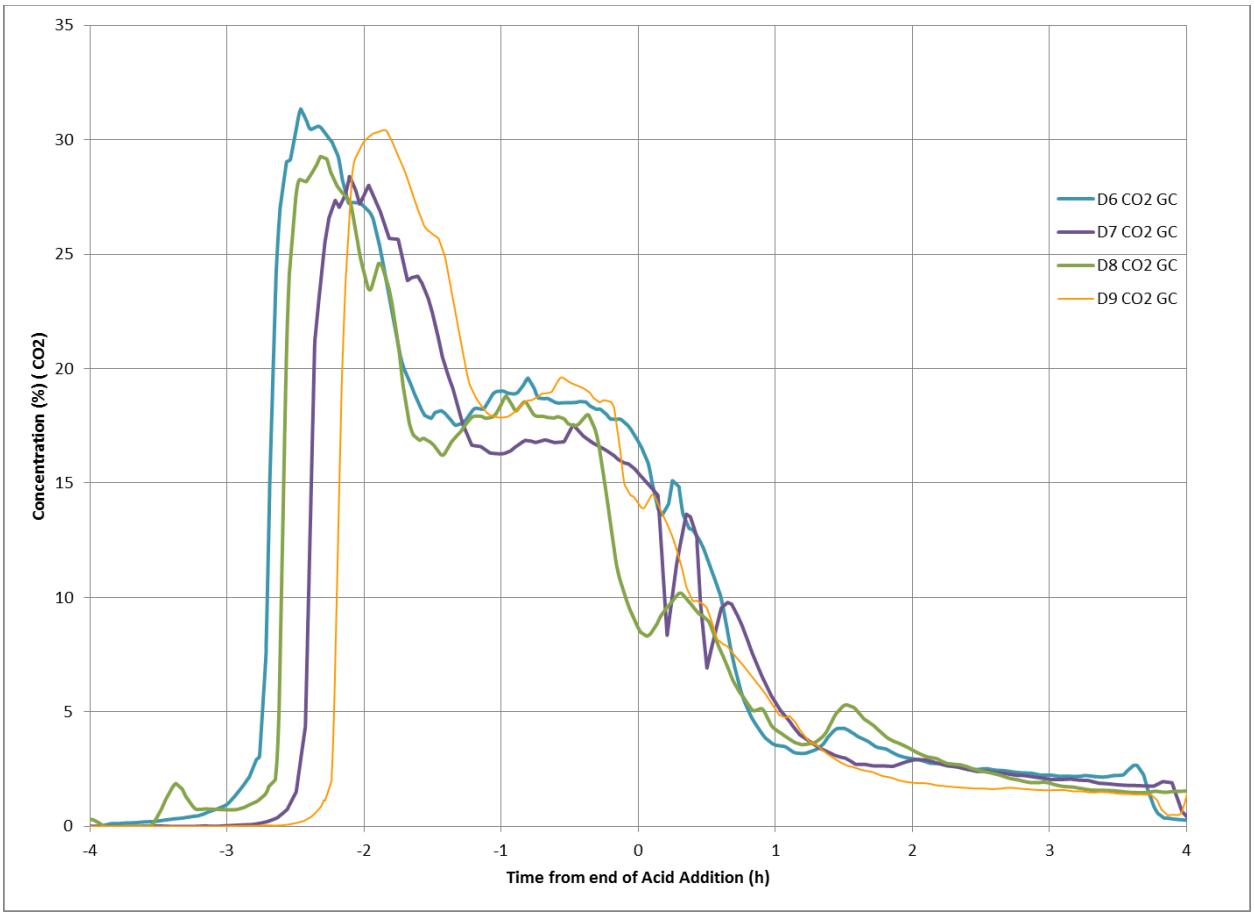

Figure 3-22. Early SRAT Cycle Carbon Dioxide Concentration for all runs, Volume %

The CO_2 generation throughout the rest of the SRAT and SME cycle was significant. The addition of formic acid with the process frit in the SME cycle led to high CO_2 peaks as boiling was approached and to high CO_2 concentrations the last 30 hours of the SME cycles. Figure 3-23 is a graph of the CO_2 concentration for the end of the SRAT cycle and the SME cycle.

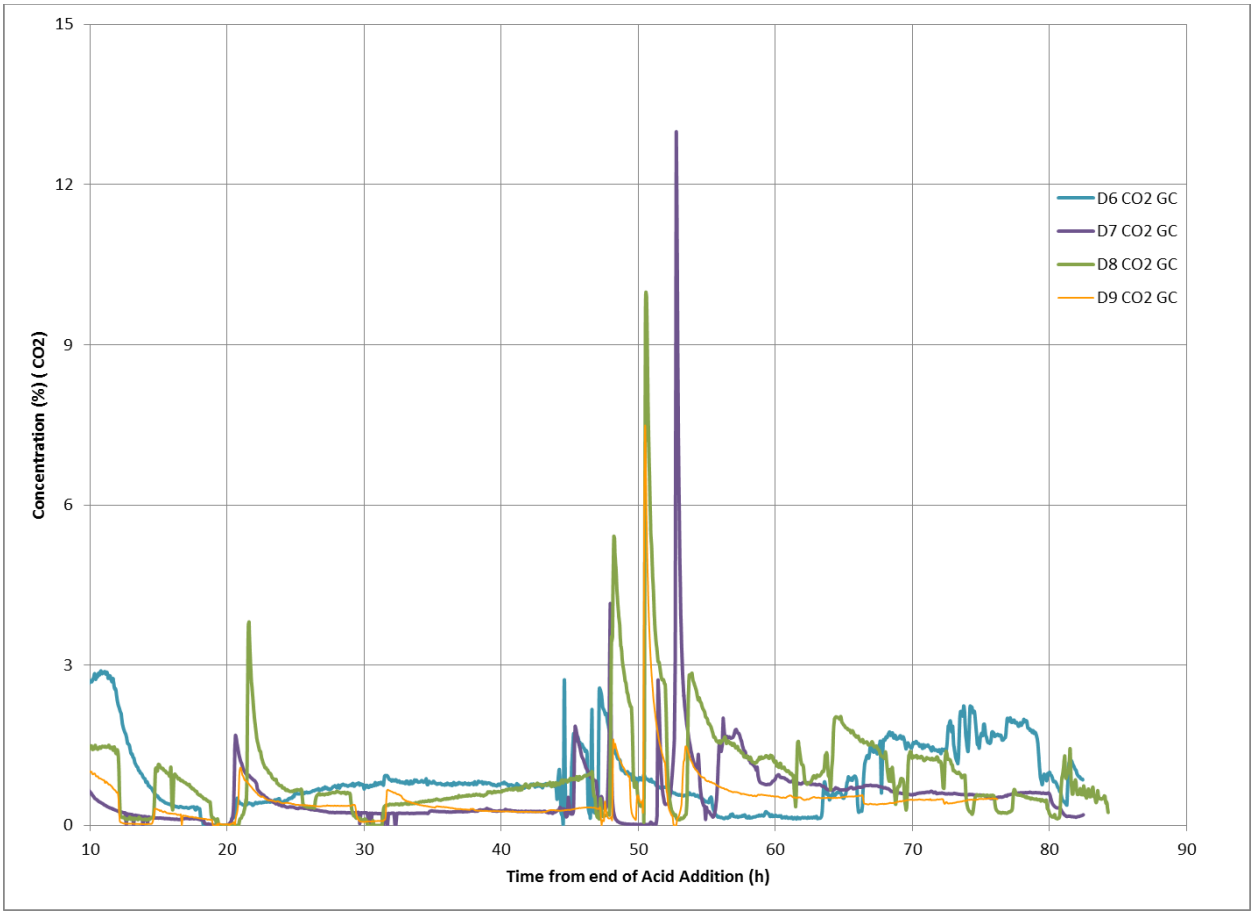

Figure 3-23. Late SRAT and SME Cycle Carbon Dioxide Concentration for all runs, Volume %

3.2.4 SRAT/SME Condensate

The tests generated large quantities of condensate. Approximately 5 liters of condensate were generated in the SRAT cycle and 12 liters of condensate were generated in the SME cycle. The samples were analyzed for both anions (IC) and cations (ICP).

Three condensate samples were pulled during SRAT processing. During ARP addition, approximately 500 mL of condensate was collected before any nitric or formic acid was added. After acid addition is complete, the first phase of boiling is dewatering to the SRAT solids endpoint of 27 wt % total solids. Approximately a liter of condensate is collected during dewater. The last phase of the SRAT cycle is the SE addition phase where the strip effluent is added and condensate is generated at the same rate to keep the volume constant. Approximately 4 liters of condensate is generated. In addition, the MWWT contents are drained at the end of the SRAT cycle. Any condensate collected in the FAVC is also drained.

Three condensate samples were pulled during SME processing. The first phase of the SME cycle was the first SME SE addition. 15,000 gallons of strip effluent was added and the same volume of condensate was generated to maintain constant volume. Approximately 6 liters of condensate is generated. Although process frit typically is added at the completion of the SRAT cycle, process frit was added after the first SME SE addition phase was complete. Two process frit additions and two dewater phases were completed to reach the total solids target of 45 wt % total solids. Approximately a liter of condensate is collected during the process frit dewater. Post SME cycle samples were pulled prior to continuing the last

phase of SME SE addition. The third phase of the SME cycle was a second SME SE addition. 15,000 gallons of strip effluent was added and the same volume of condensate was generated to maintain constant volume. Approximately 5.5 liters of condensate is generated. Any condensate collected in the FAVC is also drained.

3.2.4.1 SRAT/SME Dewater Condensate

SRAT SE Dewater was collected during the SRAT SE dewater phase. The samples were analyzed for anions and cations and the results are summarized in Table 3-27 and Table 3-28.

SME SE Dewater #1 was collected during the first SME SE addition. The samples were analyzed for anions and cations and the results are summarized in Table 3-29 and Table 3-30.

SME Process Frit Dewater was collected during the two process frit additions to target a SME product total solids concentration of 45 wt%. The samples were analyzed for anions and cations and the results are summarized in Table 3-29 and Table 3-30.

SME SE Dewater 2 was collected during the second SME SE addition. The samples were analyzed for anions and cations and the results are summarized in Table 3-29 and Table 3-30.

Table 3-27. Elemental Results of SRAT SE Dewater Condensate Samples, mg/L

Element	D6 SRAT Dewater	D7 SRAT Dewater	D8 SRAT Dewater	D9 SRAT Dewater
SE Acid	Nitric	Water	Boric	Boric
Solvent	Bob	None	Max	Blend
Al	<0.100	0.100	<0.100	0.234
B	<0.100	<0.100	<0.100	<0.100
Ca	0.737	0.785	0.734	2.32
Cr	<0.100	<0.100	<0.100	<0.100
Cu	<0.100	<0.100	<0.100	<0.100
Fe	<0.100	<0.100	<0.100	<0.100
K	<0.100	<0.100	<0.100	0.416
Li	<1.00	<1.00	<1.00	<1.00
Mg	<0.100	<0.100	<0.100	<0.100
Mn	<0.100	<0.100	<0.100	<0.100
Na	0.550	1.80	0.769	4.37
Ni	<0.100	<0.100	<0.100	<0.100
P	<1.00	<1.00	<1.00	<1.00
S	<1.00	<1.00	<1.00	<1.00
Si	127	96.8	151	284
Ti	<0.100	<0.100	<0.100	<0.100
Zn	<0.100	<0.100	<0.100	<0.100
Zr	<0.100	<0.100	<0.100	<0.100

Table 3-28. Anion, pH, Density Results of SRAT SE Dewater Condensate Samples

Element	D6 SRAT SE	D7 SRAT SE	D8 SRAT SE*	D9 SRAT SE
SE Acid	Nitric	Water	Boric	Boric
Solvent	Bob	None	Max	Blend
F, mg/L	<100	<100	<100	<100
Cl, mg/L	<100	<100	<100	<100
NO_2, mg/L	<100	<100	<100	<100
NO_3, mg/L	3,600	5,250	428*	5,830
PO_4, mg/L	<100	<100	<100	<100
C_2O_4, mg/L	<100	<100	<100	<100
HCO_2, mg/L	129	<100	<100	<100
SO_4, mg/L	<100	<100	<100	<100
pH	1.41	0.97	7.26*	0.75
Density, mg/L	1.028	0.995	1.001	1.007

* Sample is suspect due to unusually high pH and unusually low nitrate

Table 3-29. Elemental Results of SME Dewater Condensate Samples, mg/L

Element	D6 SME#1	D7 SME#1	D8 SME#1	D9 SME#1	D6 SME Frit	D7 SME Frit	D8 SME Frit	D9 SME Frit	D6 SME#2	D7 SME#2	D8 SME#2	D9 SME#2
SE Acid	Nitric	Water	Boric	Boric	Nitric	Water	Boric	Boric	Nitric	Water	Boric	Boric
Solvent	Bob	None	Max	Blend	Bob	None	Max	Blend	Bob	None	Max	Blend
Al	<0.100	<0.100	<0.100	0.109	0.202	<0.100	0.100	<0.100	<0.100	<0.100	0.111	0.561
B	<0.100	<0.100	<0.100	<0.100	<0.100	<0.100	<0.100	<0.100	<0.100	<0.100	<0.100	<0.100
Ca	1.37	1.07	0.827	0.749	0.725	0.737	0.785	0.734	0.739	0.807	0.751	1.60
Cr	<0.100	<0.100	<0.100	<0.100	0.166	<0.100	<0.100	<0.100	<0.100	<0.100	<0.100	<0.100
Cu	<0.100	<0.100	<0.100	<0.100	<0.100	<0.100	<0.100	<0.100	<0.100	<0.100	<0.100	<0.100
Fe	<0.100	<0.100	<0.100	<0.100	<0.100	<0.100	<0.100	<0.100	<0.100	<0.100	<0.100	<0.100
K	<0.100	<0.100	<0.100	<0.100	<0.100	<0.100	<0.100	<0.100	<0.100	<0.100	<0.100	0.257
Li	<1.00	<1.00	<1.00	<1.00	<1.00	<1.00	<1.00	<1.00	<1.00	<1.00	<1.00	<1.00
Mg	<0.100	<0.100	<0.100	<0.100	<0.100	<0.100	<0.100	<0.100	<0.100	<0.100	<0.100	<0.100
Mn	<0.100	<0.100	<0.100	<0.100	<0.100	<0.100	<0.100	<0.100	<0.100	<0.100	<0.100	<0.100
Na	2.98	4.33	4.10	0.876	0.515	0.550	1.80	0.769	0.548	4.46	0.864	3.16
Ni	<0.100	<0.100	<0.100	<0.100	<0.100	<0.100	<0.100	<0.100	<0.100	<0.100	<0.100	<0.100
P	<1.00	<1.00	<1.00	<1.00	<1.00	<1.00	<1.00	<1.00	<1.00	<1.00	<1.00	<1.00
S	<1.00	<1.00	<1.00	<1.00	<1.00	<1.00	<1.00	<1.00	<1.00	<1.00	<1.00	<1.00
Si	178	26.3	128	96.0	598	127	96.8	151	72.6	158	115	173
Ti	<1.00	<1.00	<1.00	<1.00	<1.00	<1.00	<1.00	<1.00	<1.00	<1.00	<1.00	<1.00
Zn	<0.100	<0.100	<0.100	<0.100	<0.100	<0.100	<0.100	<0.100	<0.100	<0.100	<0.100	<0.100
Zr	<0.100	<0.100	<0.100	<0.100	<0.100	<0.100	<0.100	<0.100	<0.100	<0.100	<0.100	<0.100

Table 3-30. Anion, pH, and Density Results of SME Condensate Samples

Anion	D6 SME# 1	D7 SME# 1	D8 SME# 1	D9 SME# 1	D6 SME Frit	D7 SME Frit	D8 SME Frit	D9 SME Frit	D6 SME# 2	D7 SME#2	D8 SME# 2	D9 SME# 2
SE Acid	Nitric	Water	Boric	Boric	Nitric	Water	Boric	Boric	Nitric	Water	Boric	Boric
Solvent	Bob	None	Max	Blend	Bob	None	Max	Blend	Bob	None	Max	Blend
F, mg/L	<100	<100	<100	<100	<100	<100	<100	<100	<100	<100	<100	<100
Cl, mg/L	<100	<100	<100	<100	<100	<100	<100	<100	<100	<100	<100	<100
NO_2, mg/L	<100	<100	<100	<100	<100	<100	<100	<100	<100	<100	<100	<100
NO_3, mg/L	<100	<100	<100	<100	<100	<100	<100	<100	141	<100	<100	<100
PO_4, mg/L	<100	<100	<100	<100	<100	<100	<100	<100	<100	<100	<100	<100
C_2O_4, mg/L	<100	<100	<100	<100	<100	<100	<100	<100	<100	<100	<100	<100
HCO_2, mg/L	<100	<100	<100	<100	<100	<100	<100	<100	<100	<100	<100	<100
SO_4, mg/L	<100	<100	<100	<100	<100	<100	<100	<100	<100	<100	<100	<100
pH	9.69	7.79	8.71	6.61	9.84	8.23	8.36	5.60	9.93	9.06	9.26	8.34
Density, mg/L	1.00	1.01	1.01	1.01	1.01	1.01	1.00	1.01	1.01	1.01	1.00	1.01

The SRAT Dewater samples analyzed had a high nitrate concentration and a low pH (equivalent to a 0.01-1.0 M nitric acid solution). No other anions were above the detection limit. The largest concentration of cation detected in the condensate was Si, likely an antifoam degradation product. The concentration of calcium and sodium was just above detection limits for all samples.

In contrast, the SME Dewater samples analyzed had a low nitrate concentration (typically below detection limit) and a high pH (5.6-9.9). No anion other than nitrate was above the detection limit. The largest concentration of cation detected in the condensate was Si, likely an antifoam degradation product. The concentration of calcium and sodium was just above detection limits for all samples.

3.2.4.2 MWWT and FAVC Condensate Samples

The MWWT was filled to overflow with DI water before the SRAT cycle began. After the SRAT cycle, the MWWT was drained to a sample bottle and the solids (primarily mercury) were separated from the condensate. The aqueous sample was submitted for anion and cation analysis. The results are summarized in Table 3-31 and Table 3-32. The mercury was placed in a dessicator and reweighed to determine the mass of Hg collected. Note that the MWWT aqueous is very similar to the SRAT SE dewater aqueous as there was such a large quantity of dewater that passed through the MWWT.

A small quantity of condensate is collected in the FAVC. The FAVC was drained to a sample bottle at the completion of the SRAT and the SME cycle. The results are summarized in Table 3-31 and Table 3-32.

Table 3-31. Elemental Results of MWWT and FAVC Condensate Samples, mg/L

Element	D6 MWWT	D7 MWWT	D8 MWWT	D9 MWWT	D6 SRAT FAVC	D7 SRAT FAVC	D8 SRAT FAVC	D9 SRAT FAVC	D6 SME FAVC	D7 SME FAVC	D8 SME FAVC	D9 SME FAVC
SE Acid	Nitric	Water	Boric	Boric	Nitric	Water	Boric	Boric	Nitric	Water	Boric	Boric
Solvent	Bob	None	Max	Blend	Bob	None	Max	Blend	Bob	None	Max	Blend
Al	<0.100	<0.100	2.17	0.428	0.465	<0.100	0.112	<0.100	<0.100	4.10	0.465	<0.100
B	<0.100	<0.100	<0.100	<0.100	<0.100	<0.100	<0.100	<0.100	<0.100	<0.100	<0.100	<0.100
Ca	0.816	0.728	1.34	1.10	0.770	0.741	0.908	0.741	0.723	0.889	0.770	0.741
Cr	<0.100	<0.100	<0.100	<0.100	<0.100	<0.100	<0.100	<0.100	<0.100	0.350	<0.100	<0.100
Cu	<0.100	<0.100	<0.100	0.120	0.105	<0.100	<0.100	<0.100	<0.100	2.48	0.105	<0.100
Fe	<0.100	<0.100	<0.100	<0.100	<0.100	<0.100	<0.100	<0.100	<0.100	0.232	<0.100	<0.100
K	<0.100	<0.100	<0.100	<0.100	<0.100	<0.100	<0.100	<0.100	<0.100	<0.100	<0.100	<0.100
Li	<1.00	<1.00	<1.00	<1.00	<1.00	<1.00	<1.00	<1.00	<1.00	<1.00	<1.00	<1.00
Mg	<0.100	<0.100	<0.100	<0.100	<0.100	<0.100	<0.100	<0.100	<0.100	<0.100	<0.100	<0.100
Mn	<0.100	<0.100	<0.100	<0.100	<0.100	<0.100	<0.100	<0.100	<0.100	<0.100	<0.100	<0.100
Na	4.55	0.960	1.83	5.23	2.38	1.15	4.75	0.690	0.600	1.28	2.38	1.15
Ni	<0.100	<0.100	<0.100	<0.100	<0.100	<0.100	<0.100	<0.100	<0.100	0.319	<0.100	<0.100
P	<1.00	<1.00	<1.00	<1.00	<1.00	<1.00	<1.00	<1.00	<1.00	<1.00	<1.00	<1.00
S	<1.00	<1.00	<1.00	<1.00	<1.00	<1.00	<1.00	<1.00	<1.00	<1.00	<1.00	<1.00
Si	240	188	154	135	232	91.0	130	198	195	53.8	232	91.0
Ti	<1.00	<1.00	<1.00	<1.00	<1.00	<1.00	<1.00	<1.00	<1.00	<1.00	<1.00	<1.00
Zn	<0.100	<0.100	<0.100	<0.100	<0.100	<0.100	<0.100	<0.100	<0.100	<0.100	<0.100	<0.100
Zr	<0.100	<0.100	<0.100	<0.100	<0.100	<0.100	<0.100	<0.100	<0.100	<0.100	<0.100	<0.100

Table 3-32. Anion, pH, Density Results of MWWT and FAVC Condensate Samples

Anion	D6 MWWT	D7 MWWT	D8 MWWT	D9 MWWT	D6 SRAT FAVC	D7 SRAT FAVC	D8 SRAT FAVC	D9 SRAT FAVC	D6 SME FAVC	D7 SME FAVC	D8 SME FAVC	D9 SME FAVC
SE Acid	Nitric	Water	Boric	Boric	Nitric	Water	Boric	Boric	Nitric	Water	Boric	Boric
Solvent	Bob	None	Max	Blend	Bob	None	Max	Blend	Bob	None	Max	Blend
F, mg/L	<100	<100	<100	<100	<100	<100	<100	<100	<100	<100	<100	<100
Cl, mg/L	<100	<100	<100	<100	<100	<100	<100	<100	<100	<100	<100	<100
NO_2, mg/L	<100	<100	<100	<100	<100	<100	<100	<100	<100	<100	<100	<100
NO_3, mg/L	376	132	<100	<100	256,000	286,000	247,000	306,000	10,800	33,100	22,300	31,500
PO_4, mg/L	<100	<100	<100	<100	<100	<100	<100	<100	<100	<100	<100	<100
C_2O_4, mg/L	<100	<100	<100	<100	<100	<100	<100	<100	<100	<100	<100	<100
HCO_2, mg/L	<100	<100	<100	<100	<100	<100	<100	<100	<100	<100	<100	<100
SO_4, mg/L	<100	<100	<100	<100	<100	<100	<100	<100	<100	<100	<100	<100
pH	9.78	8.87	9.79	7.21	2.64	2.51	2.67	2.55	0.83	0.45	0.39	0.30
Density, mg/L	1.003	1.001	1.007	1.024	1.166	1.171	1.115	1.165	1.006	1.019	1.011	1.024

The post SRAT MWWT samples analyzed were low in nitrate and high in pH (7.2-9.8). No other anions were above the detection limit. The largest concentration of cation detected in the condensate was Si, likely an antifoam degradation product. The concentration of calcium and sodium was just above detection limits for all samples.

The SRAT and SME FAVC samples analyzed had a high nitrate concentration and a low pH (0.8-2.7). Note that the nitrate concentration was much lower in the SME FAVC samples. No other anion was above the detection limit. The largest concentration of cation detected in the condensate was Si, likely an antifoam degradation product. The concentration of calcium and sodium was just above detection limits for all samples.

The mercury collected in the MWWT varied from 14-31%. This is much higher than is typical of DWPF processing where little mercury accumulates in their MWWT. The SRAT MWWT collected mercury is summarized in Table 3-33.

Table 3-33. MWWT Mercury Balance

MWWT	SB8-D6	SB8-D7	SB8-D8	SB8-D9
Mercury Added, g	6.60	6.60	6.61	6.60
MWWT Mercury, g	1.68	2.05	1.99	0.92
%Mercury Recovered	25.5%	31.0%	30.1%	13.9%

.

3.2.4.3 SRAT/SME Ammonia Results

Ammonia is generated in a series of catalytic reduction reactions in the SRAT and SME slurry that converts nitrate to more reducing species, including NH_3. Ammonia could build up in the offgas system as ammonium nitrate (potentially explosive), so ammonia scrubbers are installed in DWPF. The ammonia is scrubbed using a pH 1-3 nitric acid solution so the scrubbed ammonia is present as ammonium (NH_4^+).

The data is summarized in Table 3-34. Note that in the two runs with high hydrogen generation (SB8-D6 and SB8-D8), there was also higher ammonia production.

Table 3-34. Ammonium analysis of SRAT and SME Products and Ammonia Scrubber

Sample	Product Mass, g	NH_4^+ Result, mg/L	Scrubber Mass, g	NH_4^+ Result, mg/L
SB8-D6 SRAT	3,480.71	<100	751.29	274
SB8-D6 SME# 1	3,554.57	<100		
SB8-D6 SME# 2	3,802.25	<100	751.30	1,660
SB8-D7 SRAT	3,510.11	<100	751.47	2
SB8-D7 SME# 1	3,536.17	<100		
SB8-D7 SME# 2	3,770.62	<100	751.37	42
SB8-D8 SRAT	3,449.03	<100	733.85	157
SB8-D8 SME# 1	3,463.70	<100		
SB8-D8 SME# 2	3,720.33	<100	733.61	710
SB8-D9 SRAT	3,453.78	<100	724.01	655
SB8-D9 SME# 1	3,473.87	<100		
SB8-D9 SME#2	3,724.66	<100	722.95	55

No ammonia is present in the sludge simulant. Ammonia is produced in the SRAT or SME cycle by reducing nitrate to ammonia. The degree to which ammonia or ammonium ion is present depends on the pH of the solution. If the pH is low, the equilibrium shifts to the right: more ammonia molecules are converted into ammonium ions. If the pH is high (the concentration of hydrogen ions is low), the equilibrium shifts to the left: the hydroxide ion removes a proton from the ammonium ion, generating ammonia.

$$H_3O^+ + NH_3 \rightleftharpoons H_2O + NH_4^+$$

The equilibrium between ammonia and ammonium is controlled by pH. For solutions where the pH is <7, the equilibrium is almost completely on the right side of the equation (i.e. all ammonium, no ammonia). As the pH increases above pH 7, the equilibrium shifts to the left as shown in Figure 3-24. The equilibrium equation is:

$$\frac{[NH_3]*[H+]}{[NH_4+]} = 5.7\text{x}10^{-10}$$, where the concentrations of NH_3, H^+ and NH_4^+ are in mol/L[11]

This suggests the pH limit for the SMECT can be much higher than the current limit of 1-3. A better pH upper limit might be 5 or 6. At pH 3, 0.000057% of the species exists as ammonia. At pH 6, 0.057% of the species exists as ammonia. At pH 1, assuming pure nitric acid, the SMECT condensate is 0.1 M. At a SMECT volume of 3,000 gallons, the solution is capable of dissolving 114 kg mercury. The mass of mercury in DWPF sludge batch 735 is 78.2 kg of mercury. Thus, even at heel, the SMECT at pH 1 can dissolve all the mercury in a SRAT batch. At pH 6, the SMECT could only dissolve 1/100,000th as much mercury or 0.00114 kg (1.14 g).

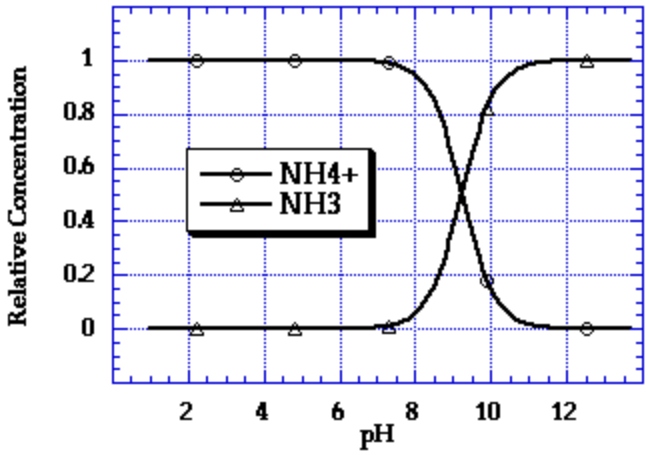

Figure 3-24. Equilibrium between ammonia and ammonium at 25˚C.

During the SRAT cycle, the pH reaches a minimum at the completion of acid addition and then slowly increases throughout the SRAT and SME cycle. As the slurry pH increases from acidic to basic, the equilibrium shifts from ammonium to ammonia. The ammonia is released to the offgas and is removed from the offgas by the ammonia scrubbers. The pH of the slurry was high by the end of the SRAT cycle (~9) and very high throughout the SME cycle (~10).

No ammonium was detected in the SRAT or SME slurries. This is because the pH was too high to retain appreciable ammonium. Ammonia generated in the slurry was likely retained for just a short time.

No ammonia was detected by the FTIR. This is likely due to near complete ammonia adsorption in the ammonia scrubber (although there could also be ammonia adsorption or removal in the Perma Pure Nafion® gas dryer). The ammonia scrubbers were designed to adsorb at least 99.9% of the ammonia, so the detection of no ammonia in the offgas is expected.

Considerable ammonium was measured in the ammonia scrubber solution, ranging from 0.03 g NH_4^+in SB8-D7 to 1.22 g in SB8-D6 (40 times more NH_4^+in SB8-D7 than SB8-D6). This is 0.06-2.34% of the added nitrogen species from the sludge and nitric acid. The mass of ammonium recovered in the experiments are summarized in Table 3-35. The time at boiling in the SME cycles was about twice as long as the SRAT cycles and the bulk of the ammonia was scrubbed in the SME cycles (66-95%). The extended processing in the SME cycles led to much higher ammonia generation and necessitated more scrubbing, consistent with expectations.

Table 3-35. Post SME Ammonia Mass Balance

	SB8-D6	**SB8-D7**	**SB8-D8**	**SB8-D9**
SME Product NH_4^+ Mass, g	None Detected			
Ammonia Scrubber NH_4^+ Mass, g	1.22	0.03	0.34	0.04
Offgas NH_3 mass, g	None Detected			
Total Mass NH_4^+ Mass, g	1.22	0.03	0.34	0.04
% of nitrogen species	2.34%	0.06%	0.65%	0.08%

The ammonia scrubber samples were also analyzed for anions. The results are summarized in Table 3-36. Note also that the presence of formate, chloride, sulfate and oxalate in the SB8-D7 SME product was due to a foamover.

Table 3-36. Ammonia Scrubber Anions, mg/L

Sample SB8-	Formate	Chloride	Nitrate	Sulfate	Oxalate
D6 SRAT	<10	<10	26,000	<10	<10
D6 SME	<10	<10	26,000	<10	<10
D7 SRAT	<10	<10	11,700	<10	<10
D7 SME	10,100	113	14,200	322	333
D8 SRAT	11	<10	25,800	<10	<10
D8 SME	10	<10	25,200	<10	<10
D9 SRAT	36	<10	23,500	<10	<10
D9 SME	37	<10	23,200	<10	<10

Note: Br, nitrite, phosphate, fluoride were below detection limits in all samples

There was a foamover in the SB8-D7 SME cycle as noted above. It is the run with the highest formate, nitrate, chloride, sulfate, and oxalate in the scrubber solution. Note it would have taken a foamover of approximately 330-500 g (to 750 g of scrubber liquid) to increase the concentration of formate to 14,200 in the scrubber liquid.

A nitrate balance was performed in the ammonia scrubber. The ammonia scrubber was isolated from the rest of the condensate in these experiments. The ammonia scrubber is effective at serving as both a secondary heat exchanger in DWPF (due to the undersizing of the SRAT and SME scrubbers) and for scrubbing both particles and soluble species from the offgas. Nitrate is the main species that is scrubbed by the scrubbers. The nitrate is scrubbed during the period of high NO_x generation (late formic addition to SRAT dewater). Approximately 0.65 g of nitrate was added to 750 g of scrubber liquid to start the solution pH at about 1.7. During SRAT and SME process, the nitrate concentration increased from about 850 mg/L to 26,000 mg/L by the completion of the SRAT cycle (approximately 30x increase in concentration). The mass of nitrate in the SME scrubber sample was lower than the SRAT sample, likely due to dilution by scrubbed water. The mass balance for the nitrate in the scrubber system is shown in Table 3-37.

Table 3-37. Scrubber Nitrate Mass Balance

Scrubber Nitrate Mass Balance	SB8-D6	SB8-D7	SB8-D8	SB8-D9
Starting Ammonia Scrubber NO_3^-, mols	0.016	0.016	0.017	0.017
Starting Ammonia Scrubber NO_3^-, M	0.021	0.021	0.022	0.022
Starting Ammonia Scrubber NO_3^-,pH	1.68	1.68	1.65	1.65
Starting Ammonia Scrubber NO_3^- Mass, g	0.634	0.637	0.669	0.669
SRAT Ammonia Scrubber NO_3^- Mass, g	19.534	8.790	19.388	17.657
SME Ammonia Scrubber NO_3^- Mass, g	19.080	10.417	18.245	16.772
Delta SRAT Scrubber NO_3^- Mass, g	18.446	9.780	17.576	.16.103
x Increase in Nitrate	30.1	16.4	27.3	25.1

3.2.5 Overall Condensate Balance

An overall condensate balance was completed to predict the pH of the resulting SMECT by summing up the hydrogen ion concentrations of all the streams that would drain to the SMECT. The condensate

balance in these runs is summarized in Table 3-38. The predicted pH of all condensate streams varied from 1.3-1.7 for the four runs. This suggests that the addition of nitric acid is not needed in the SMECT for pH control. The pH of the SMECT is controlled by the nitric acid scrubbing of the offgas in the SRAT cycle. Adding more nitric acid to the SMECT than needed may lead to dissolving the SMECT mercury, which would lead to returning the mercury back to the tank farm through the RCT. Minimizing the addition of nitric to the SMECT should lead to the accumulation of more elemental mercury in the SMECT. Nitric acid may still need to be added to the SMECT if a foamover occurs.

Table 3-38. Condensate Mass Balance, g

Condensate Mass Balance	SB8-D6	SB8-D7	SB8-D8	SB8-D9
ARP Dewater	403.4	401.7	450.8	452.5
SRAT Dewater	952.9	982.9	953.2	953.1
SRAT SE Dewater	3,796.7	3,796.9	3,797.9	3,806.7
MWWT	44.2	41.0	31.5	35.1
SRAT FAVC	23.0	17.4	21.2	17.2
SME#1 Dewater	6,666.5	6,041.2	6,055.0	6,055.0
SME Process Frit Dewater	749.6	802.7	813.9	834.3
SME#2 Dewater	5,540.4	4,672.9	4,667.4	5,560.1
SME FAVC	32.9	12.5	10.3	8.6
Post SME Ammonia Scrubber	751.3	751.3	751.5	751.4
Total Mass, all condensate	18,960.9	17,520.5	17,552.7	18,473.9

3.2.6 SME Product REDOX Discussion

It should be noted that although the total moles of acid added during acid addition remained constant, the formic/total acid ratio was 0.8513 in runs SB8-D6 and SB8-D7 and 0.7945 for runs SB8-D8 and SB8-D9. This means the targeted REDOX for runs SB8-D6 and SB8-D7 (0.20 $Fe^{+2}/\Sigma Fe$) was more reducing than runs SB8-D8 and SB8-D9 (0.10 $Fe^{+2}/\Sigma Fe$).

Three product samples were pulled from each run (one SRAT product, one SME product after 15,000 gal SE, and a second SME product after 30,000 gal SE). The REDOX was predicted based on the product analyses. In the cases of the SRAT products, the SME product was predicted knowing the SRAT product analysis and the addition of frit to give a 36% waste loading.

The REDOX equation used for the predictions was:

$$REDOX\ ratio = Fe^{2+}/\sum Fe = 0.2358 + 0.1999 * (2F + 4C + 4O - 5N - 5Mn) * 45/T$$

F = formate (mol/kg feed)
C = coal (carbon) (mol/kg feed)
O = oxalate (soluble and insoluble) (mol/kg feed)
N = nitrate (mol/kg feed)
Mn = manganese (mol/kg feed)
T = Total Solids (wt %)

In addition to the calculations above, glass was produced and the concentration of both Fe^{+2} and total Fe were measured to calculate the REDOX ratio. Note that for the SRAT samples, frit was added to the SRAT product to produce a melter feed at 36 wt% waste loading. All samples were melted per the REDOX procedure[12] and the resulting glass was analyzed to determine the relative concentration of Fe^{+2} and total Fe[13] (REDOX ratio). The data necessary for calculating the predicted REDOX and the measured REDOX are summarized in Table 3-39.

Table 3-39. Summary of Predicted and Measured REDOX

	Total Solids, wt%	SRAT/SME Product Formate, gmol/kg	SRAT/SME Product Oxalate, gmol/kg	SRAT/SME Product Nitrate, gmol/kg	SRAT/SME Product Mn, gmol/kg	REDOX Target, $Fe^{+2}/\Sigma Fe$	Predicted Glass REDOX*, $Fe^{+2}/\Sigma Fe$	Measured Glass REDOX, $Fe^{+2}/\Sigma Fe$
D6 SRAT	26.50%	0.903	0.054	0.311	0.187	0.2	0.140	Not Measured
D6 SME #1	45.60%	0.631	0.064	0.311	0.209		0.022	
D6 SME #2	37.90%	0.320	0.039	0.227	0.172		-0.049	<0.03
D7 SRAT	27.00%	0.746	0.059	0.332	0.185	0.2	0.063	Not Measured
D7 SME #1	52.00%	1.033	0.072	0.366	0.218		0.138	
D7 SME #2	49.20%	0.795	0.063	0.302	0.207		0.108	0.067
D8 SRAT	27.00%	0.805	0.056	0.426	0.163	0.1	0.012	Not Measured
D8 SME #1	45.00%	0.702	0.062	0.411	0.178		-0.023	
D8 SME #2	35.50%	0.398	0.046	0.285	0.143		-0.060	<0.03
D9 SRAT	27.60%	0.788	0.057	0.437	0.171	0.1	-0.009	Not Measured
D9 SME #1	46.30%	0.833	0.062	0.466	0.183		-0.023	
D9 SME #2	47.70%	0.786	0.064	0.463	0.188		-0.033	<0.03

* A predicted glass REDOX ratio of <0 is not possible but is shown in this table to demonstrate how oxidizing the feeds are (i.e. a predicted REDOX of -0.060 is more oxidizing than a predicted REDOX of -0.023). Any predicted REDOX of less than 0.03 can be reported as <0.03. DWPF REDOX range is 0.09-0.33.

Note that the REDOX ratio ($Fe^{+2}/\Sigma Fe$) can only vary from 0 to 1. A REDOX ratio of zero is very oxidizing while a ratio of one is very reducing. The measured REDOX agreed well with the predicted REDOX. Although the predictive REDOX negative result is shown in the second to last column in Table 3-39, the limit for the REDOX measurement is approximately 0.03 so the oxidized glass REDOX is reported as <0.03. Only the SB8-D7 SME product had a REDOX ratio that was above the detection limit.

The acid (mol % reducing acid) mix is adjusted to reach the REDOX target. The concentration of formate (reducing acid) and nitrate (oxidizing acid) control the glass REDOX as they are the only significant additions that impact REDOX. Due to the long processing times and the high noble metal concentration, the nitrate concentration was fairly constant (see runs SB8-D7 and SB8-D9), while the formate concentration decreased. The result was that the SME products had a lower REDOX than expected. It also should be noted that the predicted REDOX dropped as processing continued (SRAT REDOX>SME#1 REDOX> SME#2 REDOX). The REDOX changed from SRAT product to SME#2 varied from -0.024 to -0.19. In the runs SB8-D6 and SB8-D8, the formate concentration dropped by half or more. This makes hitting the REDOX target challenging as it depends on the volume of strip effluent added.

3.3 Observations Related to DWPF Processing

In the course of this testing, several observations were made that do not directly involve processing strip effluent in the SME but rather are related to improving processing of the nitric-formic flowsheet in DWPF. The following is a summary of potential improvements to routine DWPF processing:

- The addition of 1.5 wt % formic acid with the frit slurry should be eliminated to reduce hydrogen generation in DWPF SME cycles. If an acid is needed to prevent clumping and minimize frit leaching during makeup and storage of the process frit slurry in the frit makeup tank, use the minimum quantity necessary to minimize the amount of hydrogen produced in the SME cycle.
- The addition of nitric acid to the SMECT should be minimized. Based on these experiments using an SB8 simulant, adequate nitric acid is scrubbed during processing to keep the SMECT at a sufficiently low pH for optimum scrubbing. This should lead to the accumulation of more elemental mercury in the SMECT. Nitric acid may still need to be added if a foamover occurs.
- Consideration should be given to expanding the SMECT pH limits to ≤6. Operating the SMECT at a higher pH would minimize the dissolution of mercury in the SMECT and likely would lead to less mercury returned to the tank farm.

One potential improvement postulated prior to this testing was that the strip effluent could be added to the SRAT or SME cycle at temperatures below boiling if testing showed that volatile components did not accumulate at a lower temperature (94.5 °C). Due to the apparent accumulation of Isopar-L during the SRAT cycle, there is no justification for decreasing the minimum TSR required temperature for adding SE from boiling to 94.5 °C.

4.0 Conclusions

SRR plans to add strip effluent to the SRAT and/or the SME during processing in the DWPF. At the present time, strip effluent is added only to the SRAT, but this flowsheet change is planned to allow more flexibility in processing the large volume of strip effluent produced by the MCU or the SWPF.

Four process demonstrations of the coupled flowsheet for SRAT and SME cycles were performed using SB8-Tank 40 simulant. These runs were patterned after run SB8-D5 (a previous coupled experiment completed in developing the SB8 flowsheet and utilizing the same sludge simulant, addition of Actinide Removal Product (ARP), and acid addition). Differences from run SB8-D5 included much higher noble metal concentrations and very long strip effluent addition times (equivalent to 38,000 gallons of Strip Effluent, including 30,000 gallons of Strip Effluent added to the SME), which combined to make this a very challenging set of runs.

The main difference between the runs was that three strip effluent combinations (original solvent based on BobCalix/nitric acid, new solvent based on MaxCalix/boric acid, and a blend of the two) were used. A fourth run was performed without solvent and using water as the strip effluent solution to see whether the solvent or strip effluent acid had any impact on processing, particularly hydrogen generation.

Although allowing a large addition of strip effluent to either the SRAT or SME offers obvious operational advantages, it also requires a longer time at temperature than typical DWPF batches, which may lead to higher hydrogen generation, higher ammonia production, higher formate destruction, lower REDOX, higher potential for foaming and coil fouling, and higher yield stress and consistency. Although these impacts could be carefully controlled, consistent processing (same sludge, ARP, strip effluent, and decon water volume for each SRAT and SME batch), should lead to consistent product chemistry. Processing at maximum volumes of strip effluent, whether in the SRAT, SME or both increases the likelihood of the process problems listed above and may require remediation of the SME product with nitric or formic acid

to achieve the desired glass REDOX. Due to the high pH of the SME product leading to higher yield stress and consistency, the melter feed pump may have more difficulty feeding to the melter without dilution.

Some of the highlights of the testing are summarized below:

- The destruction of formate was very high in all runs, but especially high in the two runs with the highest hydrogen generation. The SME formate destruction varied from 29.3 to 70.7% for the four runs, much higher than the 2% measured in a similar run during SB8 blend qualification. This led to a high generation of CO_2, which could increase the potential for foamovers.
- Due to the high anion destruction rates, and the fact that formate and nitrate destruction happens at different rates, the resulting SME product REDOX was much more oxidizing than targeted. In all four tests, the SME product would have required remediation with added formic acid to meet the REDOX target. If a SME product in DWPF was remediated, it would require a remediation plan to be drafted to add formic acid, resampling and reanalysis of the SME to demonstrate that the REDOX target was met before transferring the SME product to the MFT. After remediation of the SME product in DWPF, the next SME batch might be even higher in hydrogen generation due to the addition of fresh formic acid for remediation.
- The pH of the SRAT and SME products (9-10 for SRAT products, 10 for SME products) were very high compared to typical simulant testing. The high pH SME products typically are significantly thicker rheologically. The long processing times and high noble metal concentrations were responsible for the high anion destruction and high product pH. Note that although the equivalent of 30,000 gallons of strip effluent was added during SME processing, the pH of the SME product was almost the same for the three runs with acid in the strip effluent and the run with no added acid.
- It should be noted that in two of the runs, one of the two heating rods used was likely responsible for the high hydrogen generation and rod fouling. Heating rod T8 was very hot relative to the Heating rod T4, which would lead to increased fouling and hydrogen generation. Heating rod T8 averaged more than 11˚C hotter than heating rod T4 during run SB8-D6 and 12˚C hotter during run SB8-D8. Material fouling the heating rods requires an increase in power to the heating rod to maintain the boilup rate, which in turn causes higher local temperature at the point of fouling. With hydrogen generation having a strong relationship to temperature, fouling can cause a significant increase in hydrogen generation.
- Fouling of the heating rods in the SME cycles was noted in the two experiments with the highest hydrogen generation rates. This led to longer processing times for both of these experiments as the targeted boilup rate could not be maintained.
- Very high hydrogen generation was experienced in two of the four runs (SB8-D6 and SB8-D8). The hydrogen generation was so high in run SB8-D6 that the SRAT purge was used for most of the SME cycle to keep from exceeding the 1 volume % hydrogen limit. The peak SME hydrogen generation was 0.568 and 0.229 lb/hr DWPF Scale respectively in runs SB8-D6 and SB8-D8. Both runs had a peak hydrogen generation rate higher than the 0.223 lb/hr DWPF SME limit.
- One of the objectives of the testing was to determine the impact of the three combinations of strip acid and solvent on processing, especially hydrogen generation. Because of the wide variability between the two rigs, no conclusion on this impact can be drawn based on this study.
- There was significant ammonia generation in these runs.
- The calculated pH of the SMECT condensates was 1.3-1.7, suggesting that no nitric acid addition is necessary to control the SMECT pH from 1 to 3. Eliminating the nitric addition to the SMECT may minimize mercury dissolution.

5.0 Recommendations

The testing performed was very aggressive, with high noble metals concentrations and very large strip effluent additions, which led to long processing times and high anion destruction. The objective was that this testing could demonstrate that this flowsheet change could be processed for any future sludge batch, even with very high SWPF strip effluent volumes. Based on the testing completed, an endorsement of the flowsheet change for adding strip effluent to the SME is not currently warranted.

Although the planned testing did not provide a strategy for processing strip effluent in the SME, there are likely some sludge batches (with lower noble metal activity than that tested) where processing strip effluent in the SME would be feasible. In addition, smaller additions of strip effluent in the SME are also more feasible than the 15-30,000 gallons tested.

This testing is a reminder that the chemistry throughout DWPF SRAT and SME processing is complicated and can lead to variable results depending on the temperature of the heating surface, the time for processing, the boilup rate, acid addition rate, etc. Longer processing at temperature is expected to lead to more oxidizing melter feed and will likely require remediation of the SME product with formic acid. The time it takes to develop a remediation plan, add formic acid and resample/reanalyze the SME product may negate any time savings expected from using idle SME time to process strip effluent.

This flowsheet change to add strip effluent in the SRAT or SME would be much easier to implement with the nitric-glycolic flowsheet than the nitric-formic flowsheet. The lack of hydrogen generation and lower reaction rates for destruction of glycolate and nitrate make producing melter feed without remediation more likely. The higher processing volumes expected after startup of SWPF will make processing in the SRAT and SME much longer and will likely be easier to process using the nitric-glycolic flowsheet. Future testing to implement the SEFT to SME flowsheet should be performed using the nitric-glycolic flowsheet.

Additional testing should be completed prior to implementing the flowsheet change in DWPF:

1. Repeat the experiments for each sludge batch with sludge batch levels of noble metals and mercury added to the best sludge simulant for that sludge batch.
2. Complete experiments using planned sludge batch maximum amounts for sludge, ARP, strip effluent, and acid stoichiometry. If SWPF is not operational, do not use SWPF volumes of ARP and strip effluent for testing.
3. Test adding strip effluent to the SME using the nitric-glycolic flowsheet.
4. The testing should be completed using any lessons learned from this testing (see below).

The following improvements to SRNL testing methodology is recommended and will be implemented before completing experiments with high strip effluent volumes in the SRAT or SME:

1. Repeat experiments using new, temperature-matched heating rods to minimize testing differences from probe to probe. Perform a water run before testing to demonstrate a low measured differential temperature between rods.
2. Complete scoping experiments before beginning the experimental set to determine the anion destruction in order to be able to accurately predict the REDOX in subsequent experiments. This would require the anion destruction during segments of the cycles such as strip effluent addition in SRAT or SME; decon water evaporation in SME, and process frit slurry evaporation to more accurately predict the final melter feed composition.
3. Complete analysis and review data for the SME product and resulting glass REDOX before performing the next experiment in the series.

6.0 References

[1] H. Boyd, Flowsheet Testing for SEFT to SME Modifications at DWPF, X-TTR-S-00016, SRR, Aiken, SC, 29808 (July 2014).

[2] D. P. Lambert, Task Technical and Quality Assurance Plan for Testing Feasibility of Adding Strip Effluent to the Slurry Mix Evaporator, SRNL-RP-2014-00909, SRNL, Aiken, SC, 29808 (September 2014).

[3] T. L. White, D.P. Lambert, J.R. Zamecnik, W.T. Riley, Ion Chromatography (IC) Analysis of Glycolate in Simulated Waste, SRNL-STI-2015-00049, SRNL, Aiken, SC, 29808 (March 2015 draft)

[4] C. M. Jantzen and M.E. Stone, Role of Manganese Reduction/Oxidation (REDOX) on Foaming and Melt Rate in High Level Waste (HLW) Melters, WSRC-STI-2006-00066, Revision 0, SRNL, Aiken, SC, 29808 (March 2007).

[5] M. E. Stone, Laboratory Scale Chemical Process Cell Simulations, SRNL Procedure Manual: L29, ITS-0094, Revision: 7, SRNL, Aiken, SC, 29808 (June 2012).

[6] D. C. Koopman, Noble Metal Chemistry and Hydrogen Generation during Simulated DWPF Melter Feed Preparation, WSRC-STI-2008-00002, SRNL, Aiken, SC, 29808 (June 2008).

[7] D. C. Koopman, Rheology Protocols for DWPF Samples, WSRC-RP-2004-00470, Savannah River Site, Aiken, SC, 29808 (October 2004).

[8] DPSTD-80-38, Rev. 2, Technical Data Summary for the Defense Waste Processing Facility Sludge Plant, Part 10, Item 230, September, 1982.

[9] D. C. Koopman, J. R. Zamecnik, DWPF Simulant Flowsheet Studies for SB8, SRNL-STI-2013-00106, Revision 0, Savannah River Site, Aiken, SC, 29808 (June 2013).

[10] D.T. Wasan, Progress Report and Technical Assistance to Support Antifoam Development, Subcontract # AC70087N, November 3, 2011, Illinois Institute of Technology, Chicago, IL, 60616.

[11] C.N Sawyer and P.L. McCarty, 1978. Chemistry for Environmental Engineering, 3rd Edition. McGraw-Hill Book Company, NY, NY.

[12] C.M. Jantzen,SRNL Procedure Manual: L29, ITS-0052, , Rev 4, Heat Treatment of Waste Slurries for REDOX ($Fe^{2+}/\sum Fe$) & Chemical Composition Measurement, SRNL, Aiken, SC, 29808 (December 2014).

[13] D. R. Best, SRNL Procedure Manual: L29, ITS-0042, Rev 2, Determining Fe^{2+}/Fe^{3+} and Fe^{2+}/Fe(total) Using UV VIS Spectrometer, SRNL, Aiken, SC, 29808 (August 2014).

Appendixes

Appendix A. Acid Calc Input Data

Table 1a -- Sludge Analyses for Acid Calculations, Run #	SB8-D6/D7	SB8-D8/D9	Units
Fresh Sludge Mass without trim chemicals	3,300.0	3,300.0	g slurry
Fresh Sludge Weight % Total Solids	18.72	18.72	wt%
Fresh Sludge Weight % Calcined Solids	14.36	14.36	wt%
Fresh Sludge Weight % Insoluble Solids	10.19	10.19	wt%
Fresh Sludge Density	1.160	1.160	kg / L slurry
Fresh Sludge Supernate density	1.076	1.076	kg / L supernate
Fresh Sludge Nitrite	16,136	16,136	mg/kg slurry
Fresh Sludge Nitrate	10,131	10,131	mg/kg slurry
Fresh Sludge Formate	0	0	mg/kg slurry
Fresh Sludge Sulfate (mg/kg)	1,847	1,847	mg/kg slurry
Fresh Sludge Chloride (mg/kg)	0	0	mg/kg slurry
Fresh Sludge Phosphate (mg/kg)	0	0	mg/kg slurry
Fresh Sludge Oxalate	3210	3210	mg/kg slurry
Fresh Sludge Slurry TIC (treated as carbonate)	1932	1932	mg/kg slurry
Fresh Supernate TIC (treated as carbonate)	2152	2152	mg/L supernate
Fresh Sludge Hydroxide (Base Equivalents) pH = 7	0.856	0.856	Equiv Moles Base/L slurry
Fresh Sludge Manganese (% of Calcined Solids)	8.030	8.030	wt % calcined basis
Fresh Sludge Mercury (% of Total Solids in untrimmed sludge)	0.0000	0.0000	wt% dry basis
Fresh Sludge Magnesium (% of Calcined Solids)	0.290	0.290	wt % calcined basis
Fresh Sludge Sodium (% of Calcined Solids)	18.300	18.300	wt % calcined basis
Fresh Sludge Potassium (% of Calcined Solids)	0.139	0.139	wt % calcined basis
Fresh Sludge Cesium (% of Calcined Solids)	0.000	0.000	wt % calcined basis
Fresh Sludge Calcium (% of Calcined Solids)	1.410	1.410	wt % calcined basis
Fresh Sludge Strontium (% of Calcined Solids)	0.000	0.000	wt % calcined basis
Fresh Sludge Nickel (% of Calcined Solids)	2.510	2.510	wt % calcined basis
Fresh Sludge Supernate manganese	0	0	mg/L supernate

Table 1b -- ARP Analyses for Acid Calculations, Run #	SB8-D6	SB8-D8	
ARP Mass without trim chemicals	557.42	557.42	g slurry
ARP Weight % Total Solids	6.96	6.96	wt%
ARP Weight % Calcined Solids	4.93	4.93	wt%
ARP Weight % Insoluble Solids	1.51	1.51	wt%
ARP Density	1.0535	1.0535	kg / L slurry
ARP Supernate density	1.04	1.04	kg / L supernate
ARP Nitrite	2960	2960	mg/kg slurry
ARP Nitrate	13400	13400	mg/kg slurry
ARP Oxalate	6090	6090	mg/kg slurry
ARP Formate	0	0	mg/kg slurry
ARP Sulfate (mg/kg)	882	882	mg/kg slurry
ARP Chloride (mg/kg)	0	0	mg/kg slurry
ARP Phosphate (mg/kg)	0	0	mg/kg slurry
ARP Slurry TIC (treated as carbonate)	476	476	mg/kg slurry

ARP Supernate TIC (treated as carbonate)	498	498	mg/L supernate
ARP Hydroxide (Base Equivalents) pH = 7	0.4673	0.4673	Equiv Moles Base/L slurry
ARP Mercury (% of Total Solids in untrimmed sludge)	0	0	wt% dry basis
ARP Manganese (% of Calcined Solids)	0	0	wt % calcined basis
ARP Magnesium (% of Calcined Solids)	0	0	wt % calcined basis
ARP Sodium (% of Calcined Solids)	40.97	40.97	wt % calcined basis
ARP Potassium (% of Calcined Solids)	0.927	0.927	wt % calcined basis
ARP Cesium (% of Calcined Solids)	0	0	wt % calcined basis
ARP Calcium (% of Calcined Solids)	0	0	wt % calcined basis
ARP Strontium (% of Calcined Solids)	0	0	wt % calcined basis
ARP Nickel (% of Calcined Solids)	0	0	wt % calcined basis
ARP Supernate manganese	0	0	mg/L supernate

Table 1c -- SE Analyses for Acid Calculations, Run #	**SB8-D6**	**SB8-D8**	
SE Mass without trim chemicals	18035.26	18035.26	
SE Weight % Total Solids	0.2	0.062	
SE Weight % Calcined Solids	0.0	0.0	
SE Weight % Insoluble Solids	0.0	0.0	
SE Density	1.001	0.999	
SE Supernate density	1.001	0.999	
SE Nitrite	0	0	
SE Nitrate	2,044	0	
SE Slurry TIC (treated as carbonate)	0	0	
SE Supernate TIC (treated as carbonate)	0	0	
SE Hydroxide (Base Equivalents) pH = 7	-0.033	-0.03	

Table 2 -- SRAT Processing Assumptions, Run #	**SB8-D6**	**SB8-D8**	
Conversion of Nitrite to Nitrate in SRAT Cycle	8.00	8.00	gmol NO_3^-/100 gmol NO_2^-
Destruction of Nitrite in SRAT and SME cycle	100.00	100.00	% of starting nitrite destroyed
Destruction of Formic acid charged in SRAT	28.40	28.40	% formate converted to CO_2 etc.
Destruction of Glycolic acid charged in SRAT	0.00	0.00	% glycolate converted to CO_2 etc.
Conversion of Glycolic acid to Oxalate	0.00	0.00	% glycolate converted to C2O4
Destruction of Oxalate charged	10.00	10.00	% of total oxalate destroyed
Percent Acid in Excess Stoichiometric Ratio	120.00	120.00	%
SRAT Product Target Solids	29.72	29.72	%
Nitric Acid Molarity	10.129	10.129	Molar
Formic Acid Molarity	23.548	23.548	Molar
Glycolic Acid Molarity	0.000	0.000	Molar
DWPF Nitric Acid addition Rate	2.000	2.000	gallons per minute
DWPF Formic Acid addition Rate	2.000	2.000	gallons per minute
REDOX Target	0.100	0.100	Fe^{+2} / ΣFe
Trimmed Sludge Target Ag metal content	0.0164	0.0164	total wt% dry basis after trim

Trimmed Sludge Target wt% Hg dry basis	0.9840	0.9840	total wt% dry basis after trim
Trimmed Sludge Target Pd metal content	0.0925	0.0925	total wt% dry basis after trim
Trimmed Sludge Target Rh metal content	0.0445	0.0445	total wt% dry basis after trim
Trimmed Sludge Target Ru metal content	0.2542	0.2542	total wt% dry basis after trim
Trimmed Sludge Target Cr metal content	0.0000	0.0000	total wt% dry basis after trim
Trimmed Sludge Target Ba metal content	0.0000	0.0000	total wt% dry basis after trim
Trimmed Sludge Target Cd metal content	0.0000	0.0000	total wt% dry basis after trim
Trimmed Sludge Target Gd metal content	0.0000	0.0000	total wt% dry basis after trim
Trimmed Sludge Target Wt% Coal/carbon source dry basis	0.0000	0.0000	total wt% dry basis after trim
Trimmed Sludge Target oxalate after trim (wt % not mg/kg)	1.5800	1.5800	total wt% dry basis after trim
Water to dilute fresh sludge and/or rinse trim chemicals	150.00	150.00	g
Total Water added to flush both the Nitric and Formic Acid Lines	20.00	20.00	g
Sample Mass of Trimmed sludge (SRAT Receipt sample, if any)	123.76	123.76	g
Sample Mass after ARP boil-down	0.00	0.00	g
Mass of SRAT cycle samples	415.48	415.48	g
Wt% Active Agent In Antifoam Solution	10	10	%
Basis Antifoam Addition for SRAT (generally 100 mg antifoam/kg slurry)	100	100	mg/kg slurry
Number of basis antifoam additions added during SRAT cycle	8	8	
SRAT air purge	230	230	scfm
SRAT boil-up rate	5000	5000	lbs/hr
SRAT total boil-up (reflux)	60,000	60,000	lbs
SRAT Steam Stripping Factor	750	750	(g steam/g mercury)
Table 3 -- SME Processing Assumptions, Run #	**SB8-D6**	**SB8-D8**	
Enter 1 for Redox Balance with SME Cycle or 0 for Redox Balance with no SME Cycle	1	1	
Frit type	418	418	
Destruction of Formic acid in SME	1.50	1.50	% Formate converted to CO_2 etc.
Destruction of Nitrate in SME	0.50	0.50	% Nitrate destroyed in SME
Destruction of Glycolate in SME	0.00	0.00	% glycolate converted to CO_2 etc.
Assumed SME density	1.390	1.390	kg / L
Basis Antifoam Addition for SME cycle	100	100	mg/kg slurry
Number of basis antifoam additions added during SME cycle	4	4	
Sludge Oxide Contribution in SME (Waste Loading)	35.49	35.49	%
Frit Slurry Formic Acid Ratio	1.50	1.50	g 90 wt% FA/100 g Frit
Target SME Solids total Wt%	48.0	48.0	wt%
Number of frit additions in SME Cycle	2	2	
# DWPF Canister decons simulated	6.0	6.0	

Volume of water per deconed can	1,000	1,000	gal at DWPF scale
Water flush volume after frit slurry addition	0.0	0.0	gal
SME air purge	74	74	scfm
SME boil-up rate	5000	5000	lbs/hr

Appendix B. Rheology Data

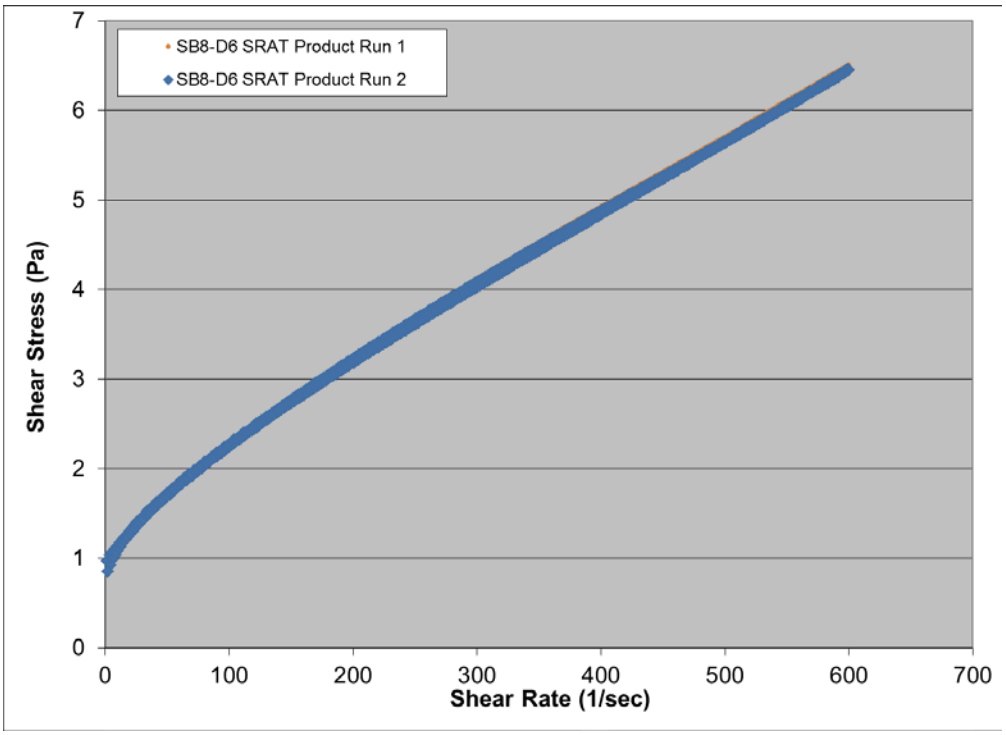

Figure B-1. SB8-D6 SRAT Product Rheology Curves

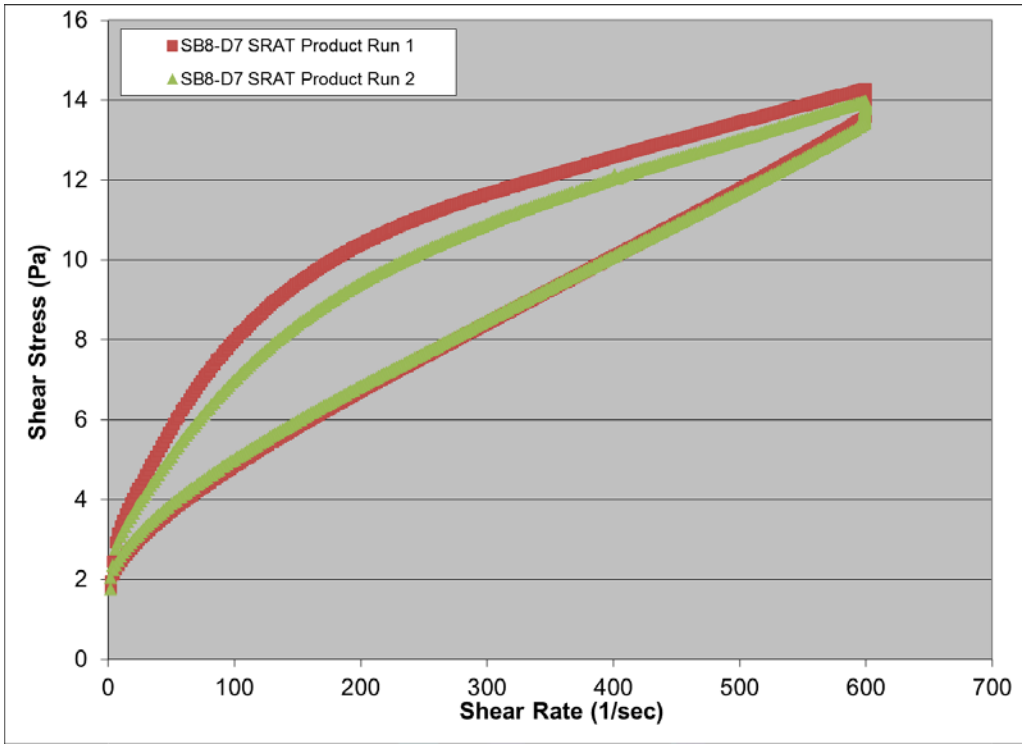

Figure B-2. SB8-D7 SRAT Product Rheology Curves

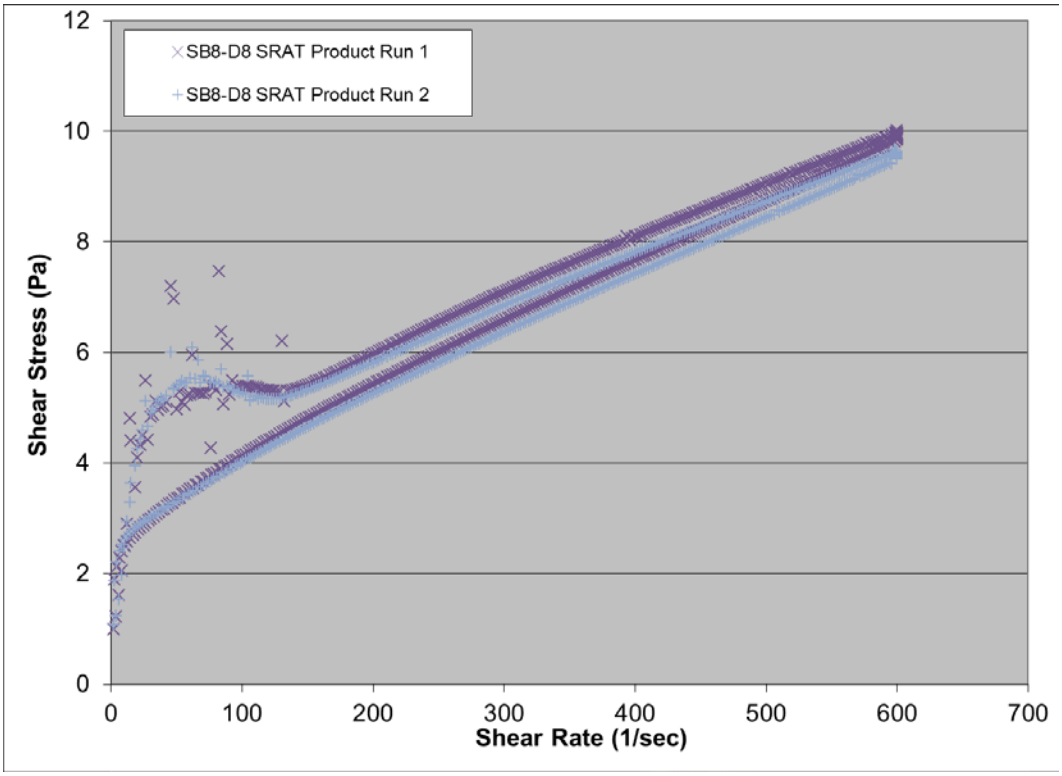

Figure B-3. SB8-D8 SRAT Product Rheology Curves

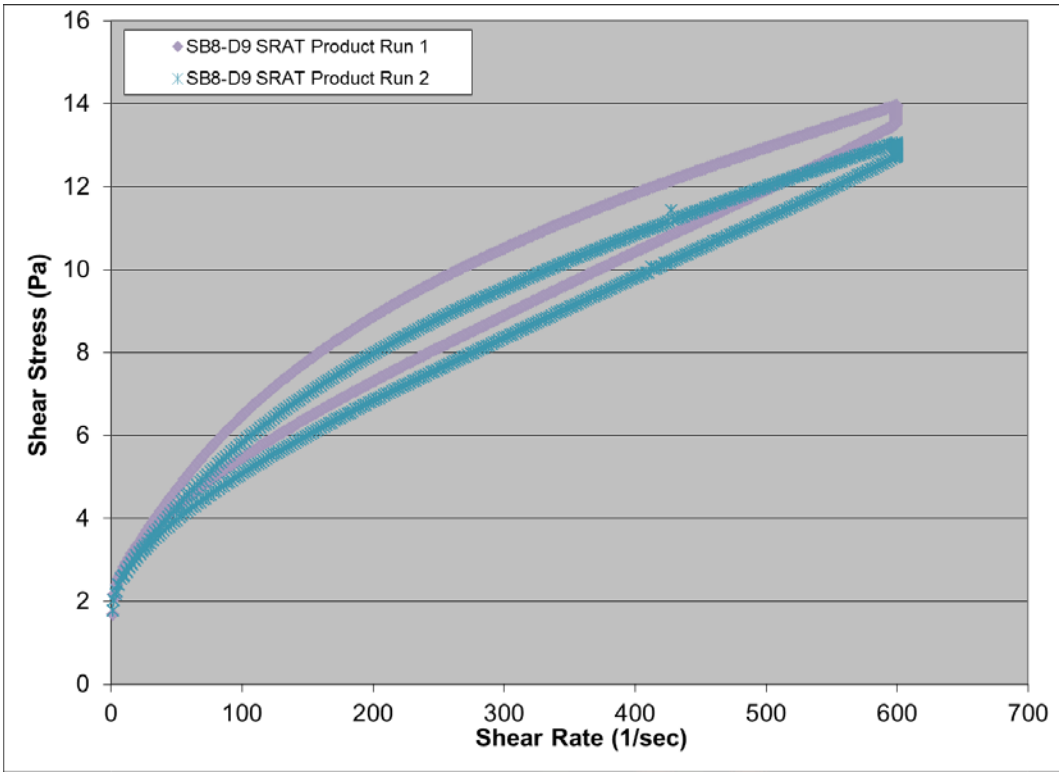

Figure B-4. SB8-D9 SRAT Product Rheology Curves

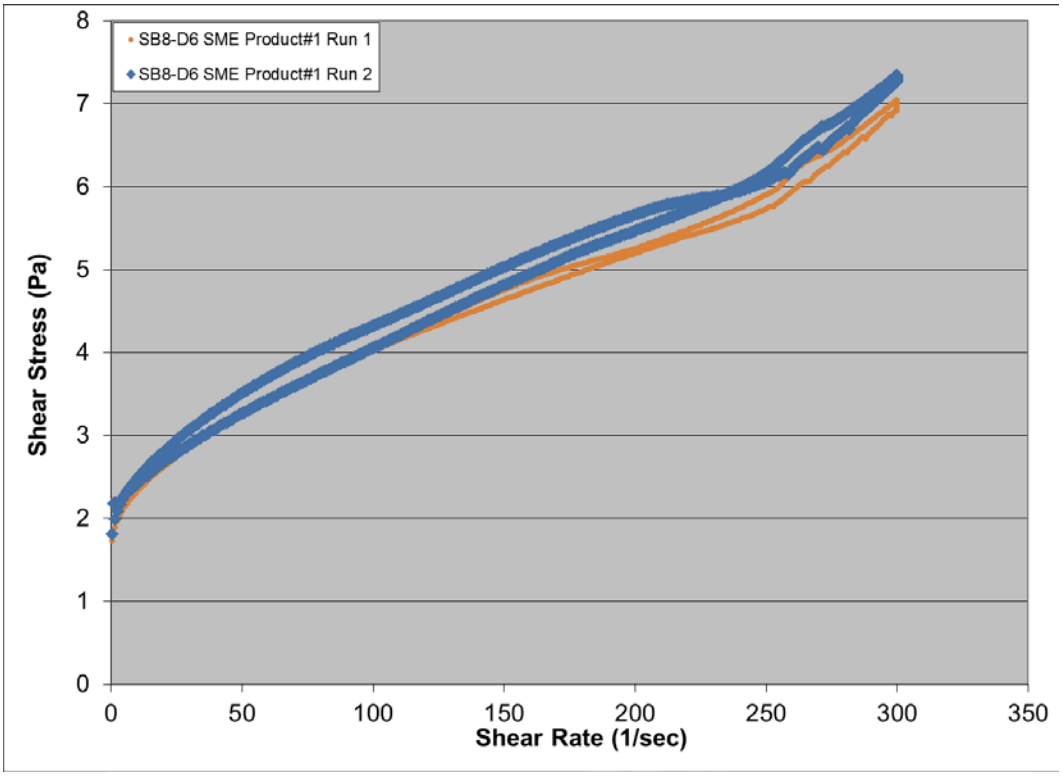

Figure B-5. SB8-D6 SME Product#1 Rheology Curves

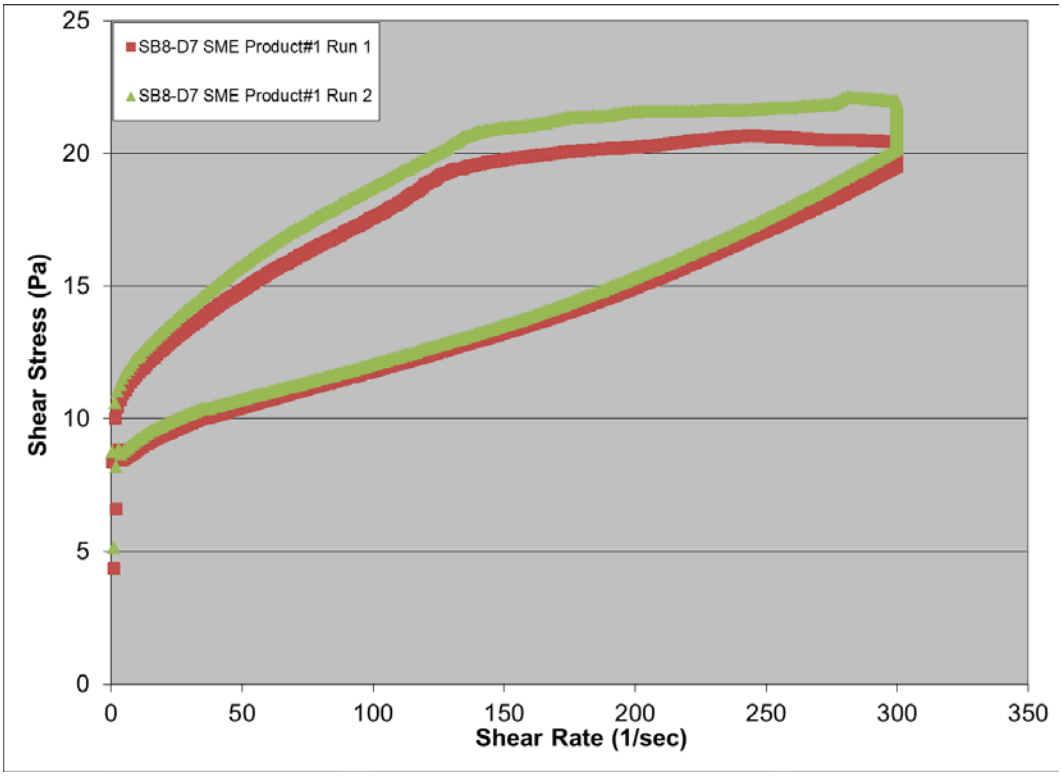

Figure B-6. SB8-D7 SME Product#1 Rheology Curves

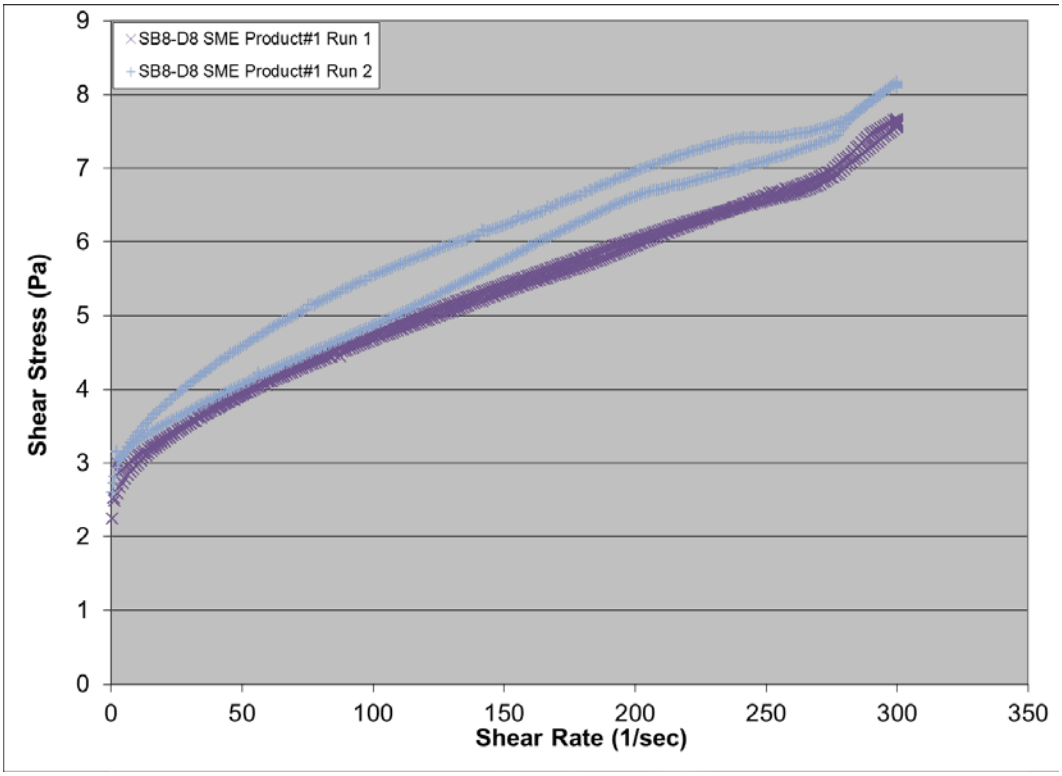

Figure B-7. SB8-D8 SME Product#1 Rheology Curves

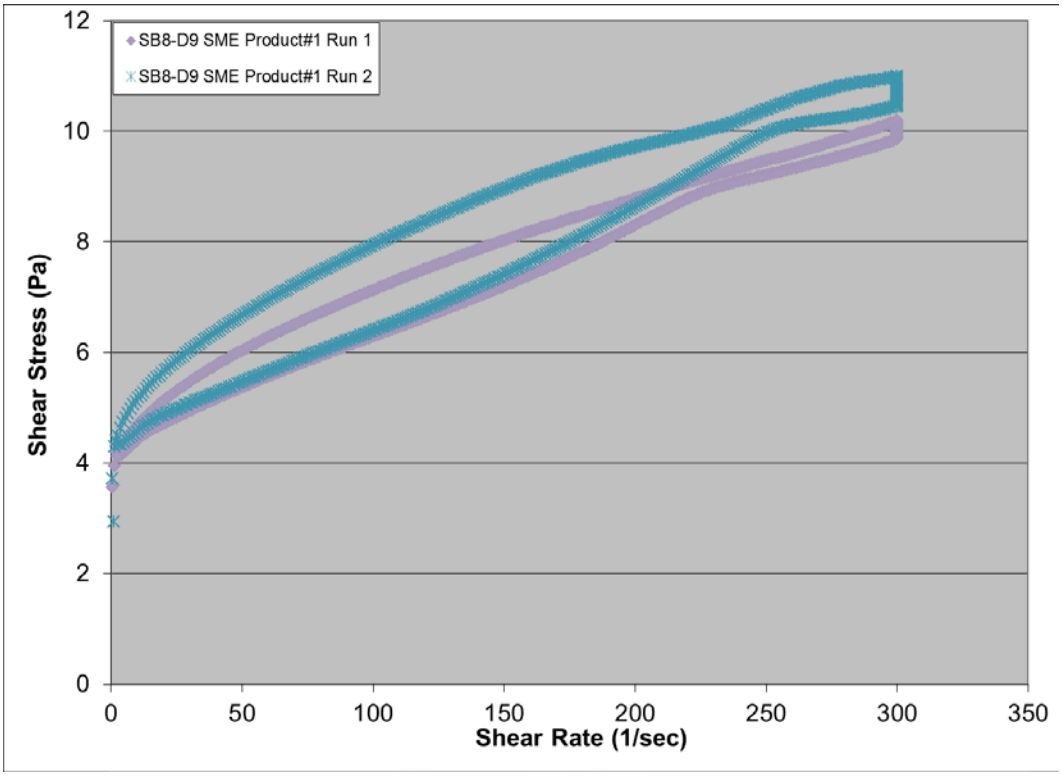

Figure B-8. SB8-D9 SME Product#1 Rheology Curves

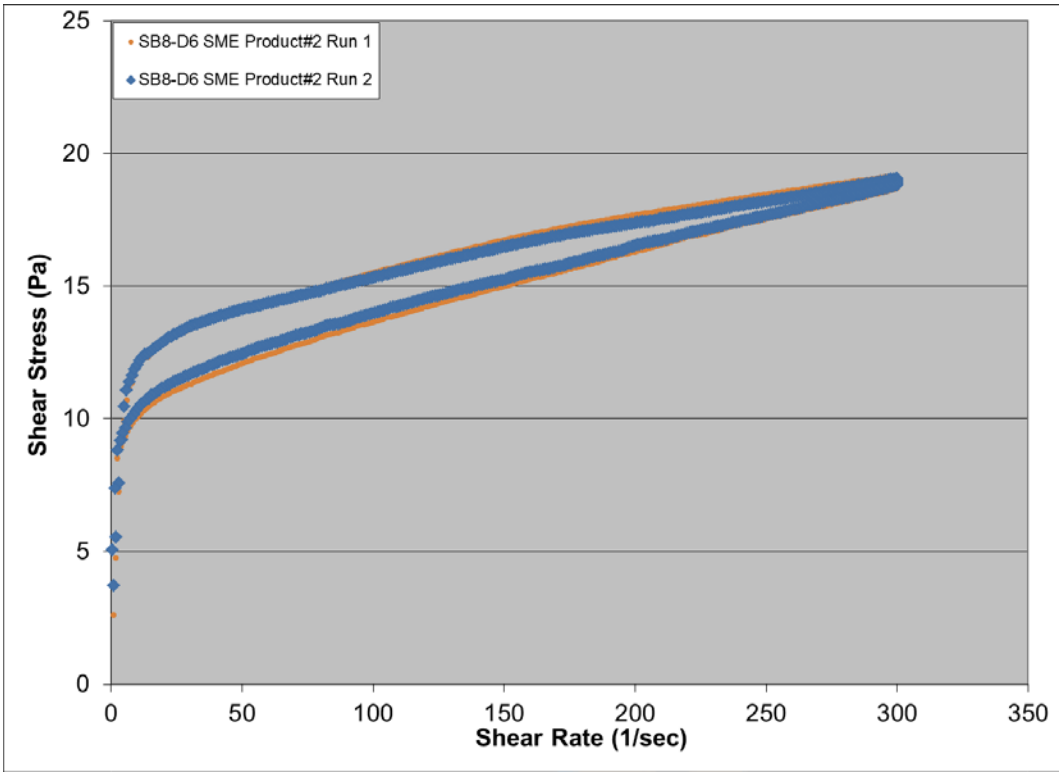

Figure B-9. SB8-D6 SME Product#2 Rheology Curves

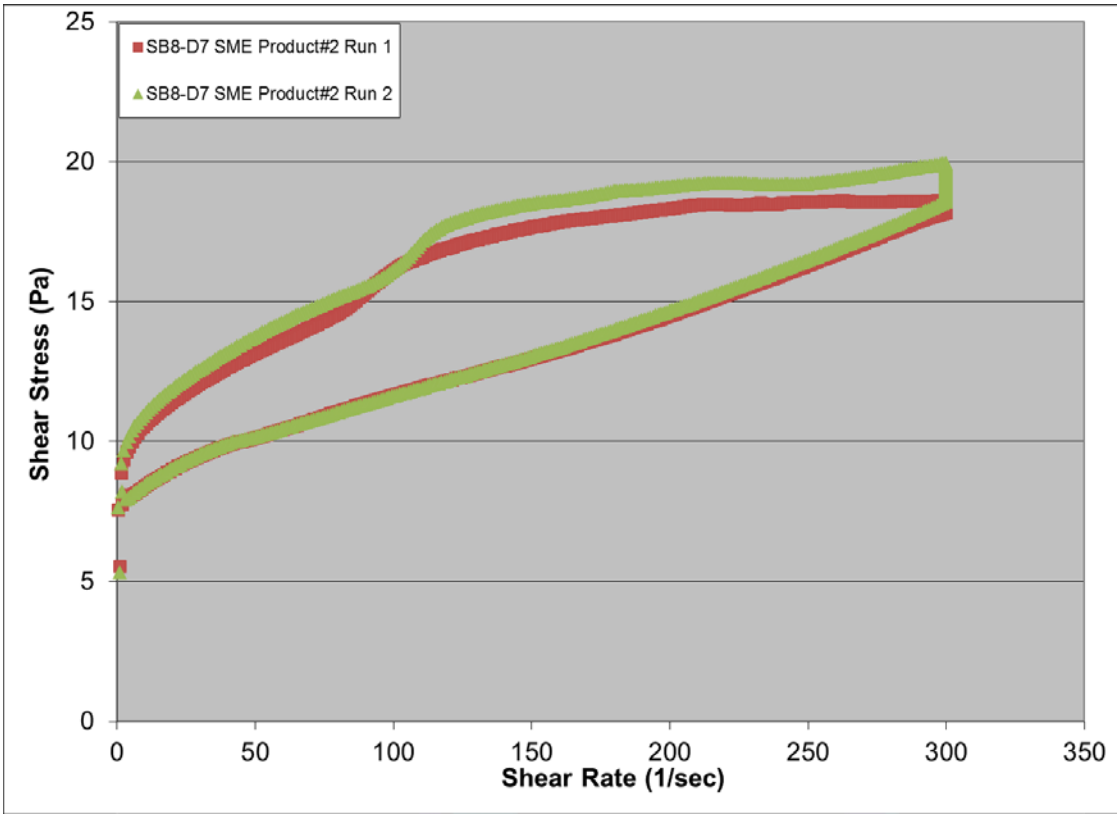

Figure B-10. SB8-D7 SME Product#2 Rheology Curves

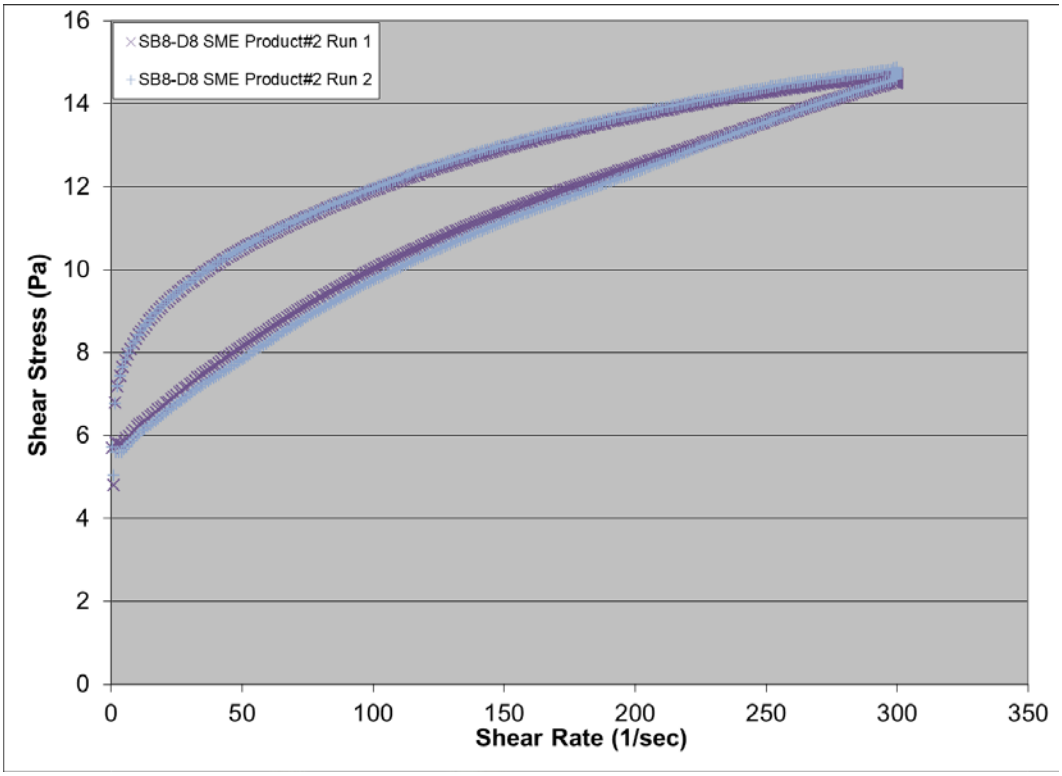

Figure B-11. SB8-D8 SME Product#2 Rheology Curves

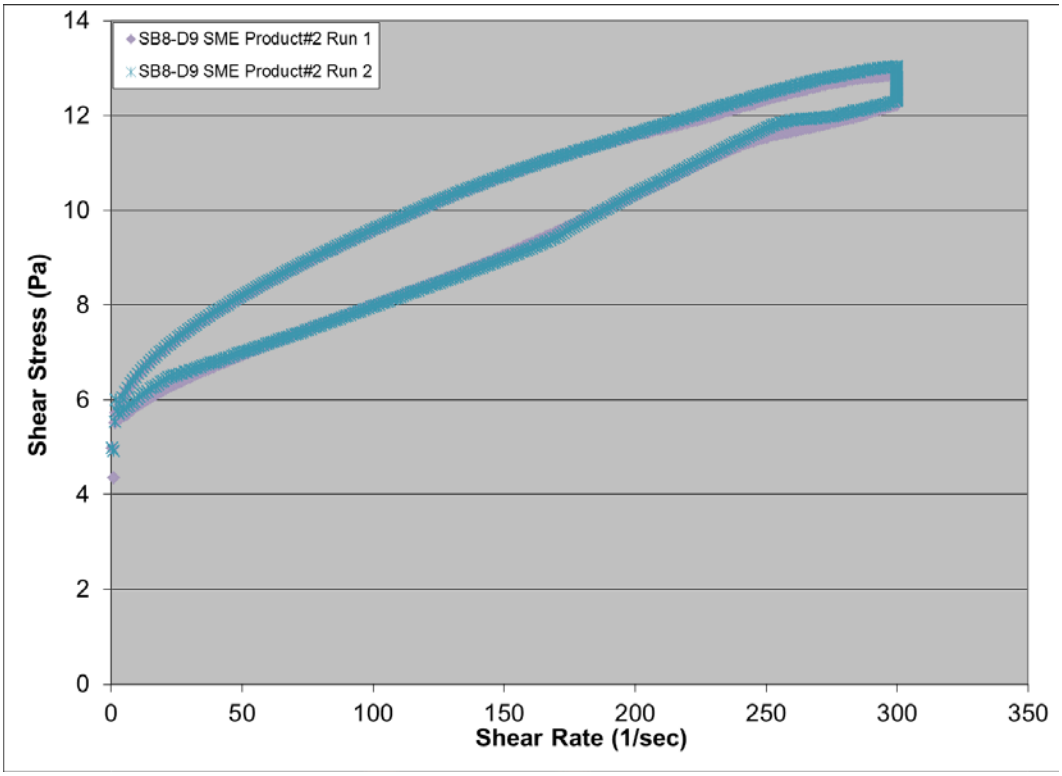

Figure B-12. SB8-D9 SME Product#2 Rheology Curves

Appendix C. Offgas Data

This appendix contains graphs of the offgas data showing the accumulated mmoles of the generated gases and volume % of gases for each run.

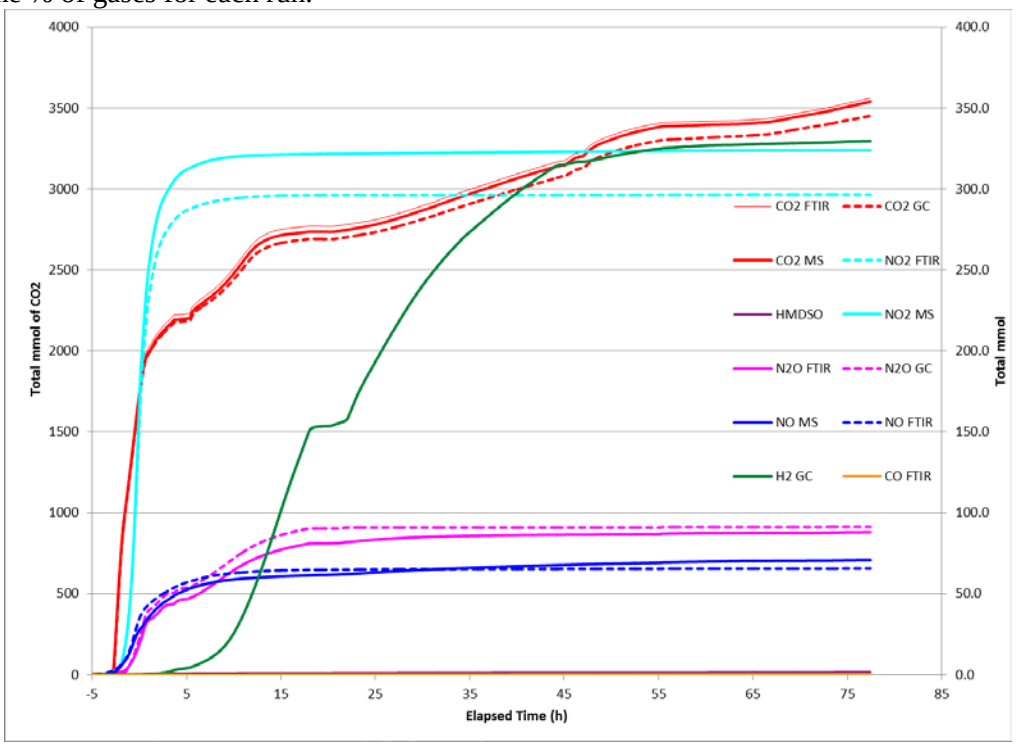

Figure C-1. SB8-D6 Cumulative Offgas Generation

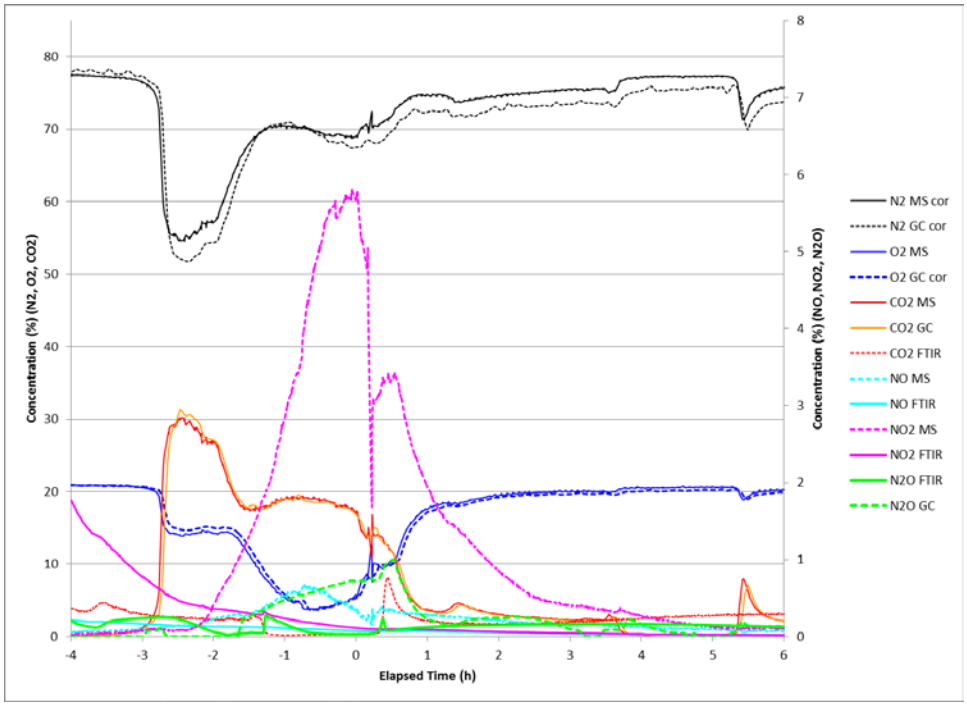

Figure C-2. SB8-D6 Offgas Concentration during Acid Addition/Early SRAT, Volume %

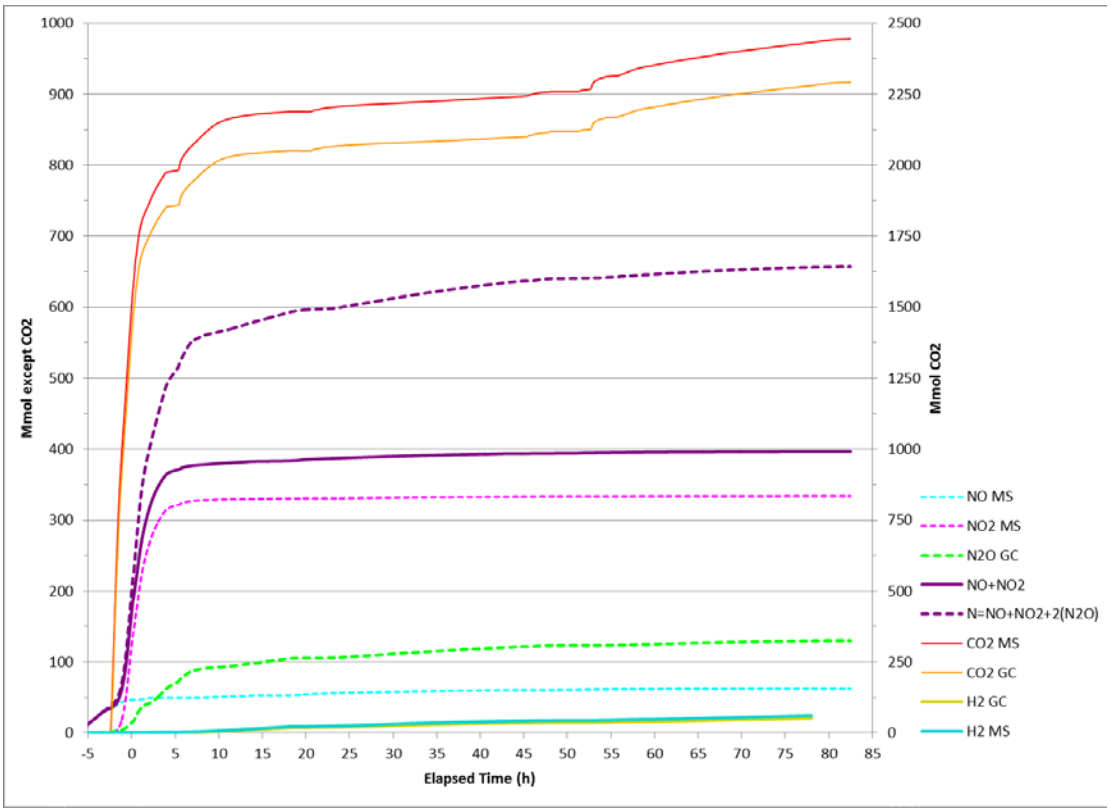

Figure C-3. SB8-D7 Cumulative Offgas Generation

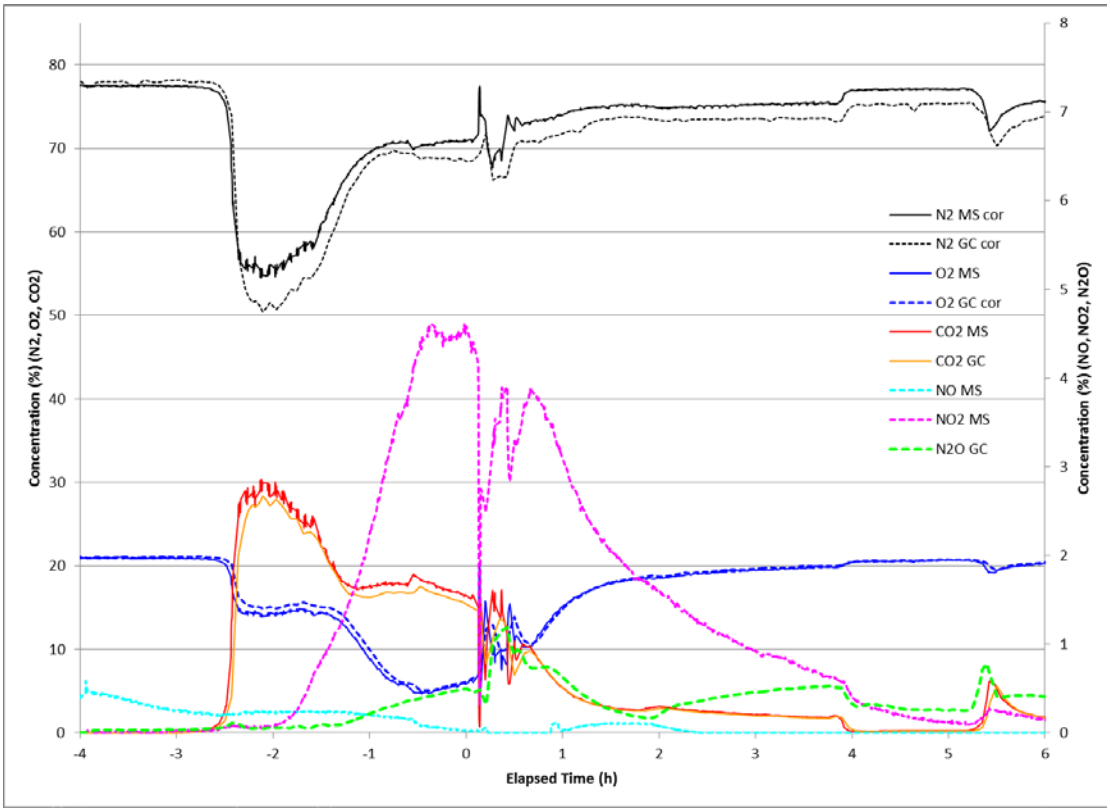

Figure C-4. SB8-D7 Offgas Concentration during Acid Addition/Early SRAT, Volume %

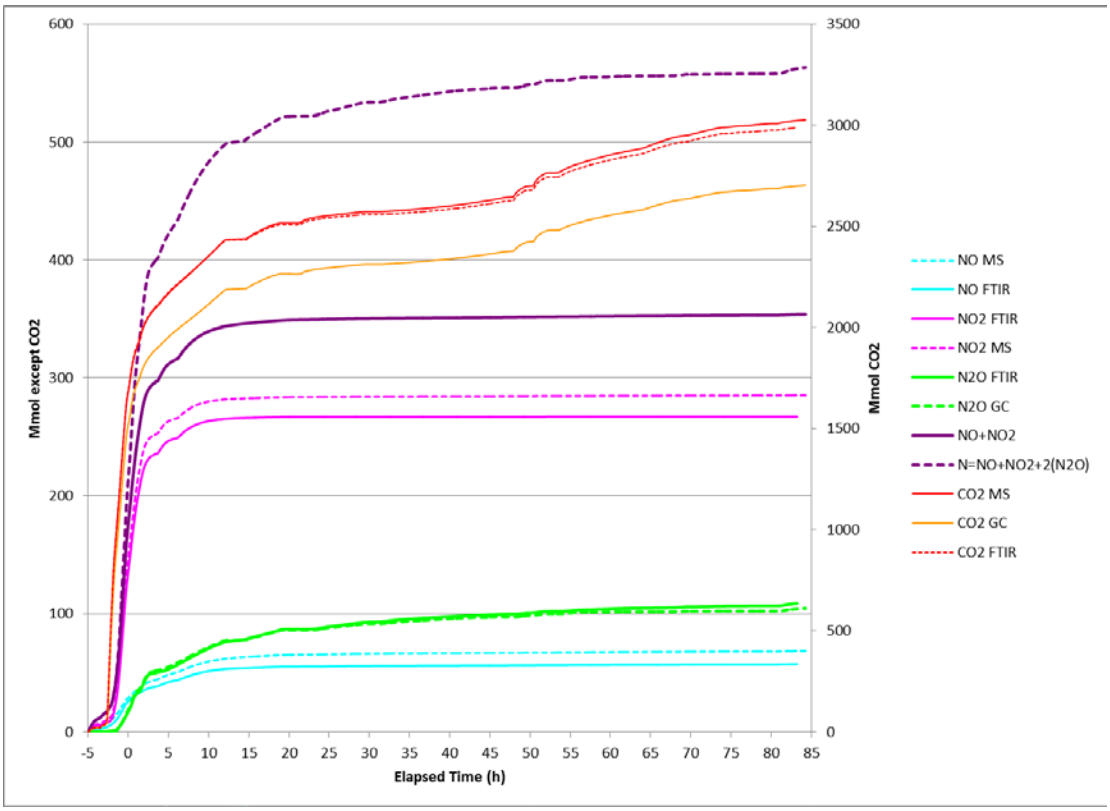

Figure C-5. SB8-D8 Cumulative Offgas Generation

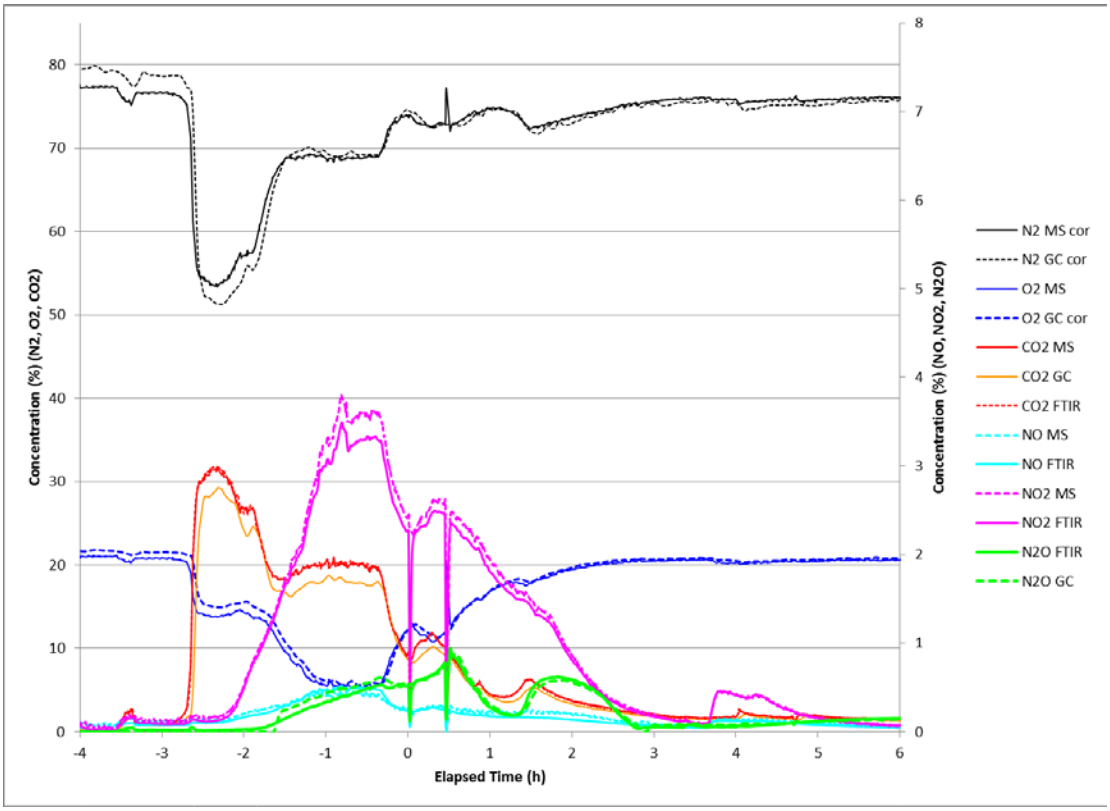

Figure C-6. SB8-D8 Offgas Concentration during Acid Addition/Early SRAT, Volume %

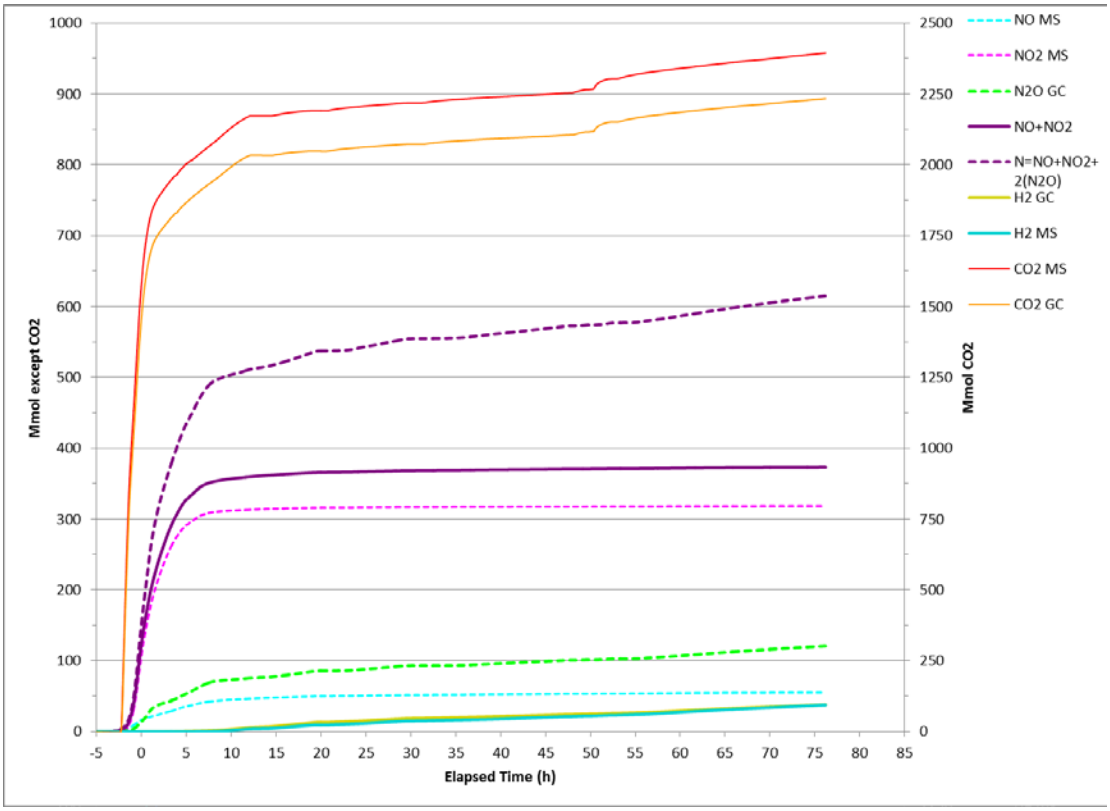

Figure C-7. SB8-D9 Cumulative Offgas Generation

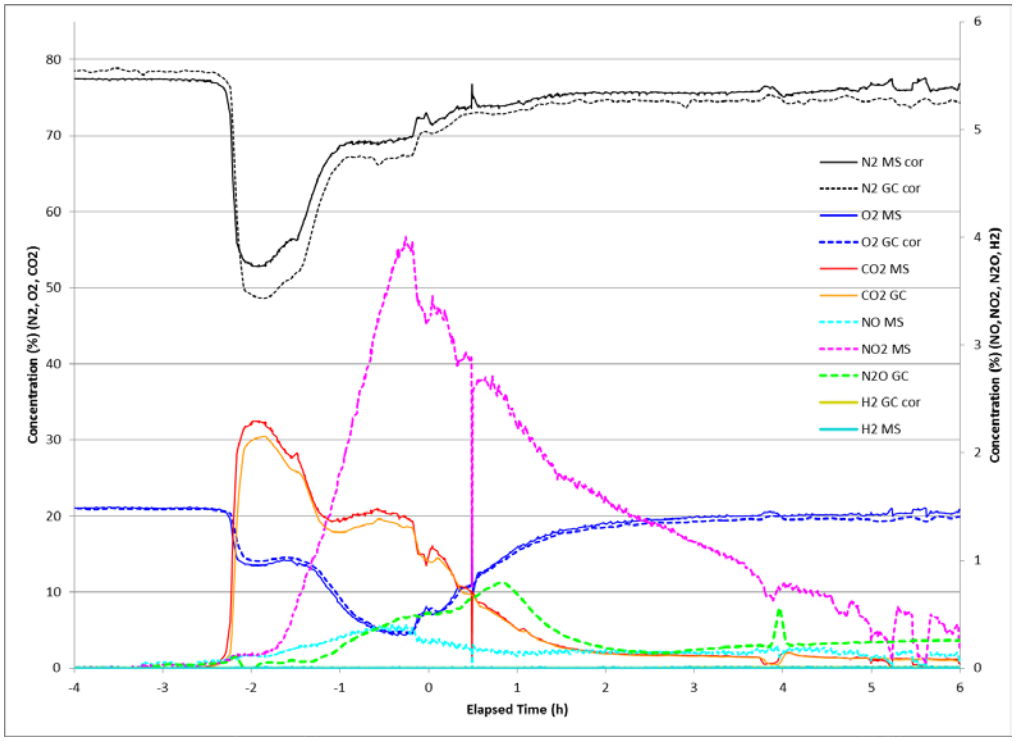

Figure C-8. SB8-D9 Offgas Concentration during Acid Addition/Early SRAT, Volume %

Distribution:

J. M. Bricker, 704-30S
J. S. Contardi, 704-56H
T. L. Fellinger, 766-H
E. J. Freed, 704-S
J. M. Gillam, 766-H
B. A. Hamm, 766-H
E. W. Holtzscheiter, 766-H
J. F. Iaukea, 704-27S
H. P. Boyd, 704-27A
J. W. Ray, 704-27S
P. J. Ryan, 704-S
M. A. Rios-Armstrong, 766-H
H. B. Shah, 766-H
D. C. Sherburne, 704-S
M. E. Stone, 999-W
B. T. Geyer, 704-72S
E. A. Brass, 241-12H
C. K. Chiu, 704-27S
E. J. Freed, 704-S
A. G. Garrison, 241-12H
B. A. Gifford, 704-56H
D. J. Martin, 241-152H
R. T. McNew, 241-152H
M. A. Rios-Armstrong, 766-H
A. R. Shafer, 704-27S
T. E. Smith,241-52H
P. R. Jackson, DOE-SR, 703-46A
J. A. Crenshaw, 703-46A
S. L. Marra, 773-A
T. B. Brown, 773-A
D. H. McGuire, 999-W
S. D. Fink, 773-A
C. C. Herman, 773-A
E. N. Hoffman, 999-W
F. M. Pennebaker, 773-42A
W. R. Wilmarth, 773-A
J. R. Zamecnik, 999-W
C. J. Martino, 999-W
M. E. Stone, 999-W
M. S. Williams, 999-W
M. F. Williams, 999-W
Holly Hall, 773-A
Records Administration (EDWS)